Modeling of Test Section Conditions in a High Enthalpy Flow Facility

Daniel R. Drabiak

A thesis
submitted in partial fulfillment of the
requirements for the degree of

Master of Science in Aeronautics and Astronautics

University of Washington

2017

Committee:

Carl Knowlen, Chair

James C. Hermanson

Program Authorized to Offer Degree:
Aeronautics and Astronautics

University of Washington

Abstract

Modeling of Test Section Conditions in a High Enthalpy Flow Facility

Daniel R. Drabiak

Chair of the Supervisory Committee:
Research Associate Professor Carl Knowlen
William E. Boeing Department of Aeronautics and Astronautics

The Shock Wave Reactor laboratory, or SWR, at the University of Washington is a high enthalpy flow facility capable of a wide range of test conditions. In this study, an analytical model has been prepared using MATLAB in an effort to predict the envelope of test conditions of which the SWR is capable for a given range of input conditions. The SWR modeling assumed one-dimensional, steady, ideal gas flow, and considered the effects of heat transfer and friction on stagnation pressure and stagnation temperature, as well as other values such as Mach number. The SWR can receive steam from a pebble bed heater at temperatures up to 1400 K and H_2(g) and O_2(g) at room temperature in a combustor section. The resulting fluid flows through a converging-diverging nozzle, which accelerates the flow to supersonic Mach numbers, typically at about Mach 2.5. Downstream of the throat, feedstock such as N_2(g) can be injected into the flow. Downstream of feedstock injection, the flow proceeds through a mixer section into a test section with a diameter of 4". It is the flow properties in the test section that were attempted to be predicted by the model in this study. The model was run using known or assumed input conditions for existing SWR experimental data, and the modeled results for the test section data were compared against the experimental data. Although the model showed good ability to predict the trends of test section conditions relative to input conditions, the model mostly did not show good ability to predict the envelope of test conditions that the SWR is capable of producing.

TABLE OF CONTENTS

LIST OF FIGURES

GLOSSARY

A: Area, m^2

A^*: Sonic throat area, m^2

a: Speed of sound, m/s

b: Time constant, 1/s

C_1: Dimensionless constant in Nusselt number relationship

C_2: Dimensionless constant in Nusselt number relationship

c_p: Specific heat at constant pressure, J/(kg*K)

c_v: Specific heat at constant volume, J/(kg*K)

D: Diameter, m

f: Friction factor

h: Specific enthalpy, J/kg

h_c: Convective heat transfer coefficient, W/(m^2*K) (unless otherwise stated)

k: Conductive heat transfer coefficient, W/(m*K) (unless otherwise stated)

L: Length, m

M: Mach number

$\mathfrak{M}$: Molecular weight, kg/kmol (unless otherwise stated)

m: Mass, kg

$\dot{m}$: Mass flow rate, kg/s (unless otherwise stated)

Nu: Nusselt number

OF: Ratio of oxidizer to fuel mass flow rates

OF_{st}: Stoichiometric ratio of oxidizer to fuel mass flow rates

p: Static pressure, Pa (unless otherwise stated)

Pr: Prandtl number

$\dot{Q}$: Heat transfer rate, W

$\dot{Q}_f$: Heat flux rate, W/m^2

$\dot{q}$: Specific heat transfer rate, W/kg

Q: Heat transfer, J

q: Specific heat transfer, J/kg

q_f: Specific heat flux, J/(kg*m^2)

R: Gas constant for a particular gas, J/(kg*K)

R_u: Universal gas law constant, J/(kmol*K)

Re: Reynolds number

T: Static temperature, K (unless otherwise stated)

T_{ad}: Adiabatic flame temperature, K (unless otherwise stated)

T_s: Wall temperature, K (unless otherwise stated)

u: Velocity, m/s

V: Volume, m^3

Greek Letters:

α: Ratio of feedstock mass flow rate to freestream mass flow rate

ϕ: Equivalence ratio

γ: Ratio of specific heats

μ: Dynamic viscosity, kg/(m*s) (unless otherwise stated)

ρ: Static density, kg/(m^3)

Subscripts:

∞: Freestream values

0: Stagnation conditions

7: Mixed fluid conditions

a: Conditions of fluid prior to feedstock mixing

am: Conditions at a temperature that is an arithmetic mean of wall temperature and the freestream fluid temperature of a particular station

b: Feedstock conditions

t: Throat conditions

TS: Test section conditions

ACKNOWLEDGMENTS

First of all, I would like to extend a special thank you to Prof. Carl Knowlen for serving as my thesis committee chair, for giving me the opportunity to conduct research in the SWR lab, for teaching me how to conduct research at the graduate level, for his availability whenever I needed his help, for teaching me how to overcome challenges that seemed insurmountable, and for his tireless and indispensible support and guidance as I worked on my thesis project.

Other professors that I would like to thank include Prof. James C. Hermanson, for serving as the second member member of my committee; Prof. Robert E. Breidenthal, whose humor is surpassed only by his humility; and Prof. Adam Bruckner, who pushed me both to do my best and to stay positive. All three provided valuable instruction, both inside and outside the classroom, during my gradute study. To Professors Hermanson and Breidenthal, *danke schön*. To Prof. Bruckner, *kösönöm*.

I would also like to thank NanoSonic for providing sponsorship for part of my graduate school education.

Additionally, I would like to thank Mr. Richard J. Schwartz of NASA Langley Research Center for the guidance and mentorship he provided during the summer between my first and second years of graduate study, and for giving me an opportunity to experience the engineering profession outside the realm of academia in the form of a summer internship at Langley. May your Italian MR2 always be filled with 93 octane.

Fellow University of Washington graduate students I would like to thank include Jake Boening, for teaching me all of the fundamentals of the SWR lab and how to operate it, and Eric Wheeler, for providing sanity checks on my work as well as unceasing encouragement.

Lastly, I would like to thank my family and many friends who provided me with support

and encouragement while I confronted the trials and challenges of pursuing a master's degree. Friends who deserve special thanks include Curtis, Nico, Basil, Dr. Mary Alice, and Col. Tom. Family members who deserve special thanks include my sisters Stephanie and Olivia; my Aunt Darlene, who has graciously allowed me to live with her as I begin my new career at NASA Glenn Research Center; and, most of all, my parents, Barb and Jerry Drabiak.

DEDICATION

to my parents, Barb and Jerry Drabiak, without whose unending love and support none of this would have been possible.

Chapter 1

INTRODUCTION

The Shock Wave Reactor laboratory, or SWR, at the University of Washington is a high enthalpy flow facility, and is capable of a wide range of test conditions. Examples of projects that have been conducted in the SWR include extraction of hydrogen from hydrocarbons; a rotating detonation engine, or RDE; and experiments involving downstream injection of additional feedstock mass flow. However, never before has the complete scope of these test conditions been modeled. In order to better inform those who might seek to employ the services of the SWR to run their experiments, an analytical modeling package written using the MATLAB software has been prepared.

In particular, the primary goal in preparing the model was to be able to predict the flow properties, including the transport properties, inside of a 4" diameter test section in the SWR. The freestream flow is typically some combination of steam and H_2(g) and O_2(g), and the feedstock is typically N_2(g). Feedstock, such as N_2, is injected with the goal of lowering the stagnation temperature, raising the stagnation pressure, and raising the Mach number. The steam in the freestream comes from a pebble bed heater, which can raise the temperatures of the steam up to about 1400 K. Additional H_2(g) and O_2(g) can be injected at room temperature. When injected, the H_2(g) and O_2(g) combust, producing more steam and raising the adiabatic flame temperature in the combustor to as high as 3300 K. For the purposes of this study, the H_2(g) and O_2(g) are assumed to react completely, with pure steam as the products of the stoichiometric reaction.

A butterfly valve downstream of the test section can be used to vary the position of a shockwave in the SWR. The shockwave can be placed in the diverging section of the nozzle, a 3" diameter feedstock injector section, or the 4" diameter mixer section, all of which would

produce subsonic flow in the test section. The shock can also be placed downstream of the test section, which would allow for supersonic flow in the test section. Depending on flow conditions, supersonic Mach numbers can be as high as Mach 2.5 for the 3" diameter section and Mach 3 for the 4" diameter section.

One of the biggest issues with the SWR facility is acquiring measurements. The walls of the SWR are solid steel and are completely opaque, prohibiting visual observations. Due to the high temperatures of the flow, only Type C thermocouples, made out of mixtures of tungsten and rhenium, can be used to record the temperatures in or near the test section, which is typically around 2300 K. However, the Type C thermocouples burn out in oxidizing flow; thus, frequent spot-welding to repair the thermocouples is necessary. The high temperatures also make acquiring pressure measurements in the test section difficult; pitot probes were used to measure the pressure but, like the thermocouples, frequently melted and needed to be repaired. PCBs and pressure transducers were used for pressure measurements upstream of the test section.

Another issue with the SWR facility is the fact that the vacuum pump can only reach pressures as low as about 3 kPa. This is due to the saturation temperature of the water vapor inside being about room temperature at about 3 kPa, meaning that some of the water vapor inside begins to liquefy at that point.

Chapter 2

THEORETICAL BACKGROUND

2.1 Isentropic, Adiabatic Calculations

Despite the name of the facility, the structure of shock waves is not considered in the modeling used. Furthermore, one-dimensional, axisymmetric, isentropic flow is assumed to occur and is used as the basis for later, more rigorous modeling, which is also part of the current study. As such, the conventional isentropic equations, shown below, are used:

$$p = p_0(1 + \frac{\gamma - 1}{2}M^2)^{\frac{\gamma}{\gamma-1}} \tag{2.1}$$

$$T = T_0(1 + \frac{\gamma - 1}{2}M^2) \tag{2.2}$$

$$\frac{A}{A*} = \sqrt{\frac{1}{M^2}[\frac{2}{\gamma+1}(1 + \frac{\gamma-1}{2}M^2)]^{\frac{(\gamma+1)}{(\gamma-1)}}} \tag{2.3}$$

Equations (2.1) and (2.2) can be found in Ref. [1], and Eq. (2.3) can be found in Ref. [2] Note that in Eq. (2.3), the relation for Mach number is a function of the specific heat ratio γ and area ratio, exclusively. Furthermore, Eq. (2.3) is only valid under adiabatic, isentropic, one-dimensional, steady-state flow.

The model used in the current study is designed such that the user is expected to define the freestream conditions, including the properties of the incoming gas. The user also has

the opportunity to modify the geometry and thus the area ratio. The stagnation values for temperature and pressure are calculated from the user-defined freestream conditions using Eqs. (2.1) and (2.2). An iterative process is then used to calculate the isentropic Mach number using Eq. (2.3), in which the area ratio is taken from the user-defined geometry. Eqs. (2.1) and (2.2) are used again to calculate the static values for temperature and pressure at all points downstream of the inlet, under the assumption that the stagnation values for temperature and pressure remain constant and using the Mach numbers given by Eq. (2.3).

Unless stated otherwise, the following Reynolds number is used throughout the analysis, most notably to determine the friction factor and Nusselt number:

$$Re = \frac{\rho u D}{\mu} \tag{2.4}$$

where D is the diameter of the duct at a given point, μ is the viscosity of the flow, ρ is the local freestream density, and u is the local freestream velocity. The viscosity μ is calculated from CEA and is assumed to be constant for a given gas composition. Chemical reactions are assumed to be frozen. The density ρ is calculated according to the ideal gas law:

$$\rho = \frac{p}{RT} \tag{2.5}$$

Moreover, the velocity u is calculated according to the definition of Mach number:

$$u = aM \tag{2.6}$$

It is worth noting that the values on the right hand side of both Eqs. (2.5) and (2.6) are the values obtained from the adiabatic, isentropic calculations. This is worth noting because the Reynolds number is derived from adiabatic, isentropic values is the same Reynolds num-

ber that is used for calculating the friction factor and Nusselt number. Applying the friction factor and Nusselt number to the analysis would change velocity u and density ρ, among other variables, and thus the Reynolds number. Thus, this approach is not perfectly accurate. However, this approach does give a close enough approximation for current modeling purposes.

2.2 Heat Flux between Fluid and Walls

For the calculation of the specific heat flux to the walls, more rigorous calculations were necessary. The Chemical Equilibrium with Applications program, or CEA, was identified early on as a potential aid for the modeling efforts. A version of CEA compatible with MATLAB, known as CEAM, is available, and this is the version of CEA used in the model.

In order to compute transport properties, which are then used to calculate the convective heat transfer coefficient, the "hp" case of CEAM, in which the specific enthalpy and the pressure are held constant, is used to calculate the properties of the freestream fluid mixture at the entrance of the combustor, including calculating the results of combustion, if H_2(g) and O_2(g) have been added. Values that were calculated using CEAM included adiabatic flame temperature, T_{ad}; speed of sound, a; specific heat at constant pressure, c_p; conductive heat transfer coefficient, k; Prandtl number, Pr; the ratio of specific heats, γ; the molecular weight, $\mathfrak{M}$; and the dynamic viscosity, μ.

It was understood prior to this project that the SWR experienced a streamwise stagnation temperature loss of approximately 100 K per meter. However, a more rigorous modeling of the stagnation temperature losses was desired. To calculate this, the heat transfer needed to be calculated.

Two different sets of empirically-derived relations were used to determine the value of the convective heat transfer coefficient, depending on the section's geometry.

For all regions of the flow except the contraction section of the throat, the Petukhov equation for friction factor and the Gnielinski equation for Nusselt number were used, both of which can be found in Ref. [3].

The following value of Petukhov friction factor is valid for Reynolds numbers of $3000 < Re < 5 * 10^6$:

$$f = (0.79\log(Re) - 1.64)^{-2} \tag{2.7}$$

The following Gnielinski equation is valid for Reynolds numbers of $10^4 < Re < 5 * 10^6$ and Prandtl numbers of $0.5 < Pr < 2000$:

$$Nu = \frac{(f/8)(Re - 1000)Pr}{1 + 12.7(f/8)^{1/2}(Pr^{2/3} - 1)} \tag{2.8}$$

In the contraction section of the throat, the geometry was known to be similar to a quarter circle, and was thus approximated as a perfect quarter circle for the purposes of the current study. It was decided that the Bartz equation, shown in Eq. (2.9), was better suited for a case with curved wall geometry than the Gnielinski and Petukhov relations.

The following expression for the Bartz equation can be found in Ref [8]:

$$h_c = \frac{0.026}{D^{0.2}}(\frac{c_p\mu^{0.2}}{Pr^{0.6}})(\rho u)^{0.8}(\frac{\rho_{am}}{\rho})(\frac{\mu_{am}}{\mu_0})^{0.2} \tag{2.9}$$

In the expression for the Bartz equation given in Eq. (2.9), D is the inner diameter of the duct, a subscript "am" denotes the properties calculated at a temperature that is an arithmetic mean of the local freestream temperature and the wall temperature. The subscript zero indicates stagnation conditions.

It is worth noting that use of the Bartz equation in the subsonic region of the throat produced values of Mach number and stagnation temperature that agreed well with the Petukhov and Gnielinski version of the analysis.

For all sections other than the contraction area of the nozzle, the definition of Nusselt

number, Nu, was used to calculate the value of the convective heat transfer coefficient, h_c:

$$Nu = \frac{h_c L}{k} \tag{2.10}$$

which becomes

$$h_c = \frac{(Nu)k}{L} \tag{2.11}$$

Using a user-defined temperature for the wall, the model then calculates the rate of heat flux into the walls due to convection using the following equation, derived from Ref. [3]:

$$\frac{\dot{Q}}{A} = h_c(T_s - T_\infty) \tag{2.12}$$

It is useful to define a rate of heat flux term, Q_f, as follows:

$$\dot{Q}_f = \frac{\dot{Q}}{A} \tag{2.13}$$

Note that $\dot{Q}_f$ has units of W/m^2. By dividing Eq. (2.12) by mass flow rate, one arrives at an equation for specific heat flux into the walls due to convection:

$$q_f = \frac{\dot{Q}_f}{\dot{m}} \tag{2.14}$$

Note that q_f has units of J/(kg*m^2). By multiplying the specific heat flux given in Eq. (2.14) by area, one arrives at the specific heat transfer q:

$$q = q_f A \tag{2.15}$$

Thus, by Eq. (2.15), it is possible to determine the specific heat transfer from the fluid to the walls.

2.2.1 Steady, 1-D, Compressible Flow Equations

Knowing the specific heat transfer, and assuming that c_p is constant, the stagnation temperature can then be calculated using the following relationship:

$$dT_0 = \frac{\delta q}{c_p} \tag{2.16}$$

In discrete form, Eq. (2.16) becomes

$$T_{0,i} = T_{0,i-1} + \frac{q_{i-1}}{c_p} \tag{2.17}$$

In Eq. (2.17), the subscript i denotes a particular point in an iterative process that begins at the inlet and proceeds downstream.

With the change in stagnation temperature acquired, it is now possible to acquire a change in Mach number using the following relationship, which can be found in Ref. [5]:

$$\frac{dM^2}{M^2} = \frac{(1 + \frac{\gamma-1}{2}M^2)}{1 - M^2}(-2\frac{dA}{A} + (1 + \gamma M^2)\frac{dT_0}{T_0} + \gamma M^2 \frac{f dx}{D}) \tag{2.18}$$

Assuming dx is constant, Eq. (2.18) can be discretized as

$$M_i = \sqrt{M_{i-1}^2(1 + \frac{(1 + \frac{\gamma-1}{2}M_{i-1}^2)}{1 - M_{i-1}^2}(-2\frac{dA_{i-1}}{A_{i-1}} + (1 + \gamma M_{i-1}^2)\frac{dT_{0,i-1}}{T_{0,i-1}} + \gamma M_{i-1}^2\frac{f_{i-1}dx}{D_{i-1}}))} \quad (2.19)$$

With the Mach number known, the stagnation pressure can be calculated from the following relationship, also found in Ref. [5]:

$$\frac{dP_0}{P_0} = -\frac{\gamma M^2}{2}(\frac{dT_0}{T_0} + \frac{f dx}{D}) \quad (2.20)$$

In discretized form, Eq. (2.20) becomes

$$P_{0,i} = P_{0,i-1}(1 - \frac{\gamma M_{i-1}^2}{2}(\frac{dT_{0,i-1}}{T_{0,i-1}} + \frac{f_{i-1}dx}{D_{i-1}})) \quad (2.21)$$

2.3 Mixing of Freestream with Injectant

The mixing of the injectant with the freestream was assumed to be instantaneous and complete. Additionally, the effects of momentum loss due to the sidewall injection of the fluid into the freestream were ignored. The injector nozzles were angled relative to the freestream, four at angles of 60° and and four at angles of 30°. Only the components of momentum that were parallel to the freestream were considered.

The notation used for the mixing process is shown in Fig. (2.1). The properties with a subscript b represent the injectant, the properties with a subscript a represent the freestream fluid, and the properties with a subscript 7 represent the mixed fluid.

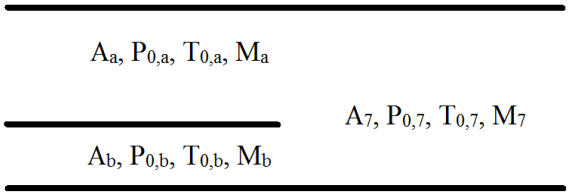

Figure 2.1: Mixing Notation

It was desired to determine the flow properties of the mixed fluid, including, but not limited to, Mach number, pressure, temperature, and transport properties such as viscosity. The laws of conservation of mass, momentum, and energy were used as a starting point from which relations for the properties of the mixed fluid could be determined based on the known properties of the freestream and the injectant fluids.

$$\dot{m}_a + \dot{m}_b = \dot{m}_7 \tag{2.22}$$

Eq. (2.22) gives the mass conservation. Furthermore, it is helpful to define a mass flow rate fraction α such that

$$\alpha = \frac{\dot{m}_b}{\dot{m}_a} \tag{2.23}$$

Eq. (2.23) allows us to re-write $\dot{m}_b$ in terms of $\dot{m}_a$ by saying that $\dot{m}_b = \alpha \dot{m}_a$. By substituting this into the mass conservation, we can also re-write $\dot{m}_7$ in terms of $\dot{m}_a$, as follows:

$$\dot{m}_7 = (1 + \alpha)\dot{m}_a \tag{2.24}$$

Keeping in mind the mass flow rate relationships given in Eqs. (2.24), the conservation of energy given in the form of a balance of enthalpy and kinetic energy is as follows:

$$\dot{m}_7(h_7 + \frac{u_7^2}{2}) = \dot{m}_b(h_b + \frac{u_b^2}{2}) + \dot{m}_a(h_a + \frac{u_a^2}{2}) \tag{2.25}$$

Using the definition of enthalpy,

$$h = c_p T \tag{2.26}$$

one can re-write Eq. (2.25) as

$$\dot{m}_7(c_{p,7}T_7 + \frac{u_7^2}{2}) = \dot{m}_b(c_{p,b}T_b + \frac{u_b^2}{2}) + \dot{m}_a(c_{p,a}T_a + \frac{u_a^2}{2}) \tag{2.27}$$

By rearranging Eq. (2.27), one can express T_7 as follows:

$$\frac{T_7}{T_a} = -\frac{u_7^2}{2c_{p,7}T_a} + \frac{\alpha}{c_{p,7}T_a(\alpha+1)}(c_{p,b}T_b + \frac{u_b^2}{2}) + \frac{1}{c_{p,7}T_a(\alpha+1)}(c_{p,a}T_a + \frac{u_a^2}{2}) \tag{2.28}$$

Eq. (2.28) is important, because it allows one to define the static temperature of the mixed fluid exclusively in terms of properties of the injectant and the freestream.

It was also desired to find the Mach number of the mixed fluid. By assuming that all fluids involved are calorically perfect gases, the following definition for mass flow rate, found in Ref. [6], can be used:

$$\dot{m} = pA\sqrt{\frac{\gamma}{R}}\frac{1}{\sqrt{T_0}}M(1 + \frac{\gamma-1}{2}M^2)^{1/2} \tag{2.29}$$

Additionally, if wall friction is neglected, the conservation of momentum can be written as the following equation, found in Ref. [7]:

$$p_b A_b(1+\gamma_b M_b^2) + p_a A_a(1+\gamma_a M_a^2) = p_7 A_7(1+\gamma_7 M_7^2) \tag{2.30}$$

By redefining Eq. (2.29) in terms of pA, as follows,

$$pA = \dot{m}\sqrt{\frac{R}{\gamma}}\sqrt{T_0}\frac{1}{M}(1+\frac{\gamma-1}{2}M^2)^{-1/2} \tag{2.31}$$

and then combining Eqs. (2.30) and (2.31), and assuming that flow is uniform at all stations, one can then derive an equation for the mixed Mach number:

$$\begin{aligned}
&\dot{m}_7\sqrt{\frac{R_7}{\gamma_7}}\sqrt{T_{0,7}}\frac{1}{M_7}(1+\frac{\gamma_7-1}{2}M_7^2)^{-1/2}(1+\gamma_7 M_7^2) \\
&= \dot{m}_b\sqrt{\frac{R_b}{\gamma_b}}\sqrt{T_{0,b}}\frac{1}{M_b}(1+\frac{\gamma_b-1}{2}M_b^2)^{-1/2}(1+\gamma_b M_b^2) \\
&+ \dot{m}_a\sqrt{\frac{R_a}{\gamma_a}}\sqrt{T_{0,a}}\frac{1}{M_a}(1+\frac{\gamma_a-1}{2}M_a^2)^{-1/2}(1+\gamma_a M_a^2)
\end{aligned} \tag{2.32}$$

At this stage, it becomes important to consider the angles of the injector ports. Four of the injector ports are angled at 60° relative to the freestream flow and the other four are angled at 30°. The transverse components of the velocity are ignored. The area of the injectant can be expressed as an average of the mass flow rates from the 60° ports and the 30° ports that are projected onto a plane that is perpendicular to the freestream flow direction, as follows:

$$\dot{m}_b = \frac{1}{2}\dot{m}_{b,full}\cos(30^\circ) + \frac{1}{2}\dot{m}_{b,full}\cos(60^\circ) \tag{2.33}$$

where $m_{b,full}$ is the full mass flow rate of the injectant through the original area. Equation (2.33) simplifies to

$$\dot{m}_b = \frac{1}{2}\dot{m}_{b,full}(\cos(30^\circ) + \cos(60^\circ)) \tag{2.34}$$

In order to simplify the mathematical expressions, it is helpful to define a term $f = f(M)$, found in Ref. [7] such that

$$f(M) = M^2(1 + \frac{\gamma - 1}{2}M^2)(1 + \gamma M^2)^{-2} \tag{2.35}$$

Eq. (2.35) allows Eq. (2.32) to be re-written as follows:

$$\begin{aligned}&\dot{m}_7\sqrt{\frac{R_7}{\gamma_7}}\sqrt{T_{0,7}}\frac{1}{\sqrt{f(M_7)}} \\ &= \frac{1}{2}\dot{m}_{b,full}(\cos(30^\circ) + \cos(60^\circ))\sqrt{\frac{R_b}{\gamma_b}}\sqrt{T_{0,b}}\frac{1}{\sqrt{f(M_b)}} + \dot{m}_a\sqrt{\frac{R_a}{\gamma_a}}\sqrt{T_{0,a}}\frac{1}{\sqrt{f(M_a)}}\end{aligned} \tag{2.36}$$

Eq. (2.36) can be rearranged to produce an expression in terms of $f(M_7)$, as follows:

$$f(M_7) = \frac{(\alpha + 1)^2\frac{R_7}{\gamma_7}\frac{T_{0,7}}{T_{0,a}}}{[\alpha\frac{1}{2}(\cos(30^\circ) + \cos(60^\circ))\sqrt{\frac{R_b}{\gamma_b}}\sqrt{\frac{T_{0,b}}{T_{0,a}}}\frac{1}{\sqrt{f(M_b)}} + \sqrt{\frac{R_a}{\gamma_a}}\frac{1}{\sqrt{f(M_a)}}]^2} \tag{2.37}$$

Furthermore, by re-writing $T_{0,7}$ in terms of the properties of the freestream and the

injectant, as expressed in Eq. (2.28), Eq. (2.37) becomes

$$f(M_7) = \frac{(\alpha+1)^2 \frac{R_7}{\gamma_7}(-\frac{u_7^2}{2c_{p,7}T_a} + \frac{\alpha}{c_{p,7}T_a(\alpha+1)}(c_{p,b}T_b + \frac{u_b^2}{2}) + \frac{1}{c_{p,7}T_a}(c_{p,a}T_a + \frac{u_a^2}{2}))}{[\alpha\frac{1}{2}(\cos(30°)+\cos(60°))\sqrt{\frac{R_b}{\gamma_b}}\sqrt{\frac{T_{0,b}}{T_{0,a}}}\frac{1}{\sqrt{f(M_b)}} + \sqrt{\frac{R_a}{\gamma_a}}\frac{1}{\sqrt{f(M_a)}}]^2} \tag{2.38}$$

Moreover, since the value of u_7 is expected to be unknown, one must re-write the equation even further by using the definition of Mach number,

$$u = aM \tag{2.39}$$

where a is the speed of sound.

It is at this stage that the angles of the injector ports are again considered. Four of the injector ports are angled at 60° relative to the freestream flow and the other four are angled at 30°. The transverse components of the velocity are ignored. The velocity of the injectant can be expressed as an average of the velocities from the 60° ports and the 30° ports, as follows:

$$u_b = \frac{1}{2}a_{b,30°}M_{b,30°}\cos(30°) + \frac{1}{2}a_{b,60°}M_{b,60°}\cos(60°) \tag{2.40}$$

Noting that speed of sound a and Mach number M are the same for all injector ports, regardless of angle, Eq. (2.40) becomes

$$u_b = \frac{1}{2}a_b M_b(\cos(30°)+\cos(60°)) \tag{2.41}$$

Thus, Eq. (2.38) becomes

$$f(M_7) = \frac{(\alpha+1)^2 \frac{R_7}{\gamma_7}}{[\alpha\frac{1}{2}(\cos(30°)+\cos(60°))\sqrt{\frac{R_b}{\gamma_b}}\sqrt{\frac{T_{0,b}}{T_{0,a}}}\frac{1}{\sqrt{f(M_b)}} + \sqrt{\frac{R_a}{\gamma_a}}\frac{1}{f(M_a)}]^2}(-\frac{(a_7 M_7)^2}{2c_{p,7}T_a}$$
$$+ \frac{\alpha}{c_{p,7}T_a(\alpha+1)}(c_{p,b}T_b + \frac{(\frac{1}{2}a_b M_b(\cos(30°)+\cos(60°)))^2}{2})$$
$$+ \frac{1}{c_{p,7}T_a}(c_{p,a}T_a + \frac{(a_a M_a)^2}{2})) \tag{2.42}$$

where

$$f(M_7) = M_7^2(1 + \frac{\gamma_7 - 1}{2}M_7^2)(1+\gamma_7 M_7^2)^{-2} \tag{2.43}$$

Eq. (2.43) is a quadratic expression for M_7, and can be rearranged into the following, given in Ref. [7]:

$$M_7^2 = \frac{2f(M_7)}{1 - 2\gamma_7 f(M_7) \pm \sqrt{1 - 2(\gamma_7+1)f(M_7)}} \tag{2.44}$$

where the + sign is used in the case of subsonic flow and the - sign is used in the case of supersonic flow, as described in Ref. [6]. Unfortunately, there is a slight problem the formula contained in Eqs. (2.42) through (2.39), and that is that, as a result of accounting for the change in kinetic energy, the Mach number for the mixed fluid appears in the definition of both variants of $f(M_7)$. This means that the equation would be very difficult or even impossible to solve analytically. Therefore, the fzero function in MATLAB was used to find M_7 using the value of M_a as the initial guess, since it is assumed that M_7 will be close to M_a.

Furthermore, by combining Eqs. (2.31) and (2.28), it can be easily shown that

$$\frac{p_{0,7}}{p_{0,a}} = (1+\alpha)\frac{M_a}{M_7}\sqrt{\frac{T_{0,7}R_7\gamma_a}{T_{0,a}R_a\gamma_7}}\frac{(1+\frac{\gamma_7-1}{2}M_7^2)^{\frac{\gamma_7+1}{2(\gamma_7-1)}}}{(1+\frac{\gamma_a-1}{2}M_a^2)^{\frac{\gamma_a+1}{2(\gamma_a-1)}}} \tag{2.45}$$

Eq. (2.45) was used for calculating the stagnation pressure of the mixed fluid immediately prior to mixing. However, unlike Eq. (2.42), Eq. (2.45) was derived without considering the angles of the injector ports.

2.4 Normal Shocks

In cases in which a normal shock was considered, the following relations, found in Ref. [1], were used:

$$M_2^2 = \frac{1+\frac{\gamma-1}{2}M_1^2}{\gamma M_1^2 - \frac{\gamma-1}{2}} \tag{2.46}$$

Eq. (2.46) was used to find the Mach number after the shock, M_2, based on the Mach number just before the shock, M_1, assuming a constant γ. Static temperature was calculated using Eq. (2.47), shown below:

$$\frac{T_2}{T_1} = [1+\frac{2\gamma}{\gamma+1}(M_1^2-1)]\frac{2+(\gamma-1)M_1^2}{(\gamma+1)M_1^2} \tag{2.47}$$

Static pressure change across the shock was calculated using Eq. (2.48)

$$\frac{p_2}{p_1} = 1+\frac{2\gamma}{\gamma+1}(M_1^2-1) \tag{2.48}$$

2.5 A Sample Case: Heat Transfer into a Test Article

2.5.1 Description of Problem

As stated above, the SWR lab is capable of a wide range of test functions and experiments. One such experiment, which has been conducted, was to calculate the heat transfer into a test article placed in the test section. The test articles in question were stainless steel cylinders approximately 0.5" in diameter and 4" in length. The test objects were exposed to two different types of freestream flows. In the first case, the freestream flow consisted of a mixture of steam from the pebble bed heater and steam resulting from the combustion of H_2 and O_2 in the combustor section. The second case was the same, except that no pebble bed steam was used. During the course of these experiments, the combustor section was changed from a tubular deflagration combustion chamber to an annular combustion chamber that could operate in both deflagration mode, to produce subsonic exhaust flow, or in rotating detonation mode, to produce supersonic exhaust. No injection of N_2 feedstock was used for these experiments. For these tests the range of flow conditions used included velocities from 200 to 600 m/s, corresponding to Mach numbers of about 0.2 to about 0.4, and temperatures from 800 °C to 2400 °C, with static pressures ranging from 0.6 bar to 1.1 bar. Cylindrical test articles supplied by a sponsor were exposed axially to the flow in the test section.

2.5.2 Methods Used

Empirically derived Nusselt number correlations for axially-oriented cylinders exposed to turbulent flow were used in combination with the experimental temperature and pressure data and calculated flow properties to find the convective heat transfer coefficient, and thence the heat transfer, of the test samples. The correlation for Nusselt number was found in Ref. [9], and is shown below:

$$Nu = C_1 Re^{C_2} \tag{2.49}$$

where C_1 and C_2 are empirically-derived constants that differ for different parts of the geometry. For the upstream face of the cylinder, the values are $C_1 = 0.662$ and $C_2 = 0.534$. For the side of the cylinder, the values are $C_1 = 0.14$ and $C_2 = 0.686$. For the downstream face of the cylinder, the values are $C_1 = 0.14$ and $C_2 = 0.623$. Wiberg and Lior give three different sets of values for C_1 and C_2, but it is the second of their three cases, which they call case (B), that matches the conditions of the current study most closely. Furthermore, for the current study, only the side of the cylinder was considered.

In order to find the Reynolds number, Re, values for density and velocity were necessary. The definition of Reynolds number is

$$Re = \frac{\rho u L}{\mu} \tag{2.50}$$

where L is some characteristic length. In this case, the characteristic length used was the diameter of the cylindrical test article. The density ρ, velocity u, and viscosity μ are all the values of the freestream flow.

The velocity of the freestream was calculated according to the following equation:

$$u = \frac{\dot{m}_\infty R T_\infty}{P_\infty A_{TS}} \tag{2.51}$$

where the freestream values are all either empirically derived or assumed, and the test section cross sectional area is calculated from the measured radius.

Once the Nusselt number was derived, Eq. (2.11) was used to calculate the convective heat transfer coefficient. The convective heat transfer coefficient was then used to calculate the final temperature of the cylinder using a lumped system analysis, found in Ref. [4], as shown below:

$$\frac{T(t) - T_\infty}{T_i - T_\infty} = e^{-bt} \tag{2.52}$$

where

$$b = \frac{h_c A_s}{\rho V c_p} \tag{2.53}$$

Eq. (2.53) gives the value of a time constant, b, for which the dimensions are 1/s. Furthermore, ρ, V, and c_p refer to the properties of the test article, T_i refers to the initial temperature of the test article, and A_s refers to the surface area being considered. In this case, A_s was equal to the surface area of the side of the cylinder. Eq. (2.52) can be rearranged to give the final temperature $T(t)$ after time t, as follows:

$$T(t) = T_\infty + (T_i - T_\infty)e^{-bt} \tag{2.54}$$

Using the value for final temperature after time t found using Eq. (2.54), the total heat transfer Q into the test article after time t was then found using the following equation:

$$Q = mc_p[T(t) - T_i] \tag{2.55}$$

where the values for m and c_p correspond to the values for the test article. The mass was derived by multiplying the density ρ by the volume V.

Chapter 3

EXPERIMENTAL APPARATUS

3.1 Description of the SWR Capabilities

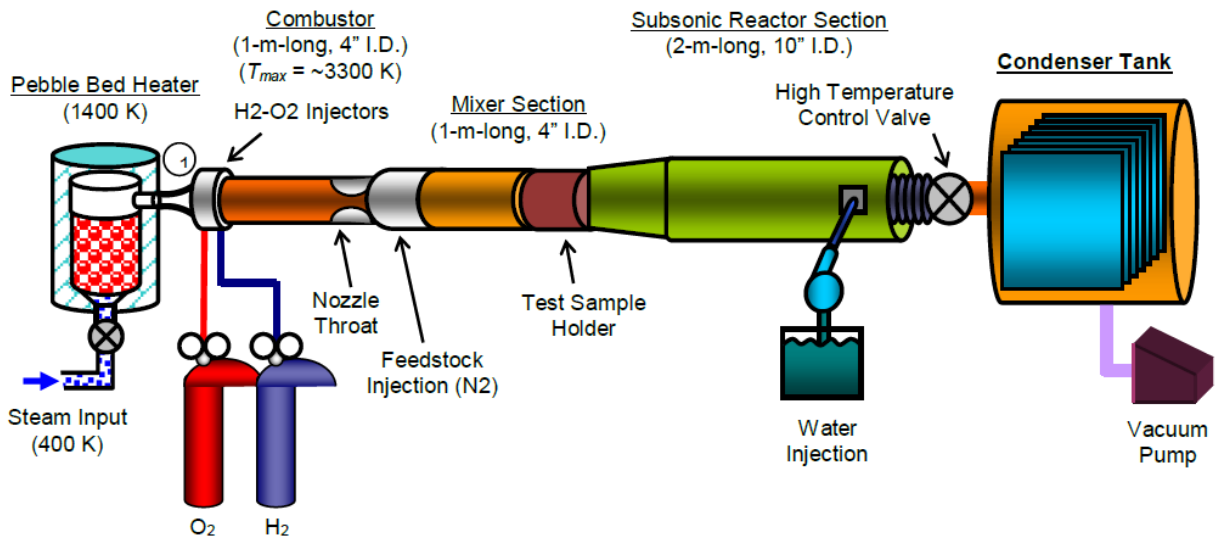

Figure 3.1: SWR Setup

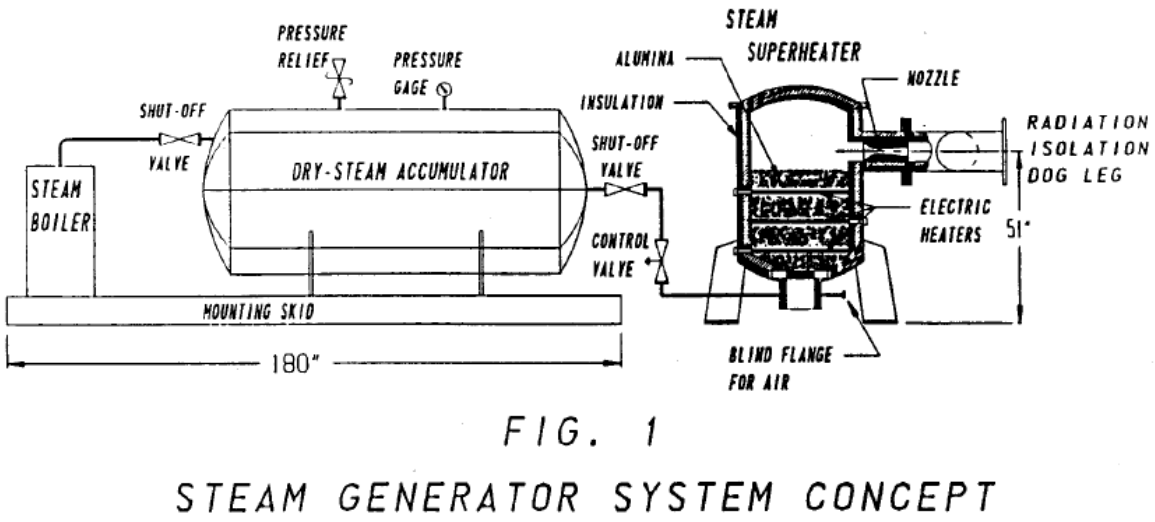

Figure 3.2: Steam Generator

Steam is the main working fluid of the SWR facility, and the steam is heated up to a maximum of approximately 1100 °C, or 1370 K, with an electrically-heated pebble bed heater, or can be produced as a result of combustion of H_2 and O_2 in the combustor or as part of a rotating detonation engine, or RDE. Furthermore, it is possible to insert additional H_2 and O_2 at room temperature (298 K). Without water cooling, the combustor can run for as long as 4 seconds, and mass flow rates as high as 0.4 kg/s are possible, though that maximum mass flow rate varies with the nature of the experiment. The mass flow in the combustor can consist of either pure steam or some mixture of steam and H_2(g) or O_2(g), depending on the equivalence ratio ϕ of the experiment. The equivalence ratio is given as

$$\phi = \frac{OF_{st}}{OF} \tag{3.1}$$

where

$$OF = \frac{\dot{m}_{oxidizer}}{\dot{m}_{fuel}} \tag{3.2}$$

and OF_{st} is the stoichiometric OF ratio, which is the OF ratio for a perfectly balanced chemical reaction. For example, for the combustion of H_2(g) with O_2(g), $OF_{st} = 8$.

Due to the limitations imposed by the pressure rating of the pebble bed heater, the maximum pressure at which one can operate the combustion chamber is approximately 4.5 bar. A butterfly valve with a diameter of 0.15 m is used to position the normal shock wave at almost any desired position in the flow channels; for the purposes of the current study, when subsonic flow was desired in the test section, a normal shock was assumed to take place either midway through the feedstock injector section or midway through the mixer section. At the end of the test apparatus is a dump tank with a volume of approximately 5 m^3, which contains approximately 500 kg of aluminum plates and maintains the pressure gradient necessary for steady-state operation by condensing the steam flow.

Figure (3.1) shows a detailed schematic of the SWR facility. In Fig. (3.1), the flow moves from left to right. At the far left end of Fig. (3.1) is the pebble bed heater. Immediately to the right of the pebble bed heater are the H_2 and O_2 injector ports. The combustor lies to the right of the H_2 and O_2 injector ports. At the exit of the combustor is a nozzle throat. To the right of the throat is a feedstock injection section, where the N_2 is injected, to the right of which lies the mixer section. Feedstock N_2 is injected with the goal of lowering the stagnation temperature, raising the stagnation pressure, and raising the Mach number. Immediately downstream of the mixer section lies the test sample holder.

These sections are of interest because the test section is the area being modeled in the current study, and the flow must pass through the mixer, throat, feedstock injector, and mixing section in order to reach the test section. Although it is not noted in Fig. (3.1), the inner radius of the feedstock injector is approximately 0.0381 m.

The flow enters the combustor 1 m prior to entering a converging-diverging nozzle. At the narrowest point of the nozzle is a throat with a diameter of 0.0397 m. The intended design capability was to accelerate steam to supersonic velocities with Mach numbers as high as 2.8. After exiting the nozzle, the flow enters a feedstock injection section section that is 0.0381 m in radius. Note that not all cases considered in this study incorporated feedstock injection. After leaving the feedstock injection chamber, the steam or other mixed fluid enters a mixer section with a radius of 0.0508 m. At the end of the mixer section is the test section in which test samples can be placed on a sting mount. Type C thermocouples placed just upstream of the test section, which in the results covered in this study were capable of recording temperatures as high as approximately 2600 °C. To measure pressure, pressure transducers were stood off from the test section using short tubes, which heated continuously in order to prevent effects from condensation on the measurements. Furthermore, PID-controlled external heat tapes were used to maintain a constant temperature on the walls of the sections including and downstream of the combustor of at least 150 °C.

Fig. (3.2) shows a schematic of the steam generator used for the experiments covered in the current study. The steam accumulator has a volume of approximately 2 m^3 and stores saturated steam at pressures up to 590 kPa, corresponding to a saturation temperature of 85 °C. Heat-taped 3" pipe routes steam through a flow regulator which isenthalpically drops pressure to set the point of the experiment, and thereby deliver dry steam to the pebble bed.

3.2 Geometry

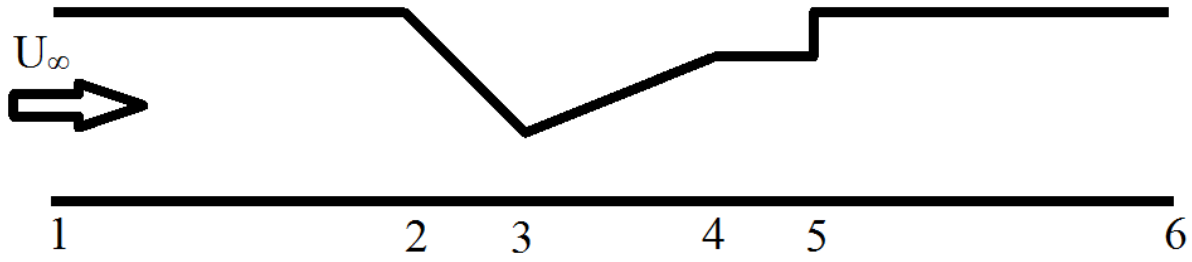

Figure 3.3: Station Notation

For the purposes of the current study, a simplified variant of the SWR geometry was considered. Fig. (3.3) shows the notation used for each of the stations in a simplified rendition of the SWR geometry. Station 1 represents the incoming freestream, as indicated by U_∞. Station 2 marks the beginning of the contraction section, leading to a throat at station 3. Choked flow with Mach number equal to 1 is assumed to occur at the throat. Station 4 marks the end of the diffuser section, in which supersonic flow is assumed to occur. Additionally, the mixing of the freestream with the injectant is assumed to occur at station 4. At station 5, the radius of the duct widens from 1.5" to 2". Though aphysical, normal shock waves are assumed to either midway between stations 4 and 5 or midway between stations 5 and 6. Station 6 represents the beginning of the test section of the SWR.

Chapter 4

METHODS AND IMPLEMENTATION

4.1 Assumptions Made

4.1.1 Nitrogen Feedstock Injection

Various assumptions were made regarding the nature of the mixing of N_2 feedstock with the freestream fluid. Firstly, the mixing was assumed to occur instantaneously and completely. Secondly, it was assumed that the components the feedstock momentum injected perpendicular to the freestream flow canceled each other out; thus, only the components of momentum injected parallel to the freestream flow were considered. However, following on the first assumption, there were assumed to be no plume interactions. This approximation is shown in Fig (2.1). Worthy of note is that the area of the injector port was not neglected; documentation from the SWR lab indicates that the injector ports had radii of 0.0970", and that there were eight of them, thus the area of the feedstock in Fig (2.1) was assumed to be the sum of the areas of the eight injector ports. Thirdly, four of the injectors were assumed to be angled at an angle of 60° relative to the freestream flow and the other four were assumed to be angled at an angle of 30° relative to the freestream flow. Finally, the feedstock was assumed to be injected at 298 K and at Mach 1.

4.1.2 Injection of Hydrogen and Oxygen into Combustor

Many of the same assumptions made for the N_2 feedstock injection were also used for the insertion of H_2 and O_2 into the combustor. First of all, the combustion of the H_2 and O_2 was assumed to be instantaneous and complete. Secondly, it was assumed that the H_2 and O_2 were inserted at a temperature of 298 K. Thirdly, it was assumed that the temperature

output from the use of the "hp" case in CEAM, in which the pressure and specific enthalpy were held constant, was the adiabatic flame temperature. Fourthly, it was assumed that although the initial pressure and the adiabatic flame temperature were stagnation values, they were close enough to the static values due to low Mach numbers that they could be used as substitutes for the static values at station 1, as indicated in Fig. (3.3).

4.1.3 Transient Heat Transfer into a Test Article

For the heat transfer calculations, various assumptions were made regarding the properties of the freestream flow and the stainless steel test article. The freestream pressure was assumed to be 80 kPa. The freestream mass flow rates varied depending on the run but ranged from approximately 90 g/s to 120 g/s. Likewise, the freestream temperatures varied depending on the run but ranged from approximately 1700 K to 2200 K. The freestream mixture's molecular mass was assumed to be that of pure steam: 18 g/mol. The viscosity of the freestream was assumed to be the viscosity of water vapor at 2000 °C, which is 0.00007808 kg/(m*s). The thermal conductivity of the steam was assumed to be the corresponding value at 2000 °C: 0.00029183 kW/(m*K).

The test article was treated as a lumped system. The initial temperature of the test article was assumed to be 45 °C. This is slightly higher than room temperature and accounts for the consideration that the test article will not have fully cooled down to room temperature between the end of one run and the start of the next. The specific heat at constant pressure of the test article was assumed to be $c_p = 0.500$ kJ/(kg*K). The density of stainless steel was assumed to be approximately 8000 kg/(m^3). Finally, only the sides of the cylinders were considered during the heat transfer calculations of this study.

4.2 Techniques Used

MATLAB was used for the majority of the calculations as well as for plotting the results. Additionally, the MATLAB version of CEA, a chemical combustion software package, was used for calculating flow properties. The model used in this study calls the "tp" and "hp"

cases of the CEAM code. In the former, temperature and pressure are among the inputs and are held constant; in the latter, pressure and specific enthalpy are the inputs and are held constant.

In order to compute transport properties, which are then used to calculate the convective heat transfer coefficient, the "hp" case was used to calculate the properties of the freestream fluid mixture at the entrance of the combustor, including calculating the results of combustion, if H_2(g) and O_2(g) have been added. Values that were calculated using CEAM included adiabatic flame temperature, T_{ad}; speed of sound, a; specific heat at constant pressure, c_p; conductive heat transfer coefficient, k; Prandtl number, Pr; the ratio of specific heats, γ; the molecular weight, $\mathfrak{M}$; and the dynamic viscosity, μ. The "hp" case was also used to calculate the same properties of the mixed fluid in cases with N_2 feedstock injection.

The "tp" case was used to calculate the arithmetic mean properties and the stagnation viscosity for the Bartz equation. The outputs procured in this case were viscosities μ_{am} and μ_0 and density, ρ_{am}.

Chapter 5

RESULTS

5.1 Study A: Case with H2, O2, Steam, and N2 Injection

Study A considers injection of additional N_2 feedstock in the feedstock injector section and is the only study considered that has this attribute. Input conditions that varied in Study A included pebble bed steam temperature; Equivalence ratio ϕ; combustor freestream temperature p_∞; mass flow rates of pebble bed steam, H_2, O_2, and N_2; and the ratio of mass flow rates α. In study A, a normal shock was assumed to occur midway through the feedstock injector section.

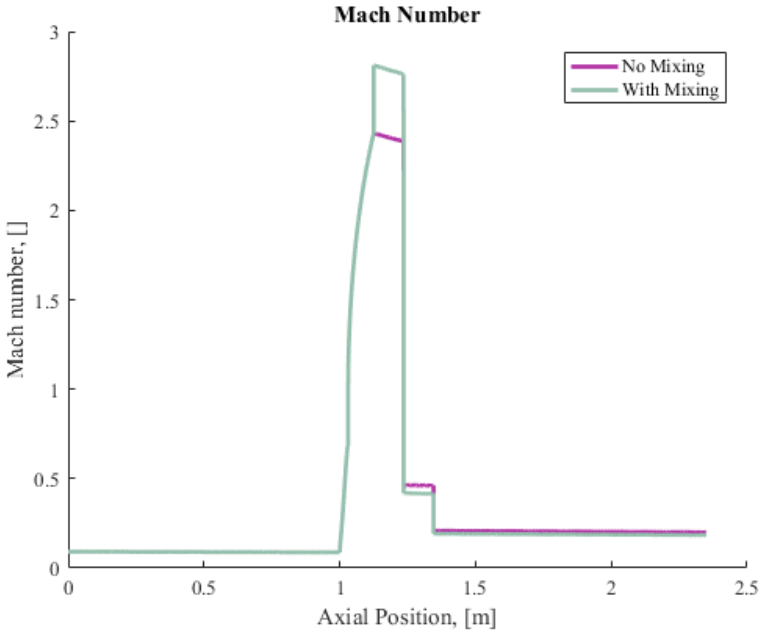

Figure 5.1: Mach number inside the SWR plotted along the streamwise, axial coordinate from the entrance of the combustor to the test section, for the same case with and without considering N_2 mixing

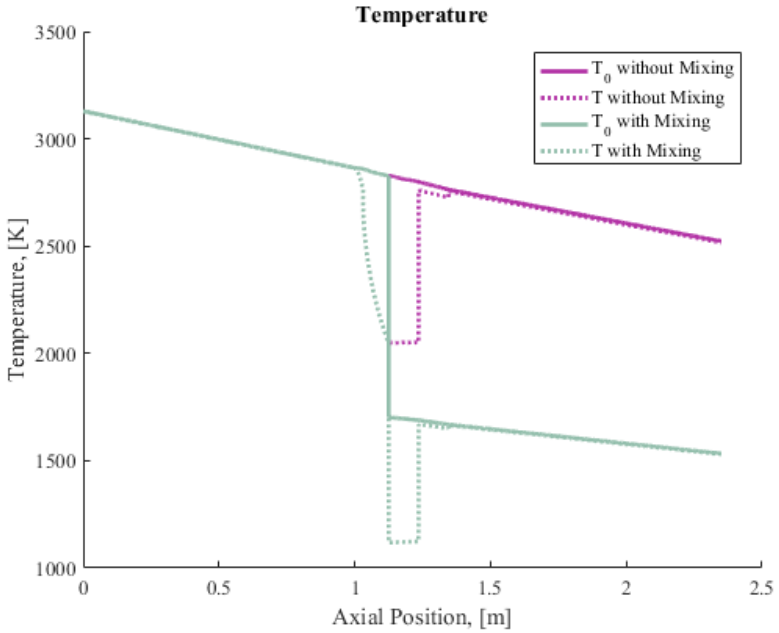

Figure 5.2: Temperature inside the SWR plotted along the streamwise, axial coordinate from the entrance of the combustor to the test section, for the same case with and without considering N_2 mixing

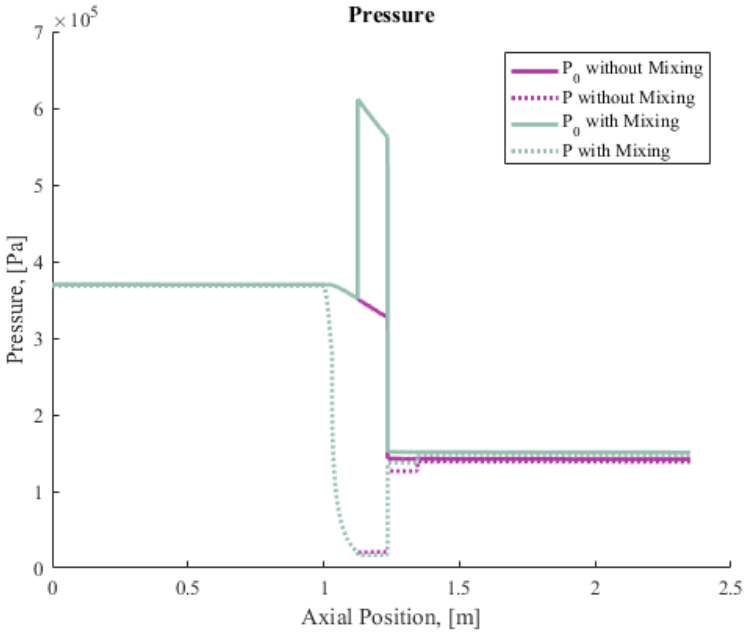

Figure 5.3: Pressure inside the SWR plotted along the streamwise, axial coordinate from the entrance of the combustor to the test section, for the same case with and without considering N_2 mixing

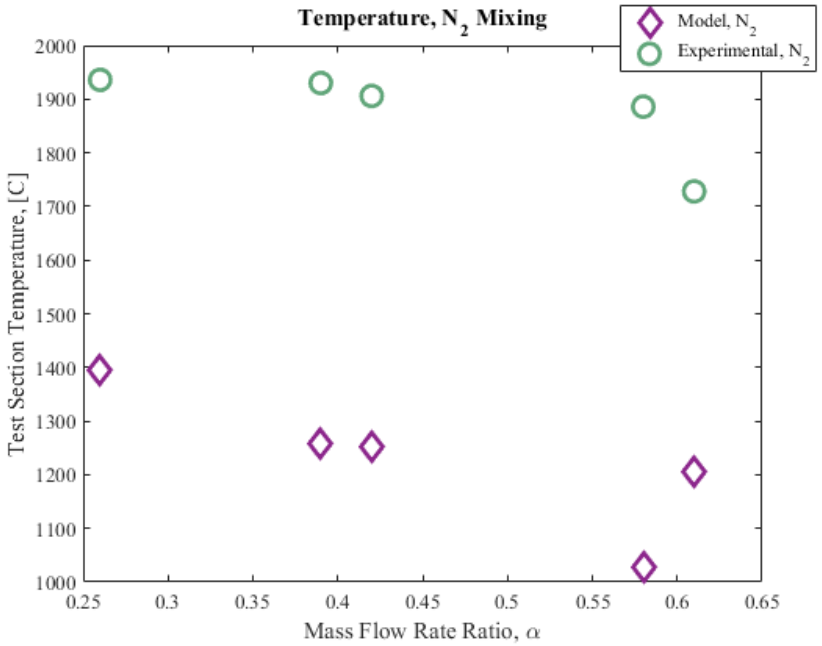

Figure 5.4: Temperature of the test section plotted against mass flow rate ratio α for cases with N_2 mixing

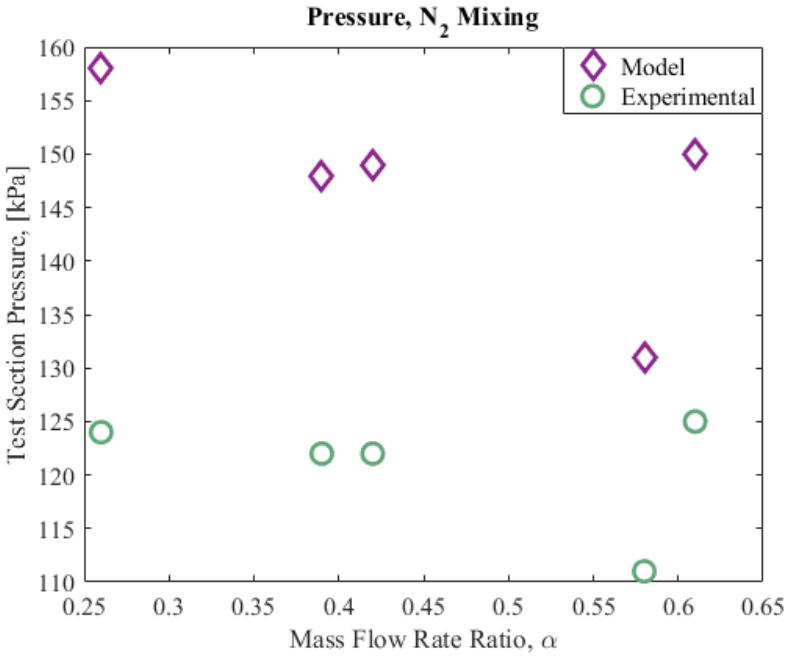

Figure 5.5: Pressure of the test section plotted against mass flow rate ratio α for cases with N_2 mixing

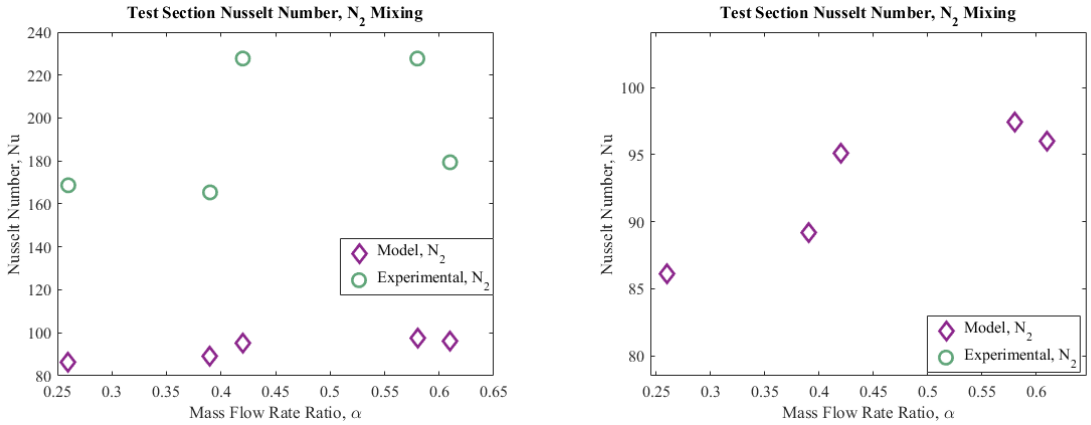

(a) Full view (b) Zoomed in

Figure 5.6: Nusselt number of the test section plotted against mass flow rate ratio α for cases with N_2 mixing

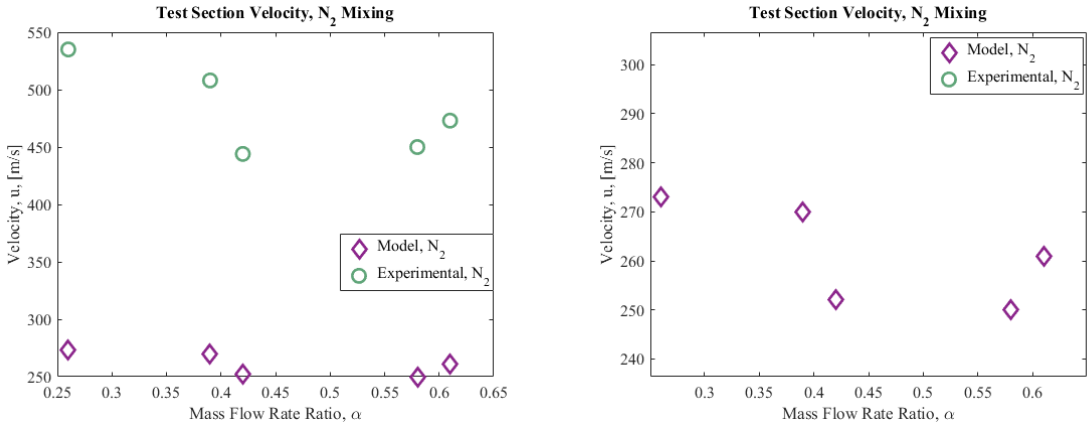

(a) Full view (b) Zoomed in

Figure 5.7: Velocity of the test section plotted against mass flow rate ratio α for cases with N_2 mixing

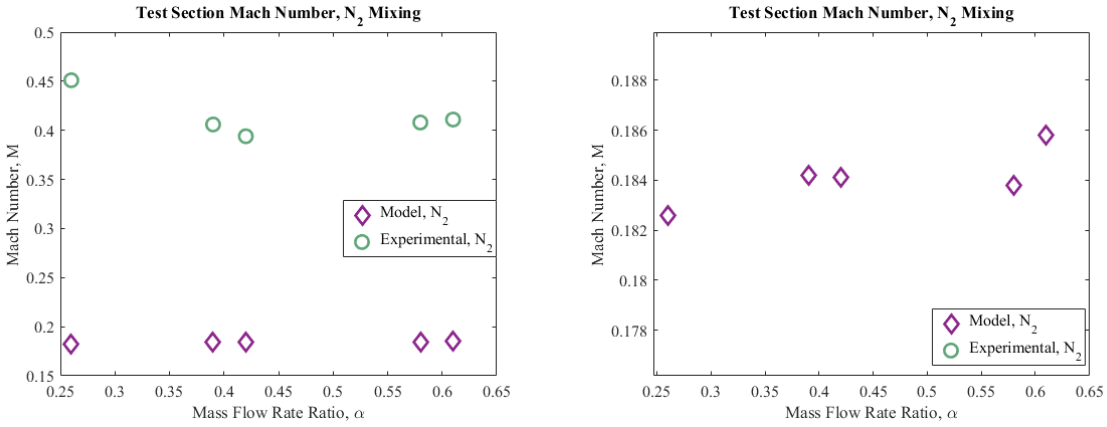

(a) Full view (b) Zoomed in

Figure 5.8: Mach number of the test section plotted against mass flow rate ratio α for cases with N_2 mixing

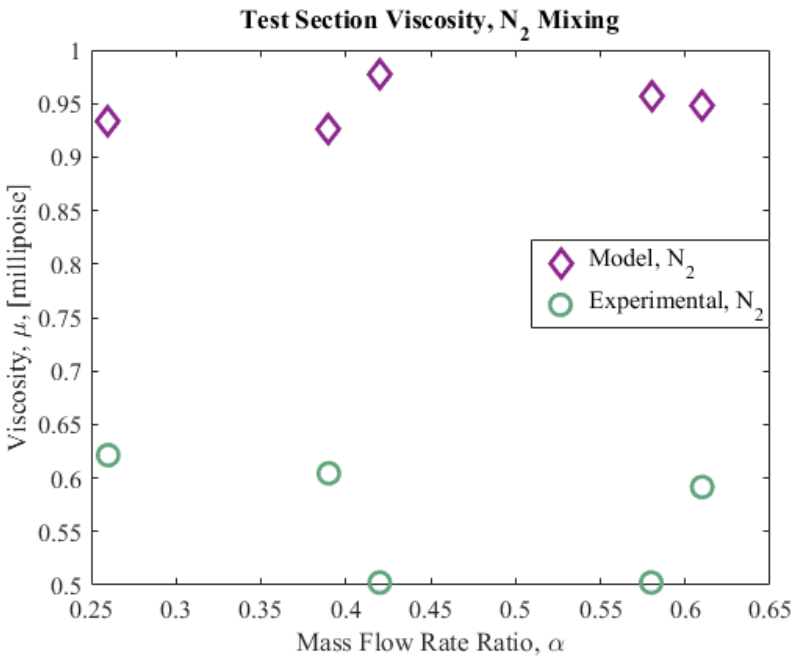

Figure 5.9: Viscosity of the test section plotted against mass flow rate ratio α for cases with N_2 mixing

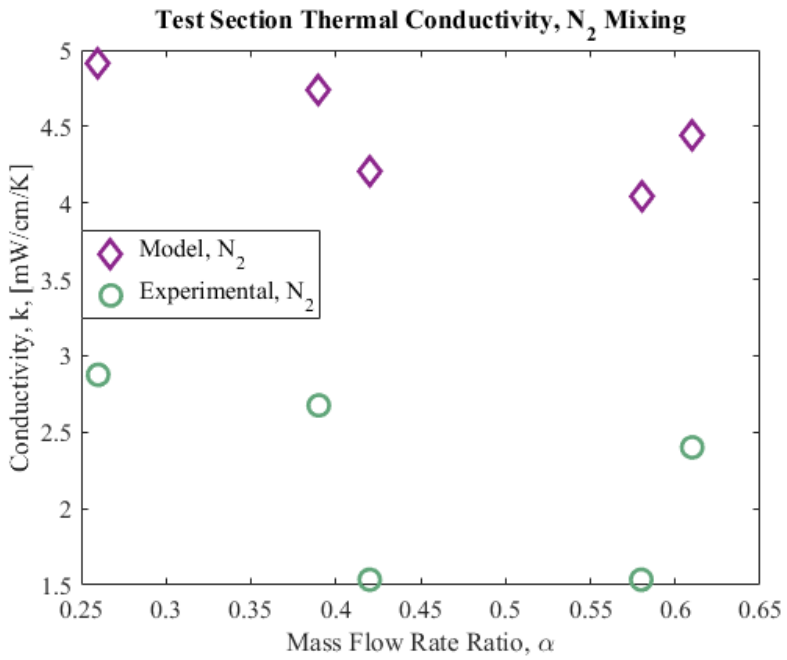

Figure 5.10: Thermal conductivity of the test section plotted against mass flow rate ratio α for cases with N_2 mixing

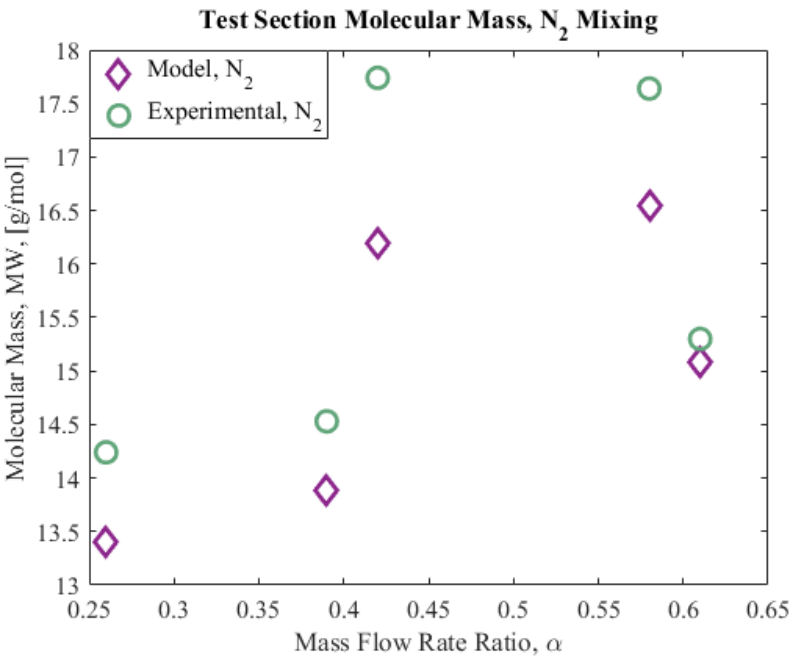

Figure 5.11: Molecular mass of the test section plotted against mass flow rate ratio α for cases with N_2 mixing

5.2 Study B: First Case with H2, O2, and Steam

In Study B, no mixing with N_2 was considered. Input conditions that were held constant include the mass flow rate of the pebble bed steam, the freestream pressure in the combustor, and the freestream temperature in the combustor. Input conditions that were varied include the mass flow rate of the H_2 and O_2 injected into the combustor and the equivalence ratio ϕ. In study B, a normal shock was assumed to occur midway through the mixer section.

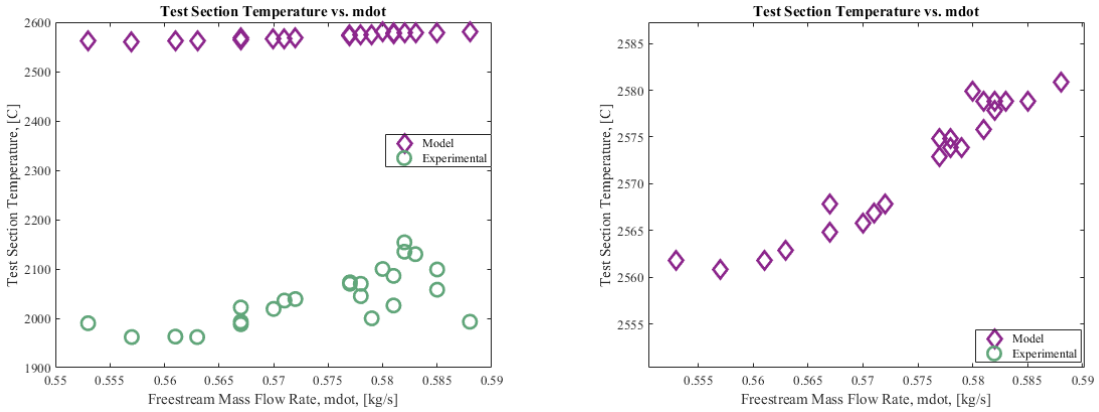

(a) Full view (b) Zoomed in

Figure 5.12: Temperature vs. $\dot{m}_\infty$

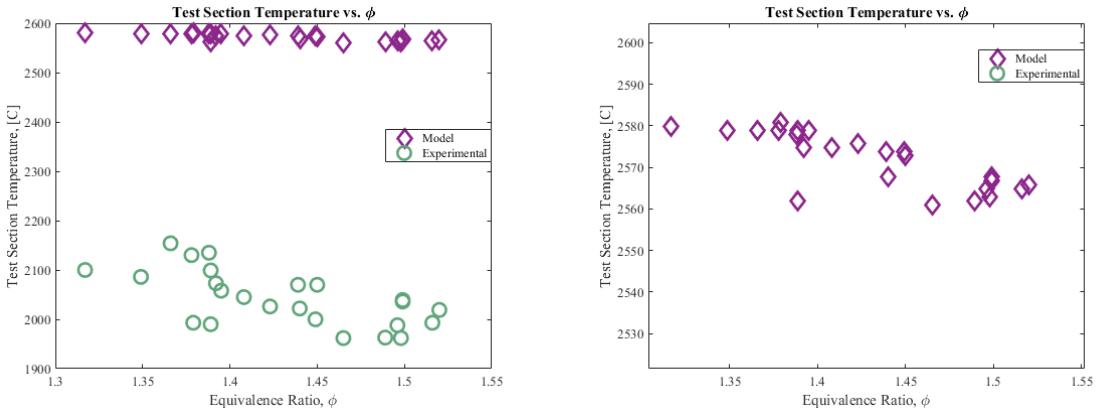

(a) Full view (b) Zoomed in

Figure 5.13: Temperature vs. ϕ

5.3 Study C: Second Case with H2, O2, and Steam

In Study C, no mixing with N_2 was considered. Input conditions that were held constant include the mass flow rate of the pebble bed steam, the mass flow rate of the H_2 and O_2 injected into the combustor, the freestream pressure in the combustor. Input conditions that

were varied include the equivalence ratio ϕ and the freestream temperature in the combustor. In study C, a normal shock was assumed to occur midway through the mixer section.

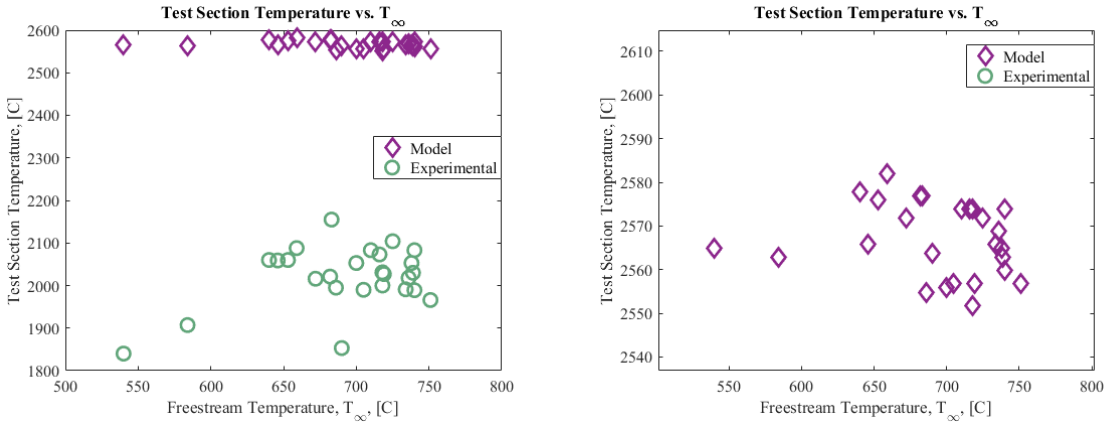

(a) Full view (b) Zoomed in

Figure 5.14: Temperature vs. T_∞

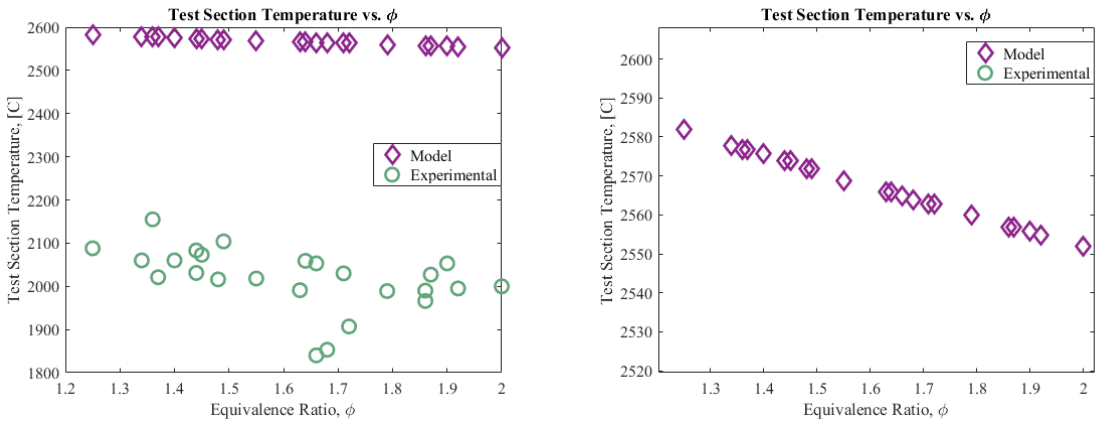

(a) Full view (b) Zoomed in

Figure 5.15: Temperature vs. ϕ

5.4 Study D: Case with H2 and O2

In Study D, no mixing with N_2 was considered. Additionally, no pebble bed steam was used; only molecular H_2 and O_2 were inserted into the combustor. Input conditions that were varied include the mass flow rate of the H_2 and O_2 injected into the combustor, the freestream pressure in the combustor, and the equivalence ratio ϕ. In study B, a normal shock was assumed to occur midway through the mixer section.

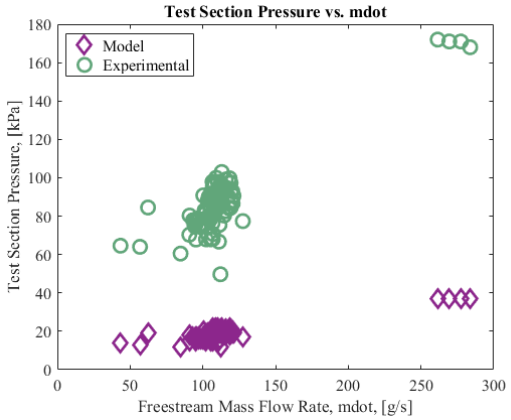

(a) Full view

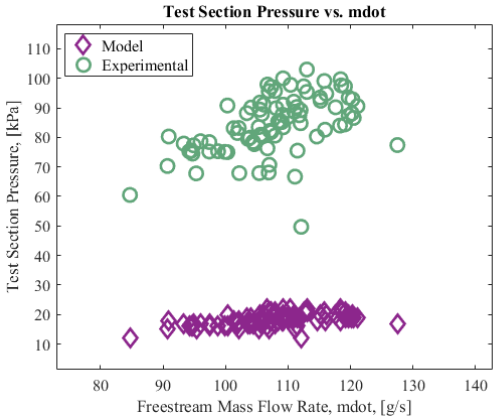

(b) Zoomed in

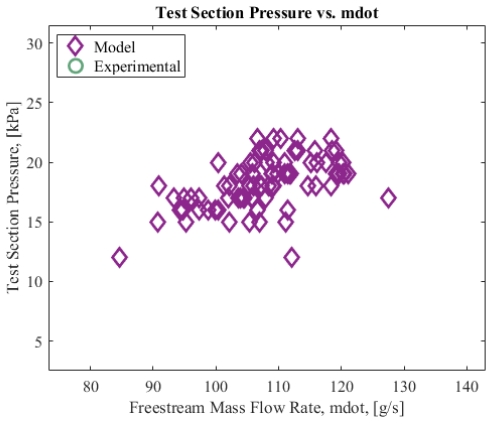

(c) Zoomed in further

Figure 5.16: Pressure vs. $\dot{m}_\infty$

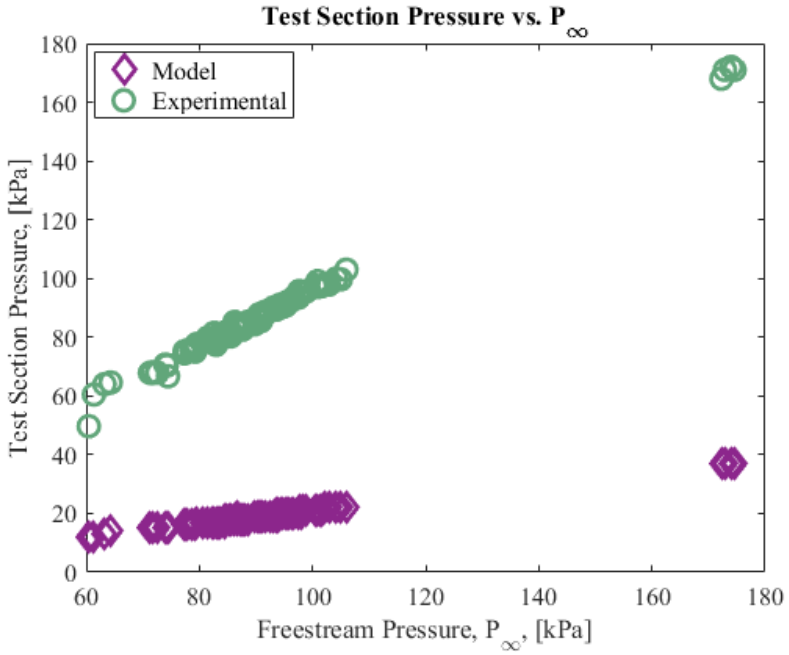

Figure 5.17: Pressure in the test section plotted against the freestream pressure P_∞

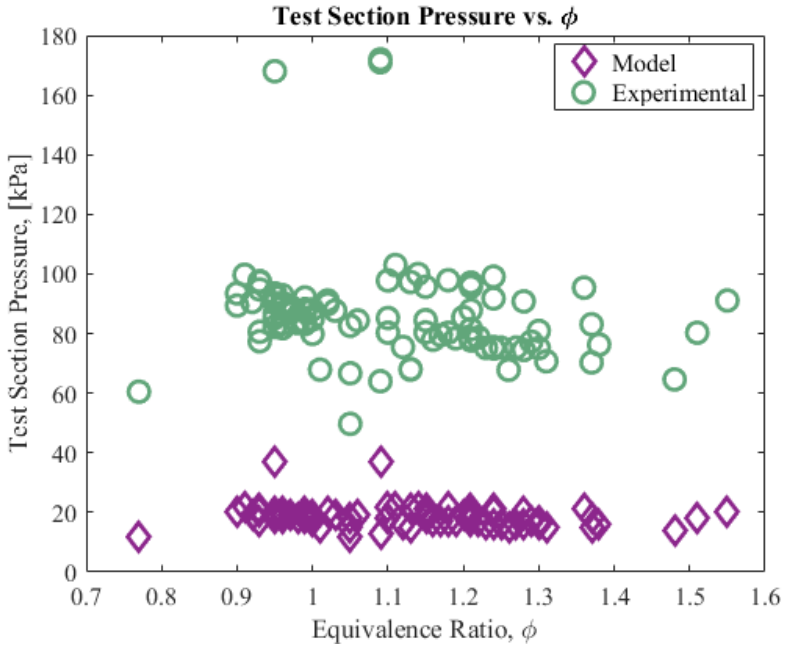

Figure 5.18: Pressure in the test section plotted against the equivalence ratio ϕ

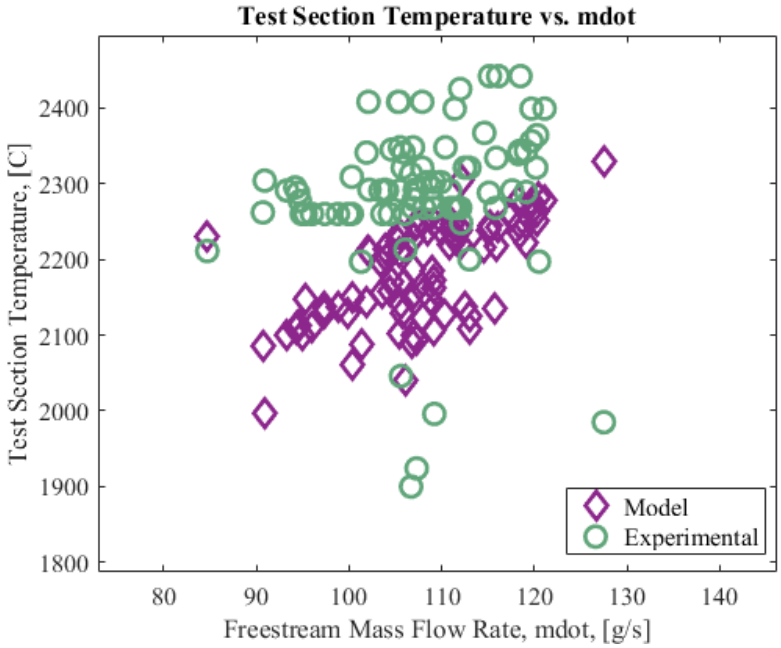

Figure 5.19: Temperature in the test section plotted against mass flow rate of the combustion reactants

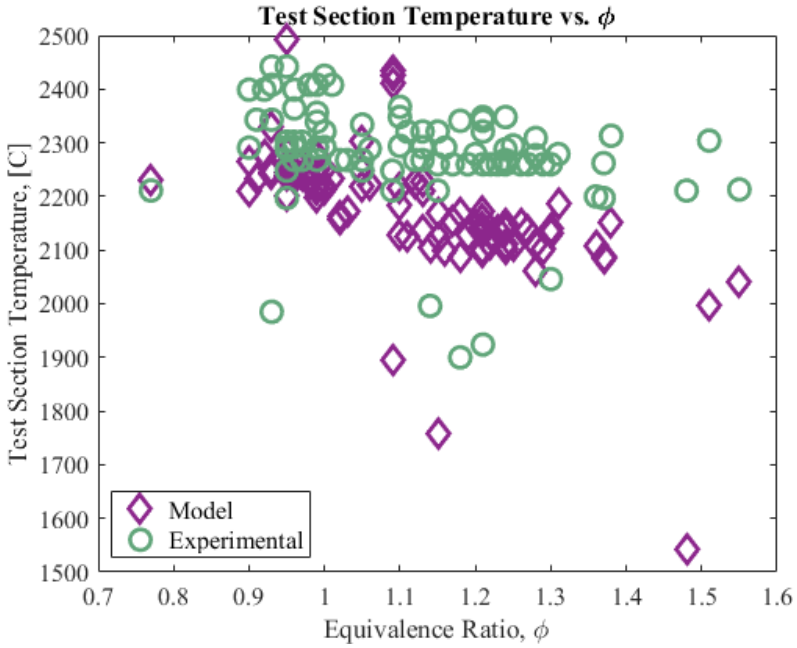

Figure 5.20: Temperature in the test section plotted against the equivalence ratio ϕ

5.5 *Transient Heat Flow into a Test Article*

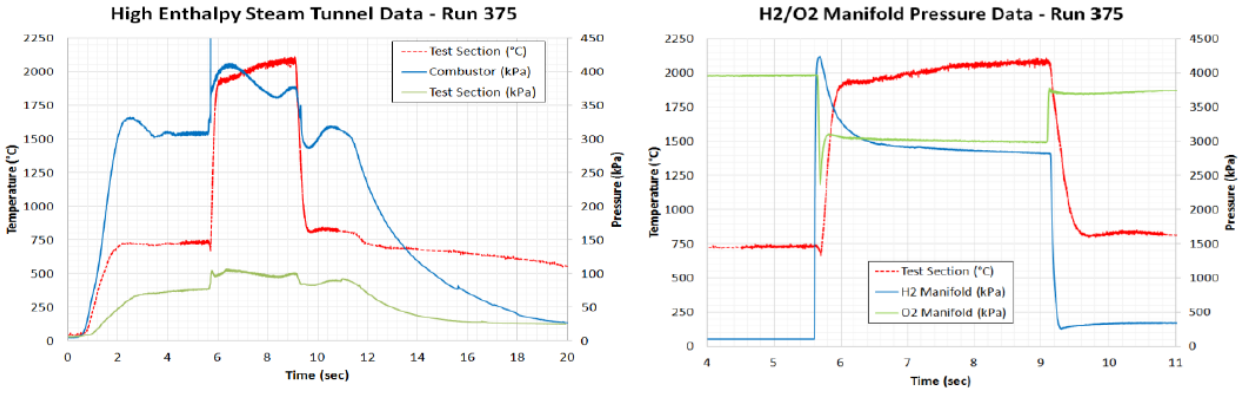

Figure 5.21: Results for a case with H_2 and O_2 combustion but no N_2 mixing

Fig. (5.21) shows a representative run from these experiments. In the left chart, one can see that the steam is at approximately 740 °C during the preheat phase, as indicated by the

red line denoting the readings from the test section thermocouple. Upon insertion of the gaseous H_2 and O_2 into the combustor, the gases ignite, and the temperature and pressure throughout the system rise. The release of energy from the combustion process completely stops the influx of steam from the pebble-bed heater, despite the fact that the combined mass flow rate for the gaseous H_2 and O_2 is less than that of the pebble-bed steam. In this experiment, the temperature rises sharply to approximately 1950 °C and continues rising gradually to about 2100 °C until the burner is shut off. The downstream flow consists of the combustion products, whose composition depends on the stoichiometry of the gaseous H_2 and O_2 flow.

The graph on the right side shows the data from the pressure sensors in the gas manifold and the thermocouple in the test section. In order to feed the igniter system that generated a pilot flame, the O_2 flow was turned on 0.5 seconds before the H_2. This allowed the H_2 to be ignited smoothly as the H_2 and O_2 were injected at the mass flow rates desired.

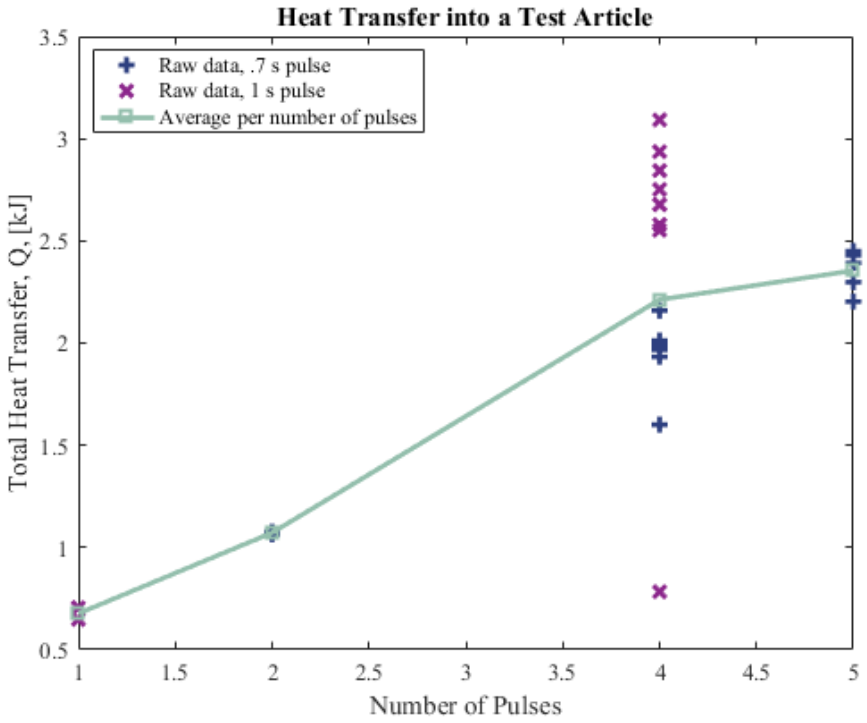

Figure 5.22: Total heat transfer into a test article plotted against number of pulses

The average heat transfer into the cylinder for the cases with four 0.7 s pulses was 1.95 kJ. The average heat transfer into the cylinder for the cases with four 1 s pulses was 2.54 kJ. This is a difference of 30.4 percent from the value for the 0.7 s pulses.

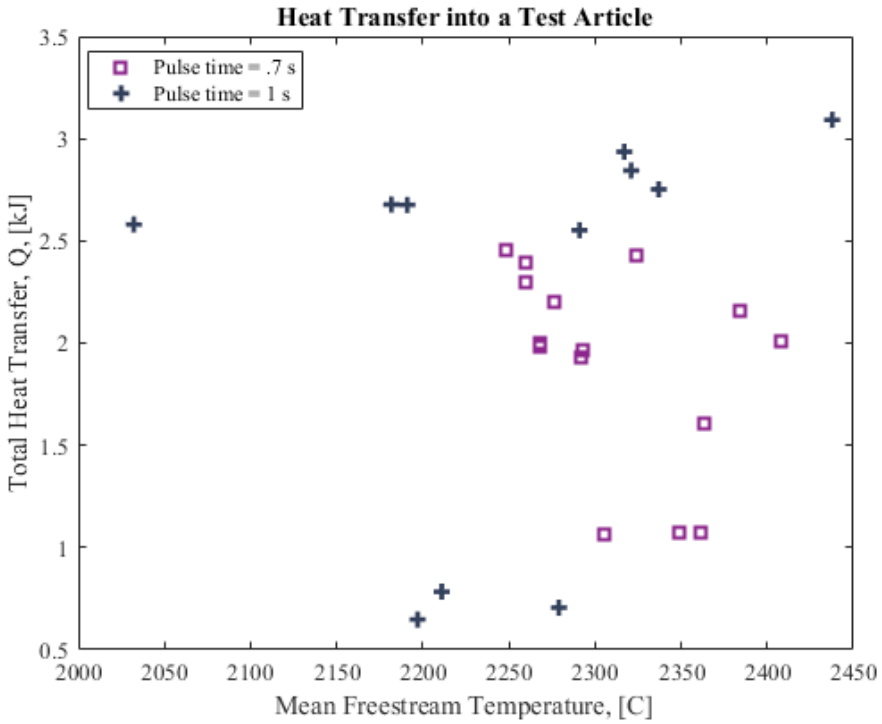

Figure 5.23: Total heat transfer into a test article plotted against average freestream tempearture, in °C

In Fig. (5.23), the "mean freestream temperature" is the average of all the freestream temperatures given in the "corrected temperature" column in Tables (E.1) and (E.2) across all pulses for a particular run.

Chapter 6

DISCUSSION

6.1 Study A: Case with H2, O2, Steam, and N2 Injection

It is difficult to draw rigorous conclusions from Study A, simply because so few data points were able to be collected for the case of interest, which was the case with N_2 mixing. Although the data from only five experimental runs were used, there were an additional three runs with N_2 mixing that were available but could not be used. This is because, unlike the five runs that were used, the three unusable runs featured values of α that were greater than one. For reasons that are not entirely clear, the model used in the current study is incapable of producing results for cases with such values of α; the approach described in section 2 produces complex values of Mach number when $\alpha > 1$. This is an aphysical result and indicates that something is likely wrong with the N_2 mixing portion of the model. Therefore, it is recommended that one proceed with caution when assessing the results of Study A.

Among the conclusions that can be drawn from Study A are general observations of the model's ability to predict trends for temperature. For example, in Fig. (5.4), one can see that both the model and the experimental results appear to show an association between temperature and α, and that both appear to show that temperature decreases as α increases. This is consistent with the theory. One of the objectives of injecting the N_2 feedstock was to decrease the stagnation temperature, which would in turn lead to a decrease in static temperature. It makes sense that for greater proportions of N_2 relative to the freestream flow, the temperature would continue to decrease.

Figures (5.1) through (5.3) display the values of Mach number, temperature, and pressure throughout the length of the SWR from the entrance of the combustor to the test section. The data in these figures are taken from the model prepared for this study. All three plots

are plotted with the input conditions of the same case, and all three display the results with and without the consideration of N_2 mixing. For temperature and pressure, both the static and stagnation values are plotted. Recall that the main objectives with injecting N_2 feedstock were to lower the stagnation temperature, raise the stagnation pressure, and raise the Mach number. On can observe that the Mach number does indeed increase at the point of N_2 injection in Fig. (5.1), that the stagnation temperature does indeed drop at the point of N_2 injection in Fig. (5.2), and that the stagnation pressure does indeed rise at the point of N_2 injection in Fig. (5.3),

As one can see in Fig. (5.5), the model appears to do a good job of matching the trends in the experimental data for Pressure. In Fig. (5.5), pressure in the test section is plotted against the ratio of mass flow rates α. In both the modeled and experimental results, the pressure appears to decrease as mass flow rate ratio α increases. However, this apparent relationship is tenuous at best. Due to the very limited number of data points, it is recommended to proceed with caution.

As one can see in Fig. (5.6), the model appears to do a good job of matching the trends in the experimental data for Nusselt number. In Fig. (5.6), Nusselt number is plotted against the ratio of mass flow rates α. In both the modeled and experimental results, the Nusselt number appears to increase sharply at about $\alpha = 0.4$ and to decrease sharply at about $\alpha = 0.6$; however, due to the very limited number of data points, it is recommended to proceed with caution.

As one can see in Fig. (5.7), the model appears to do a good job of matching the trends in the experimental data for velocity. In Fig. (5.7), velocity is plotted against the ratio of mass flow rates α. In both the modeled and experimental results, the velocity appears to decrease sharply at about $\alpha = 0.4$ and to increase sharply at about $\alpha = 0.6$; however, due to the very limited number of data points, it is recommended to proceed with caution.

As one can see in Fig. (5.8), the model does not appear to do a good job of matching the trends in the experimental data for Mach number. In Fig. (5.8), Mach number is plotted against the ratio of mass flow rates α. In the experimental results, shown in a full view

with the modeled results in Fig. (5.8a), the Mach number appears to decrease until about $\alpha = 0.42$ and then increase thereafter. On the other hand, in the modeled results, shown in a zoomed in view in Fig. (5.8b), the Mach number appears to steadily increase. However, due to the very limited number of data points, it is recommended to proceed with caution.

As one can see in Fig. (5.9), the model does not appear to do a good job of matching the trend in the experimental data for viscosity. In Fig. (5.9), viscosity is plotted against the ratio of mass flow rates α. In the experimental results, the viscosity appears to decrease sharply at about $\alpha = 0.4$ and to increase sharply at about $\alpha = 0.6$, whereas the model shows the opposite trend. However, due to the very limited number of data points, it is recommended to proceed with caution. That the model's trends are inverted from the experimental trends, however, suggests that there might be something wrong with the model that is relatively easy to fix, such as a missing negative sign.

As one can see in Fig. (5.10), the model appears to do a good job of matching the trends in the experimental data for thermal conductivity. In Fig. (5.10), thermal conductivity is plotted against the ratio of mass flow rates α. In both the modeled and experimental results, the thermal conductivity appears to decrease sharply at about $\alpha = 0.4$ and to increase sharply at about $\alpha = 0.6$; however, due to the very limited number of data points, it is recommended to proceed with caution.

As one can see in Fig. (5.11), the model appears to do a good job of matching the trends in the experimental data for molecular mass. In Fig. (5.11), molecular mass is plotted against the ratio of mass flow rates α. In both the modeled and experimental results, the molecular mass appears to increase sharply at about $\alpha = 0.4$ and to decrease sharply at about $\alpha = 0.6$; however, due to the very limited number of data points, it is recommended to proceed with caution.

6.2 Study B: First Case with H2, O2, and Steam

In Study B, many more data points were available than in Study A. Recall that in Study B, no mixing with N_2 was considered. Input conditions that were held constant include

the mass flow rate of the pebble bed steam, the freestream pressure in the combustor, and the freestream temperature in the combustor. Input conditions that were varied include the mass flow rate of the H_2 and O_2 injected into the combustor and the equivalence ratio ϕ.

Like in Study A, Study B's results allow an assessment of the model's ability to predict trends. In Fig. (5.12), temperature for both the model's results and the experimental results is plotted against the freestream mass flow rate, which is the sum of the mass flow rates for both the pebble bed steam and the H_2 and O_2. In this case, the trend in the model shows good agreement with the trend in experimental results. Both the model and the experiments appear to show that the temperature increases as mass flow rate increases. This makes sense in the context of the current experiment, since the mass flow rate of the pebble bed steam was held constant, but the mass flow rate of the combustion reactants was varied. If more combustion reactants are inserted, the adiabatic flame temperature should increase. If the adiabatic flame temperature increases, then the static temperature in the test should also increase, according to the theory.

The other case considered in Study B was one in which temperature was plotted against the equivalence ratio ϕ, as shown in Fig. (5.13). Like the results shown in Fig. (5.12), the model shows good agreement with the experimental results in terms of the trends of the data. According to both the model and the experiments, as the equivalence ratio ϕ increases for values of $\phi > 1$, the test section temperature decreases. This makes sense according to the theory, since increases in equivalence ratios for $\phi > 1$ corresponds to further departures from stoichiometric mass fractions of the combustion reactants, and thus lower adiabatic flame temperatures. Lower adiabatic flame temperatures would lead, in turn, to lower test section temperatures.

Overall, however, the model does not show very good agreement with the experimental values in terms of the temperature as opposed to the trends. In terms of the values, the model predicts values for temperature that are about 600 °C higher than the experimental values. This suggest one of three possibilities. The first possibility is that something is wrong with the model. The second possibility is that, at least under conditions to those similar in

Study B, the SWR undergoes a stagnation temperature loss that is not predicted very well by the theory used. This could include 2-D or even 3-D flow effects, as well as turbulent flow effects, all of which would likely produce greater frictional losses in stagnation temperature.

It is also worth noting that in Study B, the model invariably predicted test section pressures of 81 kPa. This is worthy of note mainly because the value is exactly the same, at least to two significant figures, for all runs. Admittedly, as one can see in Table (B.1), the pressure measurements in the experimental data only vary from 103 kPa to 114 kPa. It is possible that pressure in the test section has little or no dependence on ϕ or mass flow rate of the H_2 and O_2, which were the two input variables altered in Study B. Furthermore, it is suspected from previous experimental studies that the pressure sensors in the test section might be recording pressures that are excessively high by about 20 to 30 kPa, and the modeled results from this study seem to corroborate that.

6.3 Study C: Second Case with H2, O2, and Steam

Recall that in Study C, no mixing with N_2 was considered. Input conditions that were held constant include the mass flow rate of the pebble bed steam, the mass flow rate of the H_2 and O_2 injected into the combustor, the freestream pressure in the combustor. Input conditions that were varied include the equivalence ratio ϕ and the freestream temperature in the combustor. Like in Study B, a much greater amount of data points was available than in Study A.

Shown in Fig. (5.14) is a plot of the temperature in the test section plotted against the freestream temperature of the pebble bed steam. Neither the experimental values nor the modeled value show any easily discernible dependence. This makes sense according to the theory, since the temperature in the test section is understood to be dependent on the adiabatic flame temperature in the combustor, and the adiabatic flame temperature in the combustor is only dependent on the initial temperatures of the combustion reactants, in which the pebble bed steam is not included.

Shown in Fig. (5.15) is a plot of temperature in the test section plotted against the

equivalence ratio ϕ. There appears to be good agreement between model, and the experimental results in terms of the trends predicted, and just like in Study B, the model and the experiments both appear to indicate that temperature in the test section decreases as equivalence ratio ϕ increases for $\phi > 1$.

In Study C, just as in Study B, the model invariably predicted test section pressures of 81 kPa. This is worthy of note mainly because the value is exactly the same, at least to two significant figures, for all runs. Admittedly, as one can see in Table (C.1), the pressure measurements in the experimental data only vary from 104 kPa to 115 kPa, which is comparable to the test envelope described by the experimental results in Study B. It is possible that pressure in the test section has little or no dependence on ϕ or freestream temperature of the pebble bed steam, which were the two input variables altered in Study C. Furthermore, as stated in the previous subsection, it is suspected from previous experimental studies that the pressure sensors in the test section might be recording pressures that are excessively high by about 20 to 30 kPa, and the modeled results from this study seem to corroborate that.

6.4 Study D: Case with H2 and O2

Recall that in Study D, no mixing with N_2 was considered. Additionally, no pebble bed steam was used; only molecular H_2 and O_2 were inserted into the combustor. Input conditions that were varied include the mass flow rate of the H_2 and O_2 injected into the combustor, the freestream pressure in the combustor, and the equivalence ratio ϕ.

Shown in Fig. (5.16) are three plots of pressure in the test section plotted against the mass flow rate of the combustion reactants. In Figs. (5.16a) and (5.16b), the latter of which is zoomed in on an area of interest in the former, one can see that pressure in the test section appears to increase as mass flow rate of the combustion reactants increases. As one can see in Fig. (5.16c), which shows a zoomed in region of Fig. (5.16b), the modeled values appear to agree with the experimental values in this regard. This makes sense in terms of the theory, if the ideal gas law is assumed to be valid, since temperature and pressure are directly proportional according to the ideal gas law, and the temperature in the test

section increases as a function of the adiabatic flame temperature, which in turn increases as a function of the mass of combustion reactants present in the combustor.

Shown in Fig. (5.17) are plots of the pressure in the test section plotted against the pressure in the combustor. In all three plots, one can see that both the model and the experiments show tight correlations between the two pressures, and that the pressure in the test section appears to increase linearly with the combustor pressure.

Shown in Fig. (5.18) is a plot of the test section pressure plotted against the equivalence ratio ϕ. Both the experimental results and the modeled results appear to show that the pressure decreases as ϕ increases for $\phi > 1$, although the relationships found are admittedly tenuous.

Shown in Fig. (5.19) is a plot of the temperature in the test section plotted against the mass flow rate of the combustion reactants. Note that very few experimental data points exist below about 2250 °C. This is an artifact of an engineering approximation that was made during the data collection process. Due to the high temperatures in the test section during this study, the thermocouples used to measure the temperature frequently melted, typically after about three runs. For runs in which thermocouple data was unavailable, temperatures from runs with similar input conditions were used as approximations. Nevertheless, above about 2250 °C, the experimental data appears to suggest that temperature in the test section increases as freestream mass flow rate increases. The model also appears to predict the same trend throughout. This is consistent with the theory, because if there is a higher mass of reactants present in the combustor, one should expect the adiabatic flame temperature to be higher.

Shown in Fig. (5.20) is a plot of temperature plotted against the equivalence ratio ϕ. Above about 2250 °C, the experimental results appear to suggest that temperature decreases as equivalence ratio. The model also predicts the same trend throughout.

No apparent association was found to exist between temperature in the test section and the temperature of the freestream pebble bed steam.

6.5 Test Envelope

Overall, while the model used in the current study mostly showed good agreement predicting the trends of the experimental data, the model did not show very good agreement in predicting the test section values for a particular data point. In other words, the model did not do a very good job of predicting the test envelope for a given set of input conditions.

6.5.1 Study A: Case with H2, O2, Steam, and N2 Injection

In Study A, the model's predicted temperatures ranged from 131 kPa to 158. The experimental pressures ranged from 111 kPa to 125 kPa. The model's predicted range came close to the experimental range but was higher and did not overlap.

The model's predicted temperatures ranged from 1030 °C to 1400 °C. The experimental temperatures ranged from 1730 °C to 1940 °C. The model's predicted range was lower than the predicted range for the experimental values and the two did not overlap.

The model's predicted Mach numbers ranged from 0.183 to 0.186. The experimental Mach numbers ranged from 0.394 to 0.451. The model's predicted range was lower than the range for the experimental values and the two did not overlap.

The model's predicted velocity ranged from 250 m/s to 273 m/s. The experimental velocities ranged from 444 m/s to 535 m/s. The model's predicted range was lower than the range of the experimental values and the two did not overlap.

The model's predicted range for molecular weight ranged from 13.4 to 16.5. The experimental values for molecular weight ranged from 14.2 g/mol to 17.6 g/mol. the model's predicted range was only slightly lower than the experimental range, and the two ranges overlapped rather well.

The model's predicted values for viscosity ranged from 0.927 millipoise to 0.978 millipoise. The experimental values for viscosity ranged from 0.502 millipoise to 0.621 millipoise. The model's predicted range was higher than the experimental range and the two did not overlap.

The model's predicted values for thermal conductivity ranged from 4.05 mW/cm/K to

4.92. The experimental values for thermal conductivity ranged from 1.54 mW/cm/K to 2.88 mW/cm/K. The model's predicted range was higher than the experimental range and the two did not overlap.

The model's predicted values for Nusselt number ranged from 86.1 to 97.4. The experimental values for Nusselt number ranged from 165 to 227. The model's predicted range was lower than the experimental range and the two did not overlap.

The model's predicted value for conductive heat transfer coefficient ranged from 388 $W/m^2/K$ to 420 $W/m^2/K$. The experimental values for conductive heat transfer coefficient ranged from 344 $W/m^2/K$ to 477 $W/m^2/K$.

Among the input conditions that were considered for Study A, the values of α used ranged from 0.26 to 0.61. The total mass flow rates used ranged from 353 g/s to 461 g/s. The freestream pressures ranged from 320 kPa to 400 kPa. The freestream pebble bed steam temperatures ranged from 670 °C to 750 °C. The mass flow rates of pebble bed steam ranged from 11.4 g/s to 106 g/s. The mass flow rates of H_2 ranged from 28.5 g/s to 46.4 g/s. The mass flow rates of O_2 ranged from 171 g/s to 255 g/s.

6.5.2 Study B: First Case with H2, O2, and Steam

In Study B, the model's predicted temperatures ranged from 2560 °C to 2580 °C. The experimental values of temperature ranged from 1960 °C to 2150 °C. The model's predicted range was higher than the experimental range and the two did not overlap.

The model's predicted pressures were all exactly 81 kPa to two significant figures. The experimental values for pressure ranged from 103 kPa to 114 kPa. The model's predicted range was lower than the experimental range and the two did not overlap.

Among the input conditions that were varied in Study B, the equivalence ratio ϕ ranged from 1.32 to 1.52. The values for mass flow rate of the combustion reactants varied from 0.197 kg/s to 0.232 kg/s.

6.5.3 Study C: Second Case with H2, O2, and Steam

In Study C, the model's predicted temperatures ranged from 2550 °C to 2580 °C. The experimental values of temperature ranged from 1840 °C to 2160 °C. The model's predicted range was higher than the experimental range and the two did not overlap.

The model's predicted pressures were all exactly 81 kPa to two significant figures. The experimental values for pressure ranged from 104 kPa to 115 kPa. The model's predicted range was lower than the experimental range and the two did not overlap.

Among the input conditions that were varied in Study C, the equivalence ratio varied from 1.25 to 2. The freestream pebble bed steam temperature varied from 540 °C to 751 °C.

6.5.4 Study D: Case with H2 and O2

In Study D, the model's predicted temperatures ranged from 1540 °C to 2490 °C. The experimental values of temperature ranged from 1900 °C to 2440 °C. The model's predicted range enclosed the experimental range.

The model's predicted pressures in the test section ranged from 15 kPa to 37 kPa, but the experimentally measured pressures ranged from 49.7 kPa to 172 kPa. The model's predicted values for pressure were much lower than the experimental values for pressure and the two did not overlap.

Among the input conditions that were varied in Study D, the equivalence ratio varied from 0.77 to 1.55. The combustor pressures ranged from 60.5 kPa to 176 kPa. The freestream mass flow rates of the combustion reactants varied from 43.4 g/s to 284 g/s. Additionally, the time of each pulse was either 0.7 s or 1 s.

6.6 Transient Heat Transfer into a Test Article

The data from the heat transfer model is tabulated in Tables (E.1) and (E.2). As can be seen in Figs. (5.22) and (5.23), the total heat transfer absorbed by the test article varied from about 0.5 kJ to about 3 kJ. The mean freestream temperatures varied from about 2000

°C to about 2450 °C. The number of pulses was 1, 2, 4, or 5. The pulses, in this case, were pulsed firings of a rotating detonation engine upstream of the combustor section.

In Fig. (5.22), one can see a dependence of total heat transfer on the number of pulses. For one-pulse runs, the heat transfer absorbed by the cylinder was low, at about 0.7 kJ. For two-pulse firings, the heat transfer was higher, at about 1 kJ. In the case of four pulse firings, however something interesting appears in the data. Apart from one outlier, most of the runs with 1 s pulses resulted in higher heat transfer than the cases with 0.7 s pulses. In fact, the average value of the 1 s pulses in the four pulse case was 2.54 kJ, which was about 30 percent higher than the average of 1.95 kJ for the 0.7 s pulse runs. In the current study, the only number of pulses for which data was recorded for both 0.7 s pulses and 1 s pulses was the four pulse case.

The observation that an increase in the number of pulses produces an increase in the total heat transfer agrees with the theory. Specifically, this observation suggests that the heat transfer into the object is dependent on the amount of time that the test article is exposed to the high enthalpy flow. In the theory, Eqs. (2.54) and (2.55) indicate that final temperature and heat transfer have time dependencies. The observation that the runs with longer pulses produce higher heat transfer than the runs with shorter pulses also agrees with the same part of the theory.

Interestingly, there does not appear to be any easily discernible dependence of the total heat transfer on the mean freestream temperature. The theory suggests that such a dependence should exist; however, this dependence is likely obscured by the wide range of other variables that were being adjusted in the experiments considered. Such a dependence is perhaps further masked by the fact that the dependence indicated by the theory is on the freestream temperature of a specific pulse, not on the mean of all the freestream temperatures for all pulses. One recommendation for future research would be to apply elementary statistical learning algorithms, such as a k-nearest neighbors search or linear discriminant analysis, to the current data set to find the dominant modes in the data. Another recommendation for future research would be to run more tests with only one pulse and to calculate

the heat transfer for the additional one-pulse cases.

Chapter 7

CONCLUSIONS AND RECOMMENDATIONS FOR FUTURE WORK

7.1 Transient Heat Transfer into a Test Article

In Fig. (5.22), one can see a dependence of total heat transfer on the number of pulses. However, in the current study, the only number of pulses for which data was recorded for both 0.7 s pulses and 1 s pulses was the four pulse case. Therefore, one recommendation for future research would be to investigate the difference in average heat transfer absorbed by the test article for multiple pulse lengths at various numbers of pulses.

There does not appear to be any easily discernible dependence of the total heat transfer on the mean freestream temperature, although the theory suggests that such a dependence should exist; however, this dependence is likely obscured by the wide range of other variables that were being adjusted in the experiments considered. One recommendation for future research would be to apply elementary statistical learning algorithms, such as a k-nearest neighbors search or linear discriminant analysis, to the current data set to find the dominant modes in the data. Another recommendation for future research would be to run more tests with only one pulse and to calculate the heat transfer for the additional one-pulse cases.

A final recommendation for future research would be to adapt the heat transfer calculations to more exotic geometries. The current study only considered the sides of a cylinder exposed axially to the flow. However, examples of other geometries that might be of interest include a cylinder exposed axially to the flow with a hemispherical cap on the upstream end, a hexagonal prism exposed axially to the flow, and stacked coaxial cylinders and frusta of varying radii, all exposed axially to the flow.

In order to produce heat transfer models for such exotic geometries, it is recommended

that a literature search be conducted to find existing, empirically-derived Nusselt number correlations for such geometries. If a Nusselt number correlation with satisfactory accuracy cannot be found in the existing literature, it is recommended that the researcher conduct new experimental studies to find new, empirically-derived Nusselt number correlations for whatever geometries are of interest.

In such experiments, heat sensors of some kind should be mounted inside the test article, in order to measure the final temperature of the object at the end of the pulse. However, the temperature measured inside the object will not be the same as the corresponding temperature on the outside walls. Therefore, knowledge of the material properties of the test article would be necessary in order to calculate the temperature on the outside of the test article using basic conductive heat transfer relations. If a high-enthalpy test facility with windows is accessible, infrared cameras are highly recommended as a reliable method of measuring temperature surface temperature of the object via remote sensing.

Finally, some knowledge of the material properties of the test article both before and after the experiment, including mass loss due to ablation, would be necessary to determine how much heat transfer the object absorbed.

7.2 Study D: Case with H2 and O2

In Study D, it is interesting that the test section pressure appears to show such a strong linear dependence on the combustor pressure. This is interesting because according to the theory, the drop in stagnation pressure is a function of numerous variables, including the local values of stagnation temperature, Mach number, and friction factor, among others. Nevertheless, the relationship between test section pressure and initial pressure in the combustor appears to be linear. This seems to suggest that all of the other variables upon which the drop in stagnation pressure depends are themselves also linear functions of combustor pressure. One recommendation for future study would be to investigate the dependences of Mach number, stagnation temperature drop, friction factor, and the other variables on which stagnation pressure depends and see whether or not such dependences are linear. This could likely be

done adequately through computational modeling.

In Study D, it was found that test section temperature appeared to increase with freestream mass flow rate, but appeared to decrease with equivalence ratio. One recommendation for future study would be to conduct more controlled experiments similar to Study D but with either equivalence ratio or freestream mass flow rate held constant.

7.3 Considerations across Multiple Cases

Interestingly, the model appears to show a much tighter correlation between temperature in the test section and equivalence ratio ϕ in Study C, shown in Fig. (5.15b), than in Study B, shown in Fig. (5.13b). This is interesting because only two input variables were altered in Study B, two were altered in Study C, and one of the two was the same for both. The one that was the same for both was equivalence ratio ϕ. For Study B, the other input variable was mass flow rate of the combustion reactants H_2 and O_2. For Study C, the second input variable that was altered was the freestream pebble bed steam temperature. This seems to suggest that the test section temperature has a greater dependence on mass flow rate of the combustion reactants than on the pebble bed steam temperature. This is consistent with the existing theory, from which it is understood that temperature in the test section is dependent on the adiabatic flame temperature in the combustor. The adiabatic flame temperature in the combustor is a function of the amount of combustion reactants present, but not on the temperature of any non-reacting chemical species that might be present.

7.4 Final Conclusions

It is recommended that extreme caution be used when considering the results and conclusions from Study A. Unfortunately, only eight data points were available for cases with N_2 mixing, and of those eight, the model only worked for five of them. Therefore, the number one recommendation for future research would be to conduct more experimental studies with N_2 feedstock injection. This would allow more rigorous examination of the model used in the current study as well as any future models.

Overall, the model does not do a very good job of predicting the values, or even the test envelope, of the experimental data, despite doing a good job of predicting the trends. This could be due to imperfections in the model, but it could also be due to the existence of additional flow effects that were neglected in the construction of the model. For example, the model assumed 1-D flow. Although 1-D approximations for turbulent flow were used to determine the Nusselt number and thereby the heat transfer, it is entirely possible that the presence of turbulence could be inducing 2-D or even 3-D effects on the flow that lead to disagreement with the model. Another flow consideration that was neglected in the current study was the effect of boundary layers, including both thermal and velocity boundary layers. The presence of such boundary layers, especially thermal boundary layers, could be partially responsible for some of the disagreement between the experimental values and the modeled values. These include, notably, the temperatures in the test section, which in many of the studies were higher for the modeled predictions than for the experimental values. Considering boundary layer effects could potentially lead to lower predicted temperatures. Therefore, another recommendation for future study would be to reconstruct the model incorporating 2-D boundary layers of both the thermal and velocity varieties in the pursuit of better agreement between the modeled and experimental values. It may also be necessary to consider non-ideal gas effects such as chemically reacting flows. Considering the effects of plume interactions due to transverse injection of N_2 on the momentum conservation may also be necessary.

BIBLIOGRAPHY

[1] John D. Anderson, Jr. *Fundamentals of Aerodynamics*, chapter 8. McGraw-Hill, 5th edition, 2011.

[2] John D. Anderson, Jr. *Fundamentals of Aerodynamics*, chapter 10. McGraw-Hill, 5th edition, 2011.

[3] Yunus A. Çengel, John M. Cimbala, and Robert H. Turner. *Fundamentals of Thermal-Fluid Sciences*, chapter 19. McGraw-Hill, 4th edition, 2012.

[4] Yunus A. Çengel, John M. Cimbala, and Robert H. Turner. *Fundamentals of Thermal-Fluid Sciences*, chapter 18. McGraw-Hill, 4th edition, 2012.

[5] Jack D. Mattingly. *Elements of Gas Turbine Propulsion*, chapter 3. McGraw-Hill, Inc., 1996.

[6] Gordon C. Oates. *Aerothermodynamics of Gas Turbine and Rocket Propulsion*, chapter 2. AIAA Education Series, 1988.

[7] Gordon C. Oates. *Aerothermodynamics of Gas Turbine and Rocket Propulsion*, chapter 5. AIAA Education Series, 1988.

[8] George P. Sutton and Oscar Biblarz. *Rocket Propulsion Elements*, chapter 8. John Wiley and Sons, Inc., 8th edition, 2010.

[9] Roland Wiberg and Noam Lior. Heat transfer from a cylinder in axial turbulent flows. *International Journal of Heat and Mass Transfer*, 48(8):1505–1517, April 2005.

Appendix A

DATA FROM STUDY A: CASE WITH H2, O2, STEAM, AND N2 INJECTION

		Experimental Values								
		Test Section Conditions								
Run №	Tinf	Temp (peak)	Pres (avg)	Total Mass Flow	Velocity	Mach	Steam mdot	H2 mdot	O2 mdot	Pinf
	C	C	kPa	g/s	m/s		g/s	g/s	g/s	kPa
331	740	778	86	415	238	0.469	415	0	0	340
332	720	1572	104	325	547	0.481	193.96	22.93	108.11	400
333	690	1513	103	338	537	0.479	215.46	22.15	100.39	400
334	700	1550	105	298	551	0.483	177.02	21.74	99.24	400
335	700	1560	104	299	547	0.485	176.46	20.84	101.70	400
336	700	1569	104	299	543	0.483	179.01	20.24	99.74	400
337	720	1115	179	729	332	0.369	179.17	27.78	106.05	400
338	760	1115	185	729	328	0.369	179.09	26.19	104.73	400
339	750	1101	185	748	323	0.365	190.73	25.89	99.38	400
340	750	1728	125	461.35	473	0.411	11.40	46.40	254.55	370
341	720	1906	122	432.89	444	0.394	105.81	28.47	170.61	370
342	670	1886	111	353	450	0.408	22.92	28.47	170.61	320
343	730	1930	122	381	508	0.406	63.67	37.87	173.46	370
344	730	1936	124	362	535	0.451	74.51	37.21	174.68	400

Table A.1: Tabulated data from a second study with H_2 and O_2 inserted into the combustor, with steam from the pebble bed heater and injection of N_2 feedstock, part 1

	Experimental Values							
	Test Flow Mixture Details							
Run №	Steam	H2	N2	MW	Visc	Cond	Nu	h_coef
	g/s	g/s	g/s	g/mol	millipoise	mW/cm/K		W/m2/K
332	316	9.42	0	14.53	0.5235	2.139	113.6	243.0
333	329	9.60	0	14.53	0.4941	1.973	113.6	243.0
334	289	9.33	0	14.53	0.5174	2.149	113.6	243.0
335	290	8.13	0	14.53	0.5359	2.174	186.8	399.7
336	291	7.78	0	14.53	0.5340	2.141	235.6	496.5
337	298	14.53	416	14.53	0.3765	1.032	440.7	447.7
338	297	13.10	419	14.53	0.3793	1.011	454.0	451.6
339	303	13.47	432	14.53	0.3643	0.963	446.8	423.5
340	643	14.58	191	14.53	0.5916	2.401	179.4	424.0
341	597	7.14	128	14.53	0.5023	1.535	227.7	344.1
342	597	7.14	128	14.53	0.5023	1.535	227.7	344.1
343	259	16.18	106	14.53	0.6044	2.675	165.4	435.4
344	271	15.38	75.6	14.24	0.6214	2.875	168.7	477.4

Table A.2: Tabulated data from a second study with H_2 and O_2 inserted into the combustor, with steam from the pebble bed heater and injection of N_2 feedstock, part 2

	Modeled Values												
	Test Flow Mixture Details												
Run №	Temp	Pres	Total Mas	Velocity	Mach	Steam	H2	N2	MW	Visc	Cond	Nu	h_coef
	K	kPa	g/s	m/s		g/s	g/s	g/s	g/mol	millipoise	mW/cm/K		W/m^2/K
332	2363.85	150	315	311	0.2001	316	9.42	0	13.15	1.0103	5.334	58.5	308.3
333	2386.85	150	338	310	0.2006	329	9.60	0	13.19	1.0111	5.324	58.6	306.9
334	2308.85	150	298	312	0.1988	289	9.33	0	13.01	1.0066	5.380	58.4	309.3
335	2314.85	150	299	309	0.1987	290	8.13	0	13.27	1.0130	5.299	58.6	305.8
336	2314.85	151	299	309	0.1987	291	7.78	0	13.34	1.0148	5.275	58.7	304.8
337			729			298	14.53	416					
338			729			297	13.10	419					
339			748			303	13.47	432					
340	1206.85	150	807	261	0.1858	643	14.58	191	15.09	0.9474	4.443	96.0	419.8
341	1251.85	149	725	252	0.1841	597	7.14	128	16.20	0.9778	4.202	95.1	393.5
342	1028.85	131	353	250	0.1838	597	7.14	128	16.54	0.9570	4.048	97.4	388.1
343	1256.85	148	381	270	0.1842	259	16.18	106	13.88	0.9265	4.742	89.2	416.5
344	1395.85	158	362	273	0.1826	271	15.38	75.6	13.40	0.9339	4.915	86.1	416.6

Table A.3: Tabulated data from a second study with H_2 and O_2 inserted into the combustor, with steam from the pebble bed heater and injection of N_2 feedstock, part 3

Appendix B

DATA FROM STUDY B: FIRST CASE WITH H2, O2, AND STEAM

Run	Experimental Peak Test		Steam	Burner	Phi	P_comb	T_comb	Modeled Values Test Section			Run
	Temp (C)	Pres (kPa)	(kg/s)	(kg/s)	(f)	(kPa)	(K)	Temp (K)	Temp (C)	Pres (kPa)	
348	2000	104	0.356	0.223	1.449	370	800	2847	2573.85	81	348
349	2070	103	0.356	0.221	1.45	370	800	2846	2572.85	81	349
350	2070	105	0.356	0.222	1.439	370	800	2847	2573.85	81	350
353	2022	103	0.356	0.211	1.44	370	800	2841	2567.85	81	353
354	2039	104	0.356	0.216	1.499	370	800	2841	2567.85	81	354
355	2036	103	0.356	0.215	1.499	370	800	2840	2566.85	81	355
356	2019	105	0.356	0.214	1.52	370	800	2839	2565.85	81	356
357	1993	104	0.356	0.211	1.516	370	800	2838	2564.85	81	357
358	1988	103	0.356	0.211	1.496	370	800	2838	2564.85	81	358
359	1962	105	0.356	0.207	1.498	370	800	2836	2562.85	81	359
360	1963	104	0.356	0.205	1.489	370	800	2835	2561.85	81	360
361	1962	105	0.356	0.201	1.465	370	800	2834	2560.85	81	361
362	1990	103	0.356	0.197	1.389	370	800	2835	2561.85	81	362
363	2099	107	0.356	0.229	1.389	370	800	2852	2578.85	81	363
364	1993	109	0.356	0.232	1.379	370	800	2854	2580.85	81	364
365	2058	108	0.356	0.229	1.395	370	800	2852	2578.85	81	365
366	2135	114	0.356	0.226	1.388	370	800	2851	2577.85	81	366
367	2130	105	0.356	0.227	1.378	370	800	2852	2578.85	81	367
368	2154	105	0.356	0.226	1.366	370	800	2852	2578.85	81	368
369	2086	103	0.356	0.225	1.349	370	800	2852	2578.85	81	369
370	2100	106	0.356	0.224	1.317	370	800	2853	2579.85	81	370
372	2026	107	0.356	0.225	1.423	370	800	2849	2575.85	81	372
373	2045	107	0.356	0.222	1.408	370	800	2848	2574.85	81	373
374	2073	106	0.356	0.221	1.392	370	800	2848	2574.85	81	374

Table B.1: Tabulated data from a study with H_2 and O_2 inserted into the combustor, with steam from the pebble bed heater but no injection of N_2 feedstock

Appendix C

DATA FROM STUDY C: SECOND CASE WITH H2, O2, AND STEAM

	Experimental Values					Steam				Modeled Values		
Run №	Test Pres	Test Temp	Corrected Temp	H2+O2 mdot	Equivalence ratio, phi	Temp	Pressure	mdot	Run №	Test Pres	Test Temp	Test Temp
	kPa	C	C	kg/s		C	kPa	kg/s		kPa	K	C
375	106	2104	2304	0.223	1.49	725	370	0.356	375	81	2845	2571.85
376	108	2083	2283	0.223	1.44	740	370	0.356	376	81	2847	2573.85
377	108	2053	2253	0.223	1.9	700	370	0.356	377	81	2829	2555.85
378	105	2027	2227	0.223	1.87	719	370	0.356	378	81	2830	2556.85
379	108	1966	2166	0.223	1.86	751	370	0.356	379	81	2830	2556.85
380	107	1989	2189	0.223	1.79	740	370	0.356	380	81	2833	2559.85
381	109	2030	2230	0.223	1.71	739	370	0.356	381	81	2836	2562.85
382	107	2053	2253	0.223	1.66	738	370	0.356	382	81	2838	2564.85
383	106	1991	2191	0.223	1.63	734	370	0.356	383	81	2839	2565.85
384	108	2018	2218	0.223	1.55	736	370	0.356	384	81	2842	2568.85
385	107	2083	2283	0.223	1.44	710	370	0.356	385	81	2847	2573.85
386	105	2000	2200	0.223	2	718	370	0.356	386	81	2825	2551.85
387	115	1995	2195	0.223	1.92	686	370	0.356	387	81	2828	2554.85
388	108	1990	2190	0.223	1.86	705	370	0.356	388	81	2830	2556.85
389	104	2031	2231	0.223	1.44	718	370	0.356	389	81	2847	2573.85
390	106	2073	2273	0.223	1.45	716	370	0.356	390	81	2847	2573.85
391	107	2060	2260	0.223	1.4	653	370	0.356	391	81	2849	2575.85
392	105	2155	2355	0.223	1.36	683	370	0.356	392	81	2850	2576.85
393	109	2088	2288	0.223	1.25	659	370	0.356	393	81	2855	2581.85
394	107	2059	2259	0.223	1.64	646	370	0.356	394	81	2839	2565.85
395	106	1907	2107	0.223	1.72	584	370	0.356	395	81	2836	2562.85
396	111	1853	2053	0.223	1.68	690	370	0.356	396	81	2837	2563.85
397	106	1840	2040	0.223	1.66	540	370	0.356	397	81	2838	2564.85
398	106	2021	2221	0.223	1.37	682	370	0.356	398	81	2850	2576.85
399	107	2016	2216	0.223	1.48	672	370	0.356	399	81	2845	2571.85
400	106	2060	2260	0.223	1.34	640	370	0.356	400	81	2851	2577.85

Table C.1: Tabulated data from a second study with H_2 and O_2 inserted into the combustor, with steam from the pebble bed heater but no injection of N_2 feedstock

Appendix D

DATA FROM STUDY D: CASE WITH H2 AND O2

						Experimental			Modeled Values		
Run №	Pulse №	Total mdot [g/s]	O/F ratio	Phi	P_comb [kPa]	Test Pres [kPa]	Test Temp [C]	Corrected Temp [C]	Test Pres [kPa]	Test Temp [C]	Test Temp [K]
166	1	111.1	7.64	1.05	74.46	66.7	2068	2268	15	2246.85	2520
	2	111.8	8.07	0.99	90.57	87.5	2068	2268	19	2242.85	2516
	3	112	8.23	0.97	92.5	89.2	2068	2268	19	2238.85	2512
	4	109.2	7.82	1.02	94.4	91.1	2068	2268	20	2162.85	2436
167	1	111.5	7.12	1.12	77.8	75.5	2068	2268	16	2225.85	2499
	2	109.1	7.75	1.03	91.61	87.7	2068	2268	19	2172.85	2446
	3	111	8.32	0.96	91.69	88.7	2068	2268	19	2238.85	2512
	4	108.1	7.86	1.02	93.93	89.9	2068	2268	20	2158.85	2432
168	1	106.9	7.09	1.13	71.82	68.1	2068	2268	15	2227.85	2501
	2	109.2	8.32	0.96	86.59	83.4	2102	2302	18	2247.85	2521
	3	108.4	8.39	0.95	88.7	85.3	2102	2302	18	2237.85	2511
	4	109.9	8.27	0.97	90.18	86.8	2102	2302	19	2237.85	2511
169	1	105.4	7.94	1.01	72.59	67.9	2208	2408	15	2233.85	2507
	2	107.9	8.62	0.93	84.54	80.6	2208	2408	17	2251.85	2525
	3	102.1	8.06	0.99	86.24	83.2	2208	2408	18	2211.85	2485
	4	105.3	8.15	0.98	87.49	83.5	2208	2408	18	2223.85	2497
170	1	102.2	7.08	1.13	71.28	67.9	2092	2292	15	2208.85	2482
	2	103.9	8.03	1	81.5	79.9	2092	2292	17	2212.85	2486
	3	107.3	8.31	0.96	84.74	81.8	2092	2292	18	2245.85	2519
	4	107.1	8.42	0.95	85.33	82.2	2092	2292	18	2243.85	2517
172	1	107	6.13	1.31	74.01	70.7	2079	2279	15	2187.85	2461
	2	106.7	5.82	1.38	79.08	76.3	2113	2313	16	2150.85	2424
	3	104.6	6.62	1.21	79.54	77.7	2145	2345	17	2170.85	2444
	4	105.9	6.78	1.18	83.12	80.3	2141	2341	17	2167.85	2441
	5	101.9	6.61	1.21	82.6	81.5	2141	2341	17	2142.85	2416
173	1	100.3	6.44	1.24	77.84	75	2060	2260	16	2149.85	2423
	2	99.9	6.14	1.3	79.25	75.1	2060	2260	16	2129.85	2403
	3	104.4	6.59	1.21	82.3	78.5	2060	2260	17	2157.85	2431
	4	103.6	6.82	1.17	83.37	79.5	2060	2260	17	2155.85	2429
	5	106	6.97	1.15	84.44	80.4	2060	2260	18	2167.85	2441
174	1	97.4	6.52	1.23	77.39	75.2	2060	2260	16	2137.85	2411
	2	98.8	6.32	1.27	77.64	75.3	2060	2260	16	2136.85	2410
	3	94.9	6.22	1.29	79.43	77.3	2060	2260	17	2100.85	2374
	4	97.4	6.7	1.19	80.72	78.4	2060	2260	17	2128.85	2402
	5	96	6.54	1.22	81.46	78.7	2060	2260	17	2110.85	2384
175	1	95.3	6.33	1.26	71.66	67.8	2060	2260	15	2147.85	2421
	2	90.7	5.85	1.37	74.21	70.3	2062	2262	15	2084.85	2358
	3	94.7	6.27	1.28	77.39	74.5	2077	2277	16	2111.85	2385
	4	94.5	6.47	1.24	78.74	75.5	2088	2288	16	2111.85	2385
	5	94.2	6.41	1.25	78.69	75.3	2095	2295	16	2107.85	2381

Table D.1: Tabulated data from a study with H_2 and O_2 inserted into the combustor, with no steam from the pebble bed heater and no injection of N_2 feedstock, part 1

176	1	112.1	7.61	1.05	60.46	49.7	2048	2248	12	2303.85	2577
	2	283.8	8.42	0.95	172.3	168	2048	2248	37	2491.85	2765
	3	277.4	7.37	1.09	174.6	171	2048	2248	37	2434.85	2708
	4	269.5	7.37	1.09	172.9	171	2048	2248	37	2425.85	2699
	5	261.5	7.32	1.09	174	172	2048	2248	37	2411.85	2685
177	1	119.1	7.52	1.06	89.81	84.4	2089	2289	19	2222.85	2496
	2	120.2	7.97	1	91.2	88.1	2121	2321	19	2250.85	2524
178	1	114.6	7.3	1.1	84.79	80.3	2167	2367	18	2215.85	2489
	2	119.7	8.06	0.99	90.92	87.4	2156	2356	19	2274.85	2548
179	1	115.9	7.63	1.05	87.65	82.6	2134	2334	18	2217.85	2491
	2	120.3	8.36	0.96	96.44	92.9	2164	2364	20	2263.85	2537
180	1	118.3	8.08	0.99	87.99	84	2139	2339	18	2277.85	2551
	2	121.1	8.7	0.92	93.84	90.6	2199	2399	19	2277.85	2551
	3	111.4	8.33	0.96	93.55	90.3	2199	2399	19	2233.85	2507
	4	119.7	8.86	0.9	96.72	93.5	2199	2399	20	2264.85	2538
182	1	84.7	10.35	0.77	61.37	60.5	2011	2211	12	2229.85	2503
	2	62.3	6.93	1.15	86.69	84.5	2011	2211	19	1757.85	2031
	3	43.4	5.39	1.48	64.33	64.6	2011	2211	14	1542.85	1816
	4	56.8	7.37	1.09	63.25	64	2011	2211	13	1895.85	2169
183	1	101.3	5.84	1.37	87.12	83.1	1997	2197	18	2086.85	2360
184	1	108.8	6.66	1.2	90.89	85.5	2079	2279	19	2146.85	2420
185	1	105.8	6.64	1.21	90.65	87.9	2121	2321	19	2129.85	2403
	2	107.9	6.96	1.15	97.63	95.7	2121	2321	21	2122.85	2396
	3	112.5	7.06	1.13	101.5	97.3	2121	2321	21	2136.85	2410
	4	113	7.18	1.11	106	103	2121	2321	22	2125.85	2399
186	1	109	7.3	1.1	86.23	85.2	2094	2294	18	2183.85	2457
	2	115.1	8.44	0.95	97.54	93.5	2088	2288	20	2238.85	2512
	3	119.1	8.64	0.93	101.4	97.3	2143	2343	21	2245.85	2519
	4	118.4	8.76	0.91	105	99.7	2143	2343	22	2233.85	2507
187	1	112	7.97	1	89.81	84.8	2225	2425	19	2219.85	2493
	2	115.2	8.44	0.95	96.24	92.4	2242	2442	20	2243.85	2517
	3	116.1	8.57	0.93	98.08	94.8	2242	2442	20	2242.85	2516
	4	118.5	8.56	0.93	100.5	97.6	2242	2442	21	2245.85	2519
188	1	105.6	6.18	1.3	83.59	80.9	1846	2046	17	2140.85	2414
	2	106.1	5.17	1.55	95.41	91.1	2013	2213	20	2039.85	2313
	3	113	5.89	1.36	98.2	95.4	2000	2200	21	2107.85	2381
	4	115.8	6.44	1.24	100.9	99.1	2068	2268	21	2135.85	2409
189	1	90.9	5.3	1.51	85.58	80.3	2104	2304	18	1995.85	2269
	2	105.5	6.45	1.24	95.28	91.8	2148	2348	20	2101.85	2375
	3	106.9	6.6	1.21	98.96	95.7	2148	2348	21	2100.85	2374
	4	110.4	7.28	1.1	102.2	97.8	2148	2348	22	2127.85	2401
190	1	100.3	6.26	1.28	95.28	90.8	2109	2309	20	2061.85	2335
	2	107.3	6.62	1.21	100.9	97.1	1724	1924	21	2094.85	2368
	3	106.7	6.79	1.18	102.9	97.9	1700	1900	22	2088.85	2362
	4	109.2	7.03	1.14	104.2	100	1796	1996	22	2105.85	2379
191	1	127.5	8.59	0.93	82.95	77.4	1785	1985	17	2329.85	2603
	2	120.5	8.41	0.95	90.78	86.6	1997	2197	19	2281.85	2555
	3	117.6	8.41	0.95	94.57	90.2	2091	2291	20	2258.85	2532
	4	110.9	8.1	0.99	95.68	92.1	2091	2291	20	2220.85	2494
192	1	93.3	6.9	1.16	82.57	77.9	2091	2291	17	2099.85	2373
	2	103.4	8.1	0.99	91.64	88.2	2091	2291	19	2197.85	2471
	3	104.1	8.39	0.95	93.11	90.1	2091	2291	19	2200.85	2474
	4	105.5	8.89	0.9	93.58	89.4	2091	2291	20	2209.85	2483

Table D.2: Tabulated data from a study with H_2 and O_2 inserted into the combustor, with no steam from the pebble bed heater and no injection of N_2 feedstock, part 2

Appendix E

DATA FROM STUDY OF TRANSIENT HEAT FLOW INTO A

TEST ARTICLE

Run №	Pulse №	Total mdot [g/s]	O/F ratio	Phi	Pulse Time [s]	Test Pres [kPa]	Test Temp [C]	Corrected Temp [C]	Heat Transfer [kJ]
166	1	111.1	7.64	1.05	0.7	66.7	*2068*	*2268*	1.997
	2	111.8	8.07	0.99	0.7	87.5	*2068*	*2268*	
	3	112	8.23	0.97	0.7	89.2	*2068*	*2268*	
	4	109.2	7.82	1.02	0.7	91.1	*2068*	*2268*	
167	1	111.5	7.12	1.12	0.7	75.5	*2068*	*2268*	1.983
	2	109.1	7.75	1.03	0.7	87.7	*2068*	*2268*	
	3	111	8.32	0.96	0.7	88.7	*2068*	*2268*	
	4	108.1	7.86	1.02	0.7	89.9	*2068*	*2268*	
168	1	106.9	7.09	1.13	0.7	68.1	2068	2268	1.967
	2	109.2	8.32	0.96	0.7	83.4	2102	2302	
	3	108.4	8.39	0.95	0.7	85.3	*2102*	*2302*	
	4	109.9	8.27	0.97	0.7	86.8	*2102*	*2302*	
169	1	105.4	7.94	1.01	0.7	67.9	2208	2408	2.012
	2	107.9	8.62	0.93	0.7	80.6	*2208*	*2408*	
	3	102.1	8.06	0.99	0.7	83.2	*2208*	*2408*	
	4	105.3	8.15	0.98	0.7	83.5	*2208*	*2408*	
170	1	102.2	7.08	1.13	0.7	67.9	2092	2292	1.933
	2	103.9	8.03	1	0.7	79.9	*2092*	*2292*	
	3	107.3	8.31	0.96	0.7	81.8	*2092*	*2292*	
	4	107.1	8.42	0.95	0.7	82.2	*2092*	*2292*	
172	1	107	6.13	1.31	0.7	70.7	2079	2279	2.429
	2	106.7	5.82	1.38	0.7	76.3	2113	2313	
	3	104.6	6.62	1.21	0.7	77.7	2145	2345	
	4	105.9	6.78	1.18	0.7	80.3	2141	2341	
	5	101.9	6.61	1.21	0.7	81.5	*2141*	*2341*	
173	1	100.3	6.44	1.24	0.7	75	*2060*	*2260*	2.392
	2	99.9	6.14	1.3	0.7	75.1	*2060*	*2260*	
	3	104.4	6.59	1.21	0.7	78.5	*2060*	*2260*	
	4	103.6	6.82	1.17	0.7	79.5	*2060*	*2260*	
	5	106	6.97	1.15	0.7	80.4	*2060*	*2260*	
174	1	97.4	6.52	1.23	0.7	75.2	*2060*	*2260*	2.298
	2	98.8	6.32	1.27	0.7	75.3	*2060*	*2260*	
	3	94.9	6.22	1.29	0.7	77.3	*2060*	*2260*	
	4	97.4	6.7	1.19	0.7	78.4	*2060*	*2260*	
	5	96	6.54	1.22	0.7	78.7	*2060*	*2260*	
175	1	95.3	6.33	1.26	0.7	67.8	2060	2260	2.203
	2	90.7	5.85	1.37	0.7	70.3	2062	2262	
	3	94.7	6.27	1.28	0.7	74.5	2077	2277	
	4	94.5	6.47	1.24	0.7	75.5	2088	2288	
	5	94.2	6.41	1.25	0.7	75.3	2095	2295	

Table E.1: Tabulated data from transient heat flow into a stainless steel cylinder exposed axially to high enthalpy flow, part 1. There is H_2 and O_2 inserted into the combustor, with no steam from the pebble bed heater and no injection of N_2 feedstock.

176	1	112.1	7.61	1.05	0.7	49.7	2048	2248	2.45
	2	283.8	8.42	0.95	0.7	168	*2048*	*2248*	
	3	277.4	7.37	1.09	0.7	171	*2048*	*2248*	
	4	269.5	7.37	1.09	0.7	171	*2048*	*2248*	
	5	261.5	7.32	1.09	0.7	172	*2048*	*2248*	
177	1	119.1	7.52	1.06	0.7	84.4	2089	2289	1.065
	2	120.2	7.97	1	0.7	88.1	2121	2321	
178	1	114.6	7.3	1.1	0.7	80.3	2167	2367	1.076
	2	119.7	8.06	0.99	0.7	87.4	2156	2356	
179	1	115.9	7.63	1.05	0.7	82.6	2134	2334	1.076
	2	120.3	8.36	0.96	0.7	92.9	2164	2364	
180	1	118.3	8.08	0.99	0.7	84	2139	2339	2.159
	2	121.1	8.7	0.92	0.7	90.6	2199	2399	
	3	111.4	8.33	0.96	0.7	90.3	*2199*	*2399*	
	4	119.7	8.86	0.9	0.7	93.5	*2199*	*2399*	
181	1	76.6			0.7	62.9	*2199*	*2399*	1.601
	2	62.2			0.7	85.8	2180	2380	
	3	66.6			0.7	94.3	2266	2466	
	4	65.2			0.7	95.5	2011	2211	
182	1	84.7	10.35	0.77	1	60.5	*2011*	*2211*	0.784
	2	62.3	6.93	1.15	1	84.5	*2011*	*2211*	
	3	43.4	5.39	1.48	1	64.6	*2011*	*2211*	
	4	56.8	7.37	1.09	1	64	*2011*	*2211*	
183	1	101.3	5.84	1.37	1	83.1	1997	2197	0.648
184	1	108.8	6.66	1.2	1	85.5	2079	2279	0.706
185	1	105.8	6.64	1.21	1	87.9	2121	2321	2.844
	2	107.9	6.96	1.15	1	95.7	*2121*	*2321*	
	3	112.5	7.06	1.13	1	97.3	*2121*	*2321*	
	4	113	7.18	1.11	1	103	*2121*	*2321*	
186	1	109	7.3	1.1	1	85.2	2094	2294	2.936
	2	115.1	8.44	0.95	1	93.5	2088	2288	
	3	119.1	8.64	0.93	1	97.3	2143	2343	
	4	118.4	8.76	0.91	1	99.7	*2143*	*2343*	
187	1	112	7.97	1	1	84.8	2225	2425	3.092
	2	115.2	8.44	0.95	1	92.4	2242	2442	
	3	116.1	8.57	0.93	1	94.8	*2242*	*2442*	
	4	118.5	8.56	0.93	1	97.6	*2242*	*2442*	
188	1	105.6	6.18	1.3	1	80.9	1846	2046	2.678
	2	106.1	5.17	1.55	1	91.1	2013	2213	
	3	113	5.89	1.36	1	95.4	2000	2200	
	4	115.8	6.44	1.24	1	99.1	2068	2268	
189	1	90.9	5.3	1.51	1	80.3	2104	2304	2.752
	2	105.5	6.45	1.24	1	91.8	2148	2348	
	3	106.9	6.6	1.21	1	95.7	*2148*	*2348*	
	4	110.4	7.28	1.1	1	97.8	*2148*	*2348*	
190	1	100.3	6.26	1.28	1	90.8	2109	2309	2.58
	2	107.3	6.62	1.21	1	97.1	1724	1924	
	3	106.7	6.79	1.18	1	97.9	1700	1900	
	4	109.2	7.03	1.14	1	100	1796	1996	
191	1	127.5	8.59	0.93	1	77.4	1785	1985	2.676
	2	120.5	8.41	0.95	1	86.6	1997	2197	
	3	117.6	8.41	0.95	1	90.2	2091	2291	
	4	110.9	8.1	0.99	1	92.1	*2091*	*2291*	
192	1	93.3	6.9	1.16	1	77.9	*2091*	*2291*	2.552
	2	103.4	8.1	0.99	1	88.2	*2091*	*2291*	
	3	104.1	8.39	0.95	1	90.1	*2091*	*2291*	
	4	105.5	8.89	0.9	1	89.4	*2091*	*2291*	

Appendix F

MATLAB CODES

Transient_Flow_Problem_v8c.m:

```
%%%%%%%%%%%%%%%%%%%%%%%%%%%%%%%%
%---University of Washington---%
%---CRDE Lab---------------------%
%---Dan Drabiak------------------%
%---03 April 2016----------------%
%%%%%%%%%%%%%%%%%%%%%%%%%%%%%%%%

% Don't mess with this version! It works!

% This code calculates heat transfer into a cylinder
% of steel in axial flow using transient flow analysis.

% Works cited
% Cengel, Yunus A., John M. Cimbala, and Robert H. Turner. "Fundamentals of Thermal-Flui
%       Fourth Ed. New York: McGraw-Hill, 2008.
%
% Wiberg, Roland and Noam Lior, "Heat transfer from a cylinder in axial
%       turbulent flows". International Journal of Heat and Mass Transfer.
%       Available online 22 December 2004.

clear

% Choose your run
RunNumber = 166;
```

```
% Select a value from 166 through 170 or 172 through 192.
Compressible = 1;
% Set to 1 for compressible venturi meter mass flow rates,
% otherwise manifold

% Set up pulse square waves
if Compressible == 1
    TFP_MdotT_Comp;
    mDot_gs = mDot_v_gs;
else
    TFP_MdotT_Man;
    mDot_gs = mDot_m_gs;
end

% Convert mass flow to kg/s
mDot = mDot_gs*.001; % Mass flow of freestream, kg/s

% Record the number of pulses
[~,PulseNo] = size(mDot);

% Given values
P = 80000; % Pressure of frestream, Pa
TiC = 45; % Initial temperature of cylinder (e.g. air temperature), C
Ti = TiC + 273.15; % Initial temperature of cylinder, K
Ti2 = Ti; % Preserve value for later
M = 18; % Molecular mass of freestream mixture, kg/(kmol)
Mu = .00007808; % Viscosity of water, kg/(m*s), at T = 2000 C
% See Cengel, et al Table A-23
Rbar = 8314; % Universal Gas Constant, J/(kmol K), see Cengel, et al pg. 127 to verify u
R = Rbar/M; % Gas constant for working mixture, J/(kg K)
Cp = 500; % Specific heat of steel (Cengel, et al Table A-3), J/(kg K)
r1E = .25; % Radius of cylinder, inches
r1 = r1E*.0254; % Convert from inches to meters
```

```
58 r2E = 2; % Radius of test section, inches
59 r2 = r2E*.0254; % Convert from inches to meters
60 LE = 2; % Length of cylinder, inches
61 L = LE*.0254; % Convert from inches to meters
62 k = .29183; % Thermal conductivity, W/(m K) of steam at T = 2000 C
63 % See Cengel, et al Table A-23
64 t = PulseW; % Time of experiment, s
65
66 % Geometric bookkeeping
67 A1 = (r1^2)*pi; % Area of circular face of cylinder, m^2
68 A2 = 2*r1*pi*L; % Area of side of cylinder, m^2
69 A3 = (r2^2)*pi; % Cross-sectional area of cylindrical test section, m^2
70 V = A1*L; % Volume of cylinder, m^3
71
72 % Temperature bookkeeping
73 T0C = T; % Assume for now; ultimately, T0 is freestream stagnation temperature
74 T0 = T0C + 273.15; % Convert from Celsius to Kelvin
75 TC = T; % Redifine variable T while retaining old value (see next line)
76 T = TC + 273.15; % Convert from Celsius to Kelvin
77
78 % Radiative losses from thermocouple
79 T = T + 200;
80
81 % Nusselt number relations
82 u = mDot.*R.*T./(P*A3); % Freestream velocity according to continuity, m/s
83 Rho = P./(R.*T); % Density according to ideal gas law, kg/(m^3)
84 Rho_st = 8000; % Density of steel, approximate, kg/(m^3)
85 m = Rho_st*V; % Mass, kg
86 Re = Rho.*u.*2*r1/Mu; % Reynolds Number with respect to cylinder diameter
87 Nu2 = .140*(Re.^.686); % See Wiberg and Lior, Table 1, Configuration (B), section b-c
88 % Note: Config. (B) best approximation given our turbulent freestream
89
90 % Side walls of cylinder
```

```
h2 = Nu2.*k./L; % Heat transfer coefficient
b2 = h2.*A2./(m*Cp); % Exponential coefficient, 1/s
Ti = Ti2; % Reset initial temperature
Tt2 = zeros(1,PulseNo);
Q2 = zeros(1,PulseNo);
Tt2(1) = T(1) + (Ti - T(1))*exp(-b2(1)*t); % Final temperature, K
Q2(1) = m.*Cp.*(Tt2(1) - Ti); % Total heat transfer into cylinder front surface, kJ
for K = 2:PulseNo
    Ti = Tt2(K-1);
    Tt2(K) = T(K) + (Ti - T(K))*exp(-b2(K)*t); % Final temperature, K
    Q2(K) = m.*Cp.*(Tt2(K) - Ti); % Total heat transfer into cylinder front surface, kJ
end
% Tt2 = T + (Ti - T).*exp(-b2.*t); % Final temperature, K
Tt2total = Tt2(PulseNo);

% Total heat transfer into cylinder
Q = sum(Q2,2); % See above, J

% Note: Heat transfer output is "integrating as you go", i.e. total heat
% transfer into the surface up to a given point in time.

% Display results
% subplot(3,1,1)
% plot(t,Tt1,'-','Color',[0 .77 .57])
% grid on
% xlabel('Time, [s]'),ylabel('Temperature, [K]'),title('Surface Temperature on Front Sur
% subplot(3,1,2)
% plot(t,Tt2,'-','Color',[.22 .27 .51])
% grid on
% xlabel('Time, [s]'),ylabel('Temperature, [K]'),title('Surface Temperature on Side Wall
% subplot(3,1,3)
% plot(t,Q,'-','Color',[.5 .3 .8])
% grid on
```

```
124 % xlabel('Time, [s]'),ylabel('Heat Transfer, [J]'),title('Heat Transfer into Cylinder as
125 fprintf('------  Run No. %.f  ------\n',RunNumber) % Display run number
126 if Compressible == 1
127     fprintf('\nUsing compressible Venturi meter mass flow')
128 else
129     fprintf('\nUsing manifold mass flow')
130 end
131 fprintf('\nVelocity u = %.f m/s',u) % Display velocity
132 fprintf('\nTemperature along sides of cylinder T = %.f K',Tt2total) % Display temperatur
133 fprintf('\nHeat transfer Q = %.3f kJ\n\n',Q*.001) % Display heat transfer Q
```

TFP_MdotT_Comp.m:

```
1  %%%%%%%%%%%%%%%%%%%%%%%%%%%%%%%%
2  %----University of Washington----%
3  %----CRDE Lab--------------------%
4  %----Dan Drabiak-----------------%
5  %----22 April 2016---------------%
6  %%%%%%%%%%%%%%%%%%%%%%%%%%%%%%%%
7
8  % This code computes the compressible venturi meter mass flow rates and the
9  % temperatures for the file Transient_Flow_Problem_v2b.m
10
11 if RunNumber == 192
12     mDot_v_gs(1) = 93.32;
13     mDot_v_gs(2) = 103.41;
14     mDot_v_gs(3) = 104.13;
15     mDot_v_gs(4) = 105.5;
16 elseif RunNumber == 191
17     mDot_v_gs(1) = 100.31;
18     mDot_v_gs(2) = 107.3;
19     mDot_v_gs(3) = 117.6;
```

```
20      mDot_v_gs(4) = 110.9;
21  elseif RunNumber == 190
22      mDot_v_gs(1) = 127.5;
23      mDot_v_gs(2) = 120.51;
24      mDot_v_gs(3) = 106.69;
25      mDot_v_gs(4) = 109.18;
26  elseif RunNumber == 189
27      mDot_v_gs(1) = 90.85;
28      mDot_v_gs(2) = 105.54;
29      mDot_v_gs(3) = 106.94;
30      mDot_v_gs(4) = 110.44;
31  elseif RunNumber == 188
32      mDot_v_gs(1) = 105.64;
33      mDot_v_gs(2) = 106.08;
34      mDot_v_gs(3) = 112.98;
35      mDot_v_gs(4) = 115.75;
36  elseif RunNumber == 187
37      mDot_v_gs(1) = 111.96;
38      mDot_v_gs(2) = 115.2;
39      mDot_v_gs(3) = 116.14;
40      mDot_v_gs(4) = 118.5;
41  elseif RunNumber == 186
42      mDot_v_gs(1) = 108.97;
43      mDot_v_gs(2) = 115.09;
44      mDot_v_gs(3) = 119.05;
45      mDot_v_gs(4) = 118.44;
46  elseif RunNumber == 185
47      mDot_v_gs(1) = 105.83;
48      mDot_v_gs(2) = 107.88;
49      mDot_v_gs(3) = 112.5;
50      mDot_v_gs(4) = 113.04;
51  elseif RunNumber == 184
52      mDot_v_gs = 108.75;
```

```
53 elseif RunNumber == 183
54     mDot_v_gs = 101.3;
55 elseif RunNumber == 182
56     mDot_v_gs = 121.08;
57 elseif RunNumber == 181
58     mDot_v_gs(1) = 121.08;
59     mDot_v_gs(2) = 111.44;
60     mDot_v_gs(3) = 119.74;
61 elseif RunNumber == 180
62     mDot_v_gs(1) = 118.33;
63     mDot_v_gs(2) = 121.08;
64     mDot_v_gs(3) = 111.44;
65     mDot_v_gs(4) = 119.74;
66 elseif RunNumber == 179
67     mDot_v_gs(1) = 115.93;
68     mDot_v_gs(2) = 120.25;
69 elseif RunNumber == 178
70     mDot_v_gs(1) = 114.6;
71     mDot_v_gs(2) = 119.72;
72 elseif RunNumber == 177
73     mDot_v_gs(1) = 119.08;
74     mDot_v_gs(2) = 120.2;
75 elseif RunNumber == 176
76     mDot_v_gs(1) = 112.08;
77     mDot_v_gs(2) = 110.83;
78     mDot_v_gs(3) = 112.5;
79     mDot_v_gs(4) = 112.51;
80     mDot_v_gs(5) = 112.59;
81 elseif RunNumber == 175
82     mDot_v_gs(1) = 95.28;
83     mDot_v_gs(2) = 90.7;
84     mDot_v_gs(3) = 94.74;
85     mDot_v_gs(4) = 94.54;
```

```
86      mDot_v_gs(5) = 94.16;
87  elseif RunNumber == 174
88      mDot_v_gs(1) = 97.37;
89      mDot_v_gs(2) = 98.84;
90      mDot_v_gs(3) = 94.94;
91      mDot_v_gs(4) = 97.44;
92      mDot_v_gs(5) = 95.97;
93  elseif RunNumber == 173
94      mDot_v_gs(1) = 100.29;
95      mDot_v_gs(2) = 99.93;
96      mDot_v_gs(3) = 104.37;
97      mDot_v_gs(4) = 103.6;
98      mDot_v_gs(5) = 105.95;
99  elseif RunNumber == 172
100     mDot_v_gs(1) = 107;
101     mDot_v_gs(2) = 106.66;
102     mDot_v_gs(3) = 104.59;
103     mDot_v_gs(4) = 105.87;
104     mDot_v_gs(5) = 101.88;
105 elseif RunNumber == 170
106     mDot_v_gs(1) = 105.37;
107     mDot_v_gs(2) = 103.94;
108     mDot_v_gs(3) = 107.31;
109     mDot_v_gs(4) = 107.13;
110 elseif RunNumber == 169
111     mDot_v_gs(1) = 102.17;
112     mDot_v_gs(2) = 107.85;
113     mDot_v_gs(3) = 102.09;
114     mDot_v_gs(4) = 105.27;
115 elseif RunNumber == 168
116     mDot_v_gs(1) = 106.93;
117     mDot_v_gs(2) = 109.18;
118     mDot_v_gs(3) = 108.39;
```

```
119     mDot_v_gs(4) = 109.93;
120 elseif RunNumber == 167
121     mDot_v_gs(1) = 111.54;
122     mDot_v_gs(2) = 109.06;
123     mDot_v_gs(3) = 111.03;
124     mDot_v_gs(4) = 108.11;
125 elseif RunNumber == 166
126     mDot_v_gs(1) = 111.11;
127     mDot_v_gs(2) = 111.83;
128     mDot_v_gs(3) = 111.97;
129     mDot_v_gs(4) = 109.24;
130 end
131 
132 % Now do it all over again for temperature, you lucky duck.
133 if RunNumber == 192
134     T(1) = 1785;
135     T(2) = 1997;
136     T(3) = 2091;
137     T(4) = 2091;
138 elseif RunNumber == 191
139     T(1) = 1785;
140     T(2) = 1997;
141     T(3) = 2091;
142     T(4) = 2091;
143 elseif RunNumber == 190
144     T(1) = 2109;
145     T(2) = 1724;
146     T(3) = 1700;
147     T(4) = 1796;
148 elseif RunNumber == 189
149     T(1) = 2104;
150     T(2) = 2148;
151     T(3) = 2148;
```

```
152     T(4) = 2148;
153 elseif RunNumber == 188
154     T(1) = 1846;
155     T(2) = 2013;
156     T(3) = 2000;
157     T(4) = 2068;
158 elseif RunNumber == 187
159     T(1) = 2225;
160     T(2) = 2242;
161     T(3) = 2242;
162     T(4) = 2242;
163 elseif RunNumber == 186
164     T(1) = 2094;
165     T(2) = 2088;
166     T(3) = 2143;
167     T(4) = 2143;
168 elseif RunNumber == 185
169     T(1) = 2121;
170     T(2) = 2121;
171     T(3) = 2121;
172     T(4) = 2121;
173 elseif RunNumber == 184
174     T = 2079;
175 elseif RunNumber == 183
176     T = 1997;
177 elseif RunNumber == 182
178     T = 2180;
179 elseif RunNumber == 181
180     T(1) = 2180;
181     T(2) = 2266;
182     T(3) = 2011;
183 elseif RunNumber == 180
184     T(1) = 2139;
```

```
185      T(2) = 2199;
186      T(3) = 2199;
187      T(4) = 2199;
188  elseif RunNumber == 179
189      T(1) = 2134;
190      T(2) = 2164;
191  elseif RunNumber == 178
192      T(1) = 2167;
193      T(2) = 2156;
194  elseif RunNumber == 177
195      T(1) = 2089;
196      T(2) = 2121;
197  elseif RunNumber == 176
198      T(1) = 2048;
199      T(2) = 2048;
200      T(3) = 2048;
201      T(4) = 2048;
202      T(5) = 2048;
203  elseif RunNumber == 175
204      T(1) = 2060;
205      T(2) = 2062;
206      T(3) = 2077;
207      T(4) = 2088;
208      T(5) = 2095;
209  elseif RunNumber == 174
210      T(1) = 2079;
211      T(2) = 2113;
212      T(3) = 2145;
213      T(4) = 2141;
214      T(5) = 2141;
215  elseif RunNumber == 173
216      T(1) = 2079;
217      T(2) = 2113;
```

```
218      T(3) = 2145;
219      T(4) = 2141;
220      T(5) = 2141;
221  elseif RunNumber == 172
222      T(1) = 2079;
223      T(2) = 2113;
224      T(3) = 2145;
225      T(4) = 2141;
226      T(5) = 2141;
227  elseif RunNumber == 170
228      T(1) = 2092;
229      T(2) = 2092;
230      T(3) = 2092;
231      T(4) = 2092;
232  elseif RunNumber == 169
233      T(1) = 2208;
234      T(2) = 2208;
235      T(3) = 2208;
236      T(4) = 2208;
237  elseif RunNumber == 168
238      T(1) = 2068;
239      T(2) = 2102;
240      T(3) = 2102;
241      T(4) = 2102;
242  elseif RunNumber == 167
243      T(1) = 2068;
244      T(2) = 2102;
245      T(3) = 2102;
246      T(4) = 2102;
247  else
248      T(1) = 2068;
249      T(2) = 2102;
250      T(3) = 2102;
```

```
251     T(4) = 2102;
252 end
253
254 if RunNumber < 182
255     PulseW = .7;
256 else
257     PulseW = 1;
258 end
```

TFP_MdotT_Man.m:

```
1  %%%%%%%%%%%%%%%%%%%%%%%%%%%%%%%%
2  %---University of Washington---%
3  %---CRDE Lab---------------------%
4  %---Dan Drabiak------------------%
5  %---22 April 2016----------------%
6  %%%%%%%%%%%%%%%%%%%%%%%%%%%%%%%%
7
8  % This code computes the manifold mass flow rates and the temperatures for
9  % the file Transient_Flow_Problem_v2b.m
10
11 if RunNumber == 192
12     mDot_m_gs(1) = 126.3;
13     mDot_m_gs(2) = 110.8;
14     mDot_m_gs(3) = 106.16;
15     mDot_m_gs(4) = 102.32;
16 elseif RunNumber == 191
17     mDot_m_gs(1) = 108.51;
18     mDot_m_gs(2) = 109.98;
19     mDot_m_gs(3) = 106.05;
20     mDot_m_gs(4) = 96.48;
21 elseif RunNumber == 190
```

```
22      mDot_m_gs(1) = 134.67;
23      mDot_m_gs(2) = 126.09;
24      mDot_m_gs(3) = 123.24;
25      mDot_m_gs(4) = 120.23;
26  elseif RunNumber == 189
27      mDot_m_gs(1) = 144.47;
28      mDot_m_gs(2) = 139.19;
29      mDot_m_gs(3) = 135.56;
30      mDot_m_gs(4) = 127.81;
31  elseif RunNumber == 188
32      mDot_m_gs(1) = 134.02;
33      mDot_m_gs(2) = 142.69;
34      mDot_m_gs(3) = 135.06;
35      mDot_m_gs(4) = 130.37;
36  elseif RunNumber == 187
37      mDot_m_gs(1) = 127.34;
38      mDot_m_gs(2) = 128.53;
39      mDot_m_gs(3) = 129.43;
40      mDot_m_gs(4) = 124.58;
41  elseif RunNumber == 186
42      mDot_m_gs(1) = 137.83;
43      mDot_m_gs(2) = 130.5;
44      mDot_m_gs(3) = 128.24;
45      mDot_m_gs(4) = 126.66;
46  elseif RunNumber == 185
47      mDot_m_gs(1) = 142.41;
48      mDot_m_gs(2) = 141.46;
49      mDot_m_gs(3) = 139.79;
50      mDot_m_gs(4) = 138.63;
51  elseif RunNumber == 184
52      mDot_m_gs = 137.54;
53  elseif RunNumber == 183
54      mDot_m_gs = 144.12;
```

```
55 elseif RunNumber == 182
56     mDot_m_gs(1) = 147.21;
57 elseif RunNumber == 181
58     mDot_m_gs(1) = 147.21;
59     mDot_m_gs(2) = 138.15;
60     mDot_m_gs(3) = 136.79;
61 elseif RunNumber == 180
62     mDot_m_gs(1) = 139.6;
63     mDot_m_gs(2) = 147.21;
64     mDot_m_gs(3) = 138.15;
65     mDot_m_gs(4) = 136.79;
66 elseif RunNumber == 179
67     mDot_m_gs(1) = 140.47;
68     mDot_m_gs(2) = 142.87;
69 elseif RunNumber == 178
70     mDot_m_gs(1) = 140.66;
71     mDot_m_gs(2) = 144.57;
72 elseif RunNumber == 177
73     mDot_m_gs(1) = 141.34;
74     mDot_m_gs(2) = 145.78;
75 elseif RunNumber == 176
76     mDot_m_gs(1) = 133.46;
77     mDot_m_gs(2) = 134.26;
78     mDot_m_gs(3) = 134.79;
79     mDot_m_gs(4) = 134.86;
80     mDot_m_gs(5) = 134.61;
81 elseif RunNumber == 175
82     mDot_m_gs(1) = 118.55;
83     mDot_m_gs(2) = 119.29;
84     mDot_m_gs(3) = 118.43;
85     mDot_m_gs(4) = 117.1;
86     mDot_m_gs(5) = 116.7;
87 elseif RunNumber == 174
```

```
88      mDot_m_gs(1) = 121.35;
89      mDot_m_gs(2) = 123.54;
90      mDot_m_gs(3) = 123;
91      mDot_m_gs(4) = 122.98;
92      mDot_m_gs(5) = 121.79;
93  elseif RunNumber == 173
94      mDot_m_gs(1) = 123.63;
95      mDot_m_gs(2) = 124.41;
96      mDot_m_gs(3) = 124.83;
97      mDot_m_gs(4) = 124.02;
98      mDot_m_gs(5) = 123.18;
99  elseif RunNumber == 172
100     mDot_m_gs(1) = 124.49;
101     mDot_m_gs(2) = 128.55;
102     mDot_m_gs(3) = 126.59;
103     mDot_m_gs(4) = 124.99;
104     mDot_m_gs(5) = 124.76;
105 elseif RunNumber == 170
106     mDot_m_gs(1) = 130.86;
107     mDot_m_gs(2) = 128.39;
108     mDot_m_gs(3) = 128.28;
109     mDot_m_gs(4) = 127.03;
110 elseif RunNumber == 169
111     mDot_m_gs(1) = 135.24;
112     mDot_m_gs(2) = 131.78;
113     mDot_m_gs(3) = 131.47;
114     mDot_m_gs(4) = 130.86;
115 elseif RunNumber == 168
116     mDot_m_gs(1) = 136.8;
117     mDot_m_gs(2) = 133.35;
118     mDot_m_gs(3) = 132.62;
119     mDot_m_gs(4) = 132.18;
120 elseif RunNumber == 167
```

```
121      mDot_m_gs(1) = 139.5;
122      mDot_m_gs(2) = 135.6;
123      mDot_m_gs(3) = 134.34;
124      mDot_m_gs(4) = 134.61;
125  elseif RunNumber == 166
126      mDot_m_gs(1) = 129.29;
127      mDot_m_gs(2) = 134.54;
128      mDot_m_gs(3) = 134.71;
129      mDot_m_gs(4) = 133.43;
130  end
131
132  % Now do it all over again for temperature, you lucky duck.
133  if RunNumber == 192
134      T(1) = 1785;
135      T(2) = 1997;
136      T(3) = 2091;
137      T(4) = 2091;
138  elseif RunNumber == 191
139      T(1) = 1785;
140      T(2) = 1997;
141      T(3) = 2091;
142      T(4) = 2091;
143  elseif RunNumber == 190
144      T(1) = 2109;
145      T(2) = 1724;
146      T(3) = 1700;
147      T(4) = 1796;
148  elseif RunNumber == 189
149      T(1) = 2104;
150      T(2) = 2148;
151      T(3) = 2148;
152      T(4) = 2148;
153  elseif RunNumber == 188
```

```
154      T(1) = 1846;
155      T(2) = 2013;
156      T(3) = 2000;
157      T(4) = 2068;
158  elseif RunNumber == 187
159      T(1) = 2225;
160      T(2) = 2242;
161      T(3) = 2242;
162      T(4) = 2242;
163  elseif RunNumber == 186
164      T(1) = 2094;
165      T(2) = 2088;
166      T(3) = 2143;
167      T(4) = 2143;
168  elseif RunNumber == 185
169      T(1) = 2121;
170      T(2) = 2121;
171      T(3) = 2121;
172      T(4) = 2121;
173  elseif RunNumber == 184
174      T(1) = 2079;
175  elseif RunNumber == 183
176      T(1) = 1997;
177  elseif RunNumber == 182
178      T(1) = 2180;
179  elseif RunNumber == 181
180      T(1) = 2180;
181      T(2) = 2266;
182      T(3) = 2011;
183  elseif RunNumber == 180
184      T(1) = 2139;
185      T(2) = 2199;
186      T(3) = 2199;
```

```
187     T(4) = 2199;
188 elseif RunNumber == 179
189     T(1) = 2134;
190     T(2) = 2164;
191 elseif RunNumber == 178
192     T(1) = 2167;
193     T(2) = 2156;
194 elseif RunNumber == 177
195     T(1) = 2089;
196     T(2) = 2121;
197 elseif RunNumber == 176
198     T(1) = 2048;
199     T(2) = 2048;
200     T(3) = 2048;
201     T(4) = 2048;
202     T(5) = 2048;
203 elseif RunNumber == 175
204     T(1) = 2060;
205     T(2) = 2062;
206     T(3) = 2077;
207     T(4) = 2088;
208     T(5) = 2095;
209 elseif RunNumber == 174
210     T(1) = 2079;
211     T(2) = 2113;
212     T(3) = 2145;
213     T(4) = 2141;
214     T(5) = 2141;
215 elseif RunNumber == 173
216     T(1) = 2079;
217     T(2) = 2113;
218     T(3) = 2145;
219     T(4) = 2141;
```

```
220     T(5) = 2141;
221 elseif RunNumber == 172
222     T(1) = 2079;
223     T(2) = 2113;
224     T(3) = 2145;
225     T(4) = 2141;
226     T(5) = 2141;
227 elseif RunNumber == 171
228     fprintf('Lost run')
229 elseif RunNumber == 170
230     T(1) = 2092;
231     T(2) = 2092;
232     T(3) = 2092;
233     T(4) = 2092;
234 elseif RunNumber == 169
235     T(1) = 2208;
236     T(2) = 2208;
237     T(3) = 2208;
238     T(4) = 2208;
239 elseif RunNumber == 168
240     T(1) = 2068;
241     T(2) = 2102;
242     T(3) = 2102;
243     T(4) = 2102;
244 elseif RunNumber == 167
245     T(1) = 2068;
246     T(2) = 2102;
247     T(3) = 2102;
248     T(4) = 2102;
249 else
250     T(1) = 2068;
251     T(2) = 2102;
252     T(3) = 2102;
```

```
253     T(4) = 2102;
254 end
255
256 if RunNumber < 182
257     PulseW = .7;
258 else
259     PulseW = 1;
260 end
```

SWR_Modeling_Function.m:

```
1  %%%%%%%%%%%%%%%%%%%%%%%%%%%%%%%%%%%%%%%%
2  %---Dan Drabiak-------------------------%
3  %---University of Washington-----------%
4  %---RDE Modeling Function---------------%
5  %---File started: Mar 24, 2017---------%
6  %---Last update: Jun 17, 2017----------%
7  %%%%%%%%%%%%%%%%%%%%%%%%%%%%%%%%%%%%%%%%
8
9  % Don't mess with this version of the code. It works!
10
11 % This is the base version of the code from which all of the variants used for
12 % the final calculations were derived. The nuts and bolts are the same
13 % throughout; it's just some of the input conditions that vary, and thus
14 % require slight modifications.
15
16 % Note: This code assumes isentropic flow; thus, oblique shocks and
17 % expansion fans are ignored.
18
19 % References:
20 % 1. Anderson, John D., Jr. "Fundamentals of Aerodynamics". Fifth Ed. New
21 % York: McGraw-Hill, 2011.
```

```
% 2. Cengel, Yunus A., et al. "Fundamentals of Thermal—Fluid Sciences".
% Fourth Ed. New York: McGraw—Hill, 2012.
% 3. Hill, Philip G. and Carl R. Peterson. "Mechanics and Thermodynamics of
% Propulsion". Menlo Park, California: Addison—Wesley Publishing Company,
% 1970.
% 4. Seitzman, Jerry M. Various notes from AE3450 course at Georgia Tech.
% 5. Oates, Gordon C. "Aerothermodynamics of Gas Turbine and Rocket
% Propulsion". Washington, DC: AIAA Education Series, 1988.
% 6. Sutton, George P. and Oscar Biblarz. "Rocket Propulsion Elements".
% Hoboken, NJ: John Wiley & Sons, Inc., 2010.
% 7. Moran, Michael J., Howard N. Shapiro, Daisie D. Boettner, and
% Margaret B. Bailey. "Fundamentals of Engineering Thermodynamics".
% Seventh Edition. Hoboken, NJ: John Wiley & Sons, Inc., 2011.
% 8. Shapiro, Ascher H. "The Dynamics and Thermodynamics of Compressible
% Fluid Flow". Vol. I. New York: The Ronald Press Company, 1953.
% 9. Knowlen, Carl. "Theoretical and Experimental Investigation of the
% Thermodynamics of the Thermally Choked Ram Accelerator". PhD
% Dissertation, University of Washington, 1991.

close all; clear

ShockStation = '3';
% Determine station of the normal shock that approximates the oblique
% shock train.
% Possible values are '4' for the 4" duct and '3' for the 3" duct.

I2M = .0254; % Inches to meters conversion factor; 1 inch = .0254 meters
M2I = 1./I2M; % Meters to inchess conversion factor; 1 inch = .0254 meters

% Outer radius of the point at the beginning of each station, in inches
r(1) = 2;
r(2) = 2;
r(3) = (.0397/2).*M2I;
```

```
55 r(4) = 1.5;
56 r(5) = 1.5;
57 r(6) = 2;
58 r(7) = 2;
59
60 % Axial coordinates of each point, in inches
61 x(1) = 0;
62 x(2) = 1/I2M;
63 x(3) = x(2) + 2.5;
64 x(4) = x(3) + 1.5*sqrt(3);
65 x(5) = x(4) + .22/I2M;
66 x(6) = x(5);
67 x(7) = x(6) + 1/I2M;
68
69 xthroat = x(3);
70
71 NS = length(r); % Number of corners
72
73 % Axial length of each station, in inches
74 L = zeros(NS,1);
75 L(1) = x(1);
76 for j = 2:NS
77     L(j) = x(j) - x(j-1);
78 end
79
80 % Convert everything to SI units
81 r = r.*I2M;
82 x = x.*I2M;
83 L = L.*I2M;
84
85 NP = 2000; % Multiplier per each increment
86
87 % Outer radius as a function of axial length, m
```

```
88  Rc = cell(NS-1,1);
89  for j = 1:NS-1
90      Rc{j} = linspace(r(j),r(j+1),round(L(j+1)*NP));
91  end
92
93  % Cumulative length vector
94  Lc = cell(NS,1);
95  Lc{1} = 0;
96  for j = 2:NS
97      Lc{j} = length(Rc{j-1}) + Lc{j-1};
98  end
99
100 % Outer radius vector
101 % Rv(1:length(Rc{1})) = Rc{1};
102 for j = 1:NS-1
103     Rv(Lc{j} + 1:Lc{j+1}) = Rc{j};
104 end
105
106 for j = 1:NS-1
107     X(Lc{j}+1:Lc{j+1}) = linspace(x(j),x(j+1),Lc{j+1}-Lc{j}); % Axial position vector, m
108 end
109
110 %---Define circular subsonic region of throat---%
111
112 rstar_m = r(3); % Throat radius, m
113 rcurv = r(2)-r(3); % Radius of curvature, m
114 kcircle = rcurv + rstar_m; % y-co-ordinate of the center of the circle, m
115 y_ne = r(2); % y-co-ordinate of the entrance of the nozzle, m
116 jcircle = L(2) + rcurv;
117 % jcircle = L(2) + sqrt((rcurv^2)-((y_ne - rcurv - rstar_m)^2));
118
119 %---Re-define geometry to include circular region---%
120
```

```
121 % Axial coordinates of each point, in inches
122 x(1) = 0;
123 x(2) = 1/I2M;
124 x(3) = jcircle*M2I;
125 x(4) = x(2) + 4.925; % From drawings
126 x(5) = x(4) + .22/I2M;
127 x(6) = x(5);
128 x(7) = x(6) + 1/I2M;
129
130 xthroat = x(3);
131
132 % Axial length of each station, in inches
133 L = zeros(NS,1);
134 L(1) = x(1);
135 for j = 2:NS
136     L(j) = x(j) - x(j-1);
137 end
138
139 % Convert everything to SI units
140 x = x.*I2M;
141 L = L.*I2M;
142
143 NP = 2000; % Multiplier per each increment
144
145 % Outer radius as a function of axial length, m
146 Rc = cell(NS-1,1);
147 for j = 1:NS-1
148     Rc{j} = linspace(r(j),r(j+1),round(L(j+1)*NP));
149 end
150
151 % Cumulative length vector
152 Lc = cell(NS,1);
153 Lc{1} = 0;
```

```
154 for j = 2:NS
155     Lc{j} = length(Rc{j-1}) + Lc{j-1};
156 end
157
158 % Outer radius vector
159 % Rv(1:length(Rc{1})) = Rc{1};
160 for j = 1:NS-1
161     Rv(Lc{j} + 1:Lc{j+1}) = Rc{j};
162 end
163
164 for j = 1:NS-1
165     X(Lc{j}+1:Lc{j+1}) = linspace(x(j),x(j+1),Lc{j+1}-Lc{j}); % Axial position vector, m
166 end
167
168 Rv = real(Rv);
169
170 ycurv = kcircle - sqrt((rcurv^2)-((X(Lc{2}:Lc{3}) - jcircle).^2));
171 y2 = Rv;
172 y2(Lc{2}:Lc{3}) = ycurv;
173 Rv = y2;
174 Rv(Lc{3}) = rstar_m;
175
176 Rv = real(Rv);
177 NT = length(Rv);
178 % Corrected total number of points to account for rounding when calculating
179 % Rx vector
180
181 % Define index of the nozzle entrance in the X vector, among other vectors.
182 for j = 1:NT
183     if X(j) == L(2)
184         Idx2 = j;
185     end
186 end
```

```
187
188 %---End circular region---%
189
190 % Define index of the exit of the diffuser in the X vector, among other vectors.
191 Idx4 = Lc{4};
192
193 % Define index of the exit of the diffuser in the X vector, among other vectors.
194 Idx5 = Lc{5};
195
196 dx = x(end)/NT; % Length increment from one point to the next, in
197 %[~,Idx3] = (min(abs(Rv)));
198 Idx3 = Lc{3};
199 % Index of the throat in the X vector, among other vectors
200
201 Rv = Rv';
202
203 %---Input Conditions---%
204 mdotH2O = .06367; % Mass flow rate of steam, kg/s
205 % phi = 1.49; % Equivalence Ratio, []
206 mdotO2_tot = .17346;
207 % Mass flow rate of O2, kg/s
208 mdotH2_tot = .03787;
209 % Mass flow rate of H2, kg/s
210 mdotinj = mdotO2_tot + mdotH2_tot; % Mass flow rate of H2 and O2, kg/s
211 mdotinf = mdotH2O + mdotinj;
212 mdotinf_g = 1000*mdotinf; % Freestream mass flow rate, g/s
213 T0inf_C = 730; % Freestream temperature, degrees C
214 P0inf_kPa = 370; % Freestream pressure, kPa
215 gamma = 1.22; % Ratio of specific heats, []
216 rstar = .0397/2; % Radius of the throat, m
217 MWH2O = 18; % Molecular weight, kg/kmol
218 Ts_C = 150; % Temperature of the wall, degrees C
219 Z = mdotinj/mdotinf; % Proportion by mass of (2H2+O2) in the H2O, H2, and O2 mixture.
```

```
220 % Note: Z ranges from 0 to 1.
221 mdotH2_extra_g = 0; % Extra amount of H2 beyond stoichiometric amount, g/s
222 mdot4 = .106; % Mass flow of injectant, kg/s
223 %---End Input Conditions---%
224
225 %---Universal Constants---%
226 Rbar = 8314; % Universal gas law constant, J/(kmol K)
227 Patm = 101325; % Standard atmospheric pressure, Pa
228 %---End Universal Constants---%
229
230 mdotinf = mdotinf_g./1000; % Freestream mass flow rate, kg/s
231 Ts = Ts_C + 273.15; % Wall temperature, K
232 T0inf = T0inf_C + 273.15; % Freestream temperature, K
233 P0inf = P0inf_kPa*1000; % Freestream pressure, Pa
234 P0inf_bar = P0inf_kPa/100; % Freestream pressure, bar
235 % rstar = rstar_in*I2M;
236 % Convert radius of the throat to meters
237 Astar = pi*(rstar^2); % Area of the throat, m^2
238 RH2O = Rbar/MWH2O; % Gas constant for freestream mixture, J/(kg K)
239
240 A = pi.*(Rv.^2); % Cross-sectional area, m^2
241 A2 = 2.*pi.*Rv.*dx; % Circumferential area, m^2
242 rho0inf = P0inf./(RH2O.*T0inf); % Freestream density, kg/(m^3)
243 Uinf = mdotinf./(rho0inf.*A(1)); % Freestream velocity, m/s
244
245 % Intermediate constants to make the code less jumbled
246 B = 2/(gamma+1);
247 C = (gamma-1)/2;
248 G = (gamma+1)/(2.*(gamma-1));
249
250 Cp = (gamma*RH2O)/(gamma-1); % Specific heat at constant pressure, same units as R
251 Cv = RH2O/(gamma-1); % Specific heat at constant volume, same units as R
252
```

```
253 ainf = sqrt(gamma.*RH2O.*T0inf); % Speed of sound at the inlet, m/s
254 Minf = Uinf./ainf; % Freestream Mach number, []
255
256 Marea = .001:.001:5;
257 Marea = Marea';
258 Amach = (Astar./Marea).*((B.*(1+C.*Marea.^2)).^G);
259 % Produce a range of areas for all possible Mach numbers over an interval
260 % of .001 from 0 to 5.
261
262 IdxM1 = find(Marea == 1);
263 M(1:Idx3) = interp1(Amach(1:IdxM1),Marea(1:IdxM1),A(1:Idx3));
264 M(Idx3+1:Idx5) = interp1(Amach(IdxM1:end),Marea(IdxM1:end),A(Idx3+1:Idx5));
265
266 % However, it does account for a normal shock at the end of the feedstock
267 % injector:
268 Mps = ((1+((gamma-1)/2).*M(Idx5).^2)./((gamma.*M(Idx5).^2)-...
269     ((gamma-1)/2))).^.5;
270 % Post-shock Mach number, []
271 M(Idx5+1:NT) = Mps*ones(NT-Idx5,1);
272 % From Anderson, pg. 597
273
274 M = M';
275
276 T = T0inf./(1+C.*(M.^2)); % Stagnation temperature, K
277 P = P0inf./((1+C.*(M.^2)).^(gamma/(gamma-1))); % Stagnation pressure, Pa
278 rho = rho0inf.*((1+C.*(M.^2)).^(1/(gamma-1))); % Stagnation density, kg/(m^3)
279 % Remember, this code assumes no oblique shockwaves!
280
281 Pps = P(Idx5).*(1+((1.*gamma)./(gamma+1))*((M(Idx5).^2) - 1));
282 P(Idx5+1:end) = Pps.*ones(NT-Idx5,1);
283
284 rhops = rho(Idx5).*( ((gamma + 1).*M(Idx5).^2)./...
285     (2 + (gamma - 1).*M(Idx5).^2) );
```

```
286 rho(Idx5+1:end) = rhops.*ones(NT-Idx5,1);
287
288 %---H2 and O2 insertion in combustor---%
289
290 OFst = 8; % Stoichiometric O/F ratio for H2 and O2
291 OF = mdotO2_tot/mdotH2_tot;
292 % Oxidizer to fuel ratio for H2 and O2 at entrance
293
294     if OF > OFst
295         mdotH2_extra = 0;
296         mdotO2_extra = ((OF-OFst)/OF)*mdotO2_tot;
297     elseif OF < OFst
298         mdotH2_extra = ((OFst-OF)/OFst)*mdotH2_tot;
299         mdotO2_extra = 0;
300     elseif OF == OFst
301         mdotH2_extra = 0;
302         mdotO2_extra = 0;
303     end
304
305     mdotH2 = mdotH2_tot - mdotH2_extra;
306     mdotO2 = mdotO2_tot - mdotO2_extra;
307     mdotSteam = mdotinf - mdotH2_extra - mdotO2_extra;
308
309     gammaH2 = 1.405; % From Table A-20 on pg. 925 in 7.
310     MWH2 = 2; % Molecular mass of H2, g/mol
311     MH2 = 1; % Mach number of injectant, []
312     % Assume injectant enters at sonic velocity
313
314     gammaO2 = 1.395; % From Table A-20 on pg. 925 in 7.
315     MWO2 = 16; % Molecular mass of O2, g/mol
316     MO2 = 1; % Mach number of incoming freestream, []
317     % Assume adiabatic isentropic Mach number for now.
318
```

```
319     MWH2O = 18; % Molecular mass of O2, g/mol
320     MH2O = M(1); % Mach number of incoming freestream, []
321     % Assume adiabatic isentropic Mach number for now.
322
323     ndotH2 = mdotH2/MWH2; % Molar flow rate of H2, kmol/s
324     ndotO2 = mdotO2/MWO2; % Molar flow rate of O2, kmol/s
325     ndotH2O = mdotH2O/MWH2O; % Molar flow rate of steam, kmol/s
326
327     ndotH2_tot = mdotH2_tot/MWH2; % Molar flow rate of H2, kmol/s
328     ndotO2_tot = mdotO2_tot/MWO2; % Molar flow rate of O2, kmol/s
329
330     ndot_tot = ndotH2_tot + ndotO2_tot + ndotH2O; % Total molar flow rate, kmol/s
331
332     ndotH2_extra = mdotH2_extra/MWH2; % Molar flow rate of H2, kmol/s
333     ndotO2_extra = mdotO2_extra/MWO2; % Molar flow rate of O2, kmol/s
334
335     yH2 = ndotH2/ndot_tot;
336     yO2 = ndotO2/ndot_tot;
337     yH2O = ndotH2O/ndot_tot;
338
339     yH2_tot = ndotH2_tot/ndot_tot;
340     yO2_tot = ndotO2_tot/ndot_tot;
341
342     yH2_extra = ndotH2_extra/ndot_tot;
343     yO2_extra = ndotO2_extra/ndot_tot;
344
345     PH2 = yH2*P0inf; % Partial pressure of H2, Pa
346     PO2 = yO2*P0inf; % Partial pressure of O2, Pa
347     PH2O = P0inf*(1 - yH2_tot - yO2_tot);  % Partial pressure of steam, Pa
348     PSteam = P0inf*(1 - yH2_extra - yO2_extra);
349
350     PH2_extra = yH2_extra*P0inf; % Partial pressure of H2, Pa
351     PO2_extra = yO2_extra*P0inf; % Partial pressure of O2, Pa
```

```
352
353      PH2_bar = PH2/100000;
354      PO2_bar = PO2/100000;
355      PH2O_bar = PH2O/100000;
356      PSteam_bar = PSteam/100000;
357      % Convert pressures from Pascals to bar
358
359      PH2_extra_bar = PH2_extra/100000;
360      PO2_extra_bar = PO2_extra/100000;
361
362      RH2 = Rbar./MWH2; % Gas law constant for injectant
363      RO2 = Rbar./MWO2; % Gas law constant for injectant
364
365      CH2 = (gammaH2-1)/2;
366      BH2 = 2/(gammaH2+1);
367      GH2 = (gammaH2+1)/(2*(gammaH2-1));
368
369      % Remember, these are intermediate variables to make the code less
370      % jumbled.
371      CO2 = (gammaO2-1)/2;
372      BO2 = 2/(gammaO2+1);
373      GO2 = (gammaO2+1)/(2*(gammaO2-1));
374
375  Tatm = 298.15; % Atmospheric temperature, K
376  TH2 = Tatm;
377  TO2 = Tatm;
378
379  CEAout2 = CEA('problem','hp','frozen','p,bar',P0inf_bar,...
380              'reactants','name','H2O(g)','H',2,'O',1,...
381              'wt%',mdotH2O,'t(K)',T0inf,'name','H2(g)','H',2,...
382              'wt%',mdotH2_tot,'t(K)',TH2,'name','O2(g)','O',2,...
383              'wt%',mdotO2_tot,'t(K)',TO2,...
384              'output','transport','short','end');
```

```
385         % Run CEAM
386         Cp2_kJ = CEAout2.output.cp_tran.froz; % Specific heat at constant pressure, [kJ/
387         Cp2 = Cp2_kJ.*1000; % Convert to J/(kg*K)
388         mu2 = CEAout2.output.viscosity./10000; % Dynamic Viscosity, kg/(m*s)
389         % Note that default output from CEAM is in millipoise.
390         % 10 P = 1 kg/(m*s), 1 P = 1000 mP
391         cond2 = CEAout2.output.conduct.froz*.1; % Conductive heat transfer coefficient,
392         % Note that the default output from CEAM is in mW/(cm*K)
393         Pr2 = CEAout2.output.prandtl.froz; % Specific heat at constant pressure, kJ/(kg*
394         gamma2 = CEAout2.output.gamma; % Ratio of specific heats from CEAM, []
395         rho02 = CEAout2.output.density; % Density, kg/(m^3)
396         MW2 = CEAout2.output.mw; % Molecular weight, check units
397         % Educated guess based on order of magnitude (10^1): kg/kmol
398         a2 = CEAout2.output.sonvel; % Sonic velocity, m/s
399         Tad = CEAout2.output.temperature;
400         % Adiabatic flame temperature of mixture, K
401         h2_kJ = CEAout2.output.enthalpy; % Specific enthalpy, kJ/kg
402         h2 = h2_kJ.*1000; % Convert specific enthalpy to J/kg
403
404         R2 = Rbar/MW2;
405
406 % Intermediate constants to make the code less jumbled
407 B2 = 2/(gamma2+1);
408 C2 = (gamma2-1)/2;
409 G2 = (gamma2+1)/(2.*(gamma2-1));
410
411 % Define indices of possible shock locations
412 IdxShk3 = round((Idx4 + Idx5)/2);
413 % Assumes shock occurs halfway through the feedstock injector section
414 IdxShk4 = round((Idx5 + NT)/2);
415 % Assumes shock occurs halfway through the mixer section
416
417 Amach2 = (Astar./Marea).*((B2.*(1+C2.*Marea.^2)).^G2);
```

```
418
419 if strcmp(ShockStation,'4') == 1
420 M2(1:Idx3)= interp1(Amach2(1:IdxM1),Marea(1:IdxM1),A(1:Idx3));
421 M2(Idx3+1:IdxShk4) = interp1(Amach2(IdxM1:end),Marea(IdxM1:end),A(Idx3+1:IdxShk4));
422
423 % Account for a normal shock midway through the mixer section:
424 Mps2_b = ((1+C2.*M2(IdxShk4).^2)./((gamma2.*M2(IdxShk4).^2)-C2)).^.5;
425 % Post-shock Mach number, []
426 M2(IdxShk4+1:NT) = Mps2_b*ones(NT-IdxShk4,1);
427 % From Anderson, pg. 597
428
429 M2 = M2';
430
431 T2 = Tad./(1+C2.*(M2.^2)); % Static temperature, K
432 P2 = P0inf./((1+C2.*(M2.^2)).^(gamma2/(gamma2-1))); % Static pressure, Pa
433
434 Pratio2 = (1+((2.*gamma2)./(gamma2+1))*((M2(IdxShk4).^2) - 1));
435 Pps2 = Pratio2*P2(IdxShk4);
436 P2(IdxShk4+1:end) = Pps2.*ones(NT-IdxShk4,1);
437
438 rho2 = P2./(R2.*T2); % Static density, kg/(m^3)
439
440 elseif strcmp(ShockStation,'3') == 1
441
442 M3(1:Idx3)= interp1(Amach2(1:IdxM1),Marea(1:IdxM1),A(1:Idx3));
443 M3(Idx3+1:IdxShk3) = interp1(Amach2(IdxM1:end),Marea(IdxM1:end),A(Idx3+1:IdxShk3));
444
445 % Account for a normal shock midway through the feedstock injector:
446 Mps3 = ((1+C2.*M3(IdxShk3).^2)./((gamma2.*M3(IdxShk3).^2)-C2)).^.5;
447 % Post-shock Mach number, []
448 M3(IdxShk3+1:NT) = Mps3*ones(NT-IdxShk3,1);
449 % From Anderson, pg. 597
450
```

```
451 M3 = M3';
452
453 P3 = P0inf./((1+C2.*(M3.^2)).^(gamma2/(gamma2-1))); % Static pressure, Pa
454
455 Pratio3 = (1+((2.*gamma2)./(gamma2+1))*((M3(IdxShk3).^2) - 1));
456 Pps3 = Pratio3*P3(IdxShk3);
457 P3(IdxShk3+1:end) = Pps3.*ones(NT-IdxShk3,1);
458
459 % Calculate the Mach number post area expansion (pae = post area
460 % expansion).
461 Mpaetest = M3(Idx5+1);
462 Mpae = 0;
463 while abs(Mpae - Mpaetest) > .00002
464     Mpae = M3(Idx5).*(A(Idx5)./A(Idx5+1)).*( ((1 + C2.*M3(Idx5)).^(-G2))./((1 + C2.*Mpae
465     if Mpaetest > Mpae
466        Mpaetest = Mpaetest - .00001;
467     elseif Mpaetest < Mpae
468        Mpaetest = Mpaetest + .00001;
469     end
470 end
471
472 M3(Idx5+1:NT) = Mpae*ones(NT-Idx5,1);
473
474 P03 = P3(Idx5)*((1 + C2*M3(Idx5)^2)^(gamma2/(gamma2 - 1)));
475 % Stagnation pressure after the shock, Pa
476 Ppae_b = P03/((1 + C2*Mpae^2)^(gamma2/(gamma2 - 1)));
477 % Post area expansion static pressure, Pa
478 P3(Idx5+1:NT) = Ppae_b*ones(NT-Idx5,1);
479 % Static pressure, Pa
480
481 T3 = Tad./(1+C2.*(M3.^2)); % Static temperature, K
482
483 rho3 = P3./(R2.*T3); % Static density, kg/(m^3)
```

```
484
485 else
486     fprintf('\n\nNot a valid shock station.\nShockStation must equal either ''3'' or ''4
487 end
488 %---End H2 and O2 insertion in combustor---%
489
490 if strcmp(ShockStation, '4') == 1
491     Tf = T2;
492     Pf = P2;
493     rhof = rho2;
494     Mf = M2;
495 elseif strcmp(ShockStation, '3') == 1
496     Tf = T3;
497     Pf = P3;
498     rhof = rho3;
499     Mf = M3;
500 end
501
502 U = a2.*Mf;
503 P0f = P0inf*ones(NT,1);
504 P0f_bar = P0f/100000;
505 Pf_bar = Pf/100000;
506
507     Re = (rhof.*U.*2.*Rv)./mu2;
508     % Reynolds number
509     f = (.79*log(Re)-1.64).^(-2); % First Petukhov equation, (2, pg. 805).
510     % Friction factor, valid for 3000 < Re < 5*10^6 in smooth tubes.
511     Nu = (f/8).*(Re-1000).*Pr2./(1+12.7.*((f/8).^.5).*((Pr2.^(2/3))-1));
512     % Nusselt number, Gnielinski equation (2, pg. 806).
513     % Valid for .5 <= Pr <= 2000 and 3000 < Re < 5*10^6
514     h = Nu.*cond2./(2.*Rv); % Convective heat transfer coefficient, W/((m^2)*K)
515     Qfdotconv = h.*(Ts-Tf);
516     % Rate of heat flux to fluid, W/(m^2), (2, pg. 777)
```

```
517     qf = Qfdotconv./mdotinf; % Heat flux per unit mass, J/(kg*m^2)
518     q = qf.*A2; % Specific heat transfer, J/kg
519     T0f = Tad*ones(NT,1); % Use frictionless T0 as the value for T0f at X = Idx2
520
521     % Note that the lowercase letter "f" at the end of a variable name
522     % indicates use in the frictional calculations, unless stated
523     % otherwise. For instance, Qf indicates heat flux, and qf indicates
524     % specific heat flux, as two examples of exceptions.
525
526 %---Preallocation---%
527
528 dT0f = zeros(NT,1);
529 dA = zeros(NT,1);
530
531 %---End Preallocation---%
532
533 %---Station 1 to 2---%
534
535     % For loop to assign stagnation temperatures accounting for friction
536     for m = 2:Idx2
537         T0f(m) = T0f(m-1) + (1./Cp2).*q(m-1);
538         % Stagnation temperature accounting for friction, K
539         dT0f(m) = T0f(m) - T0f(m-1); % Differential of stagnation temperature, K
540         dA(m) = A(m) - A(m-1); % Differential of cross-sectional area, m^2
541     end
542
543     D = 2.*Rv;
544     % Diameter of the duct, m
545
546 for j = 2:Idx2
547     Mf(j) = SWR_Steady1D_Mach(gamma2,Mf(j-1),dA(j),A(j),dT0f(j),T0f(j),f(j),dx,D(j));
548     P0f(j) = SWR_Steady1D_Pressure(gamma2,Mf(j),P0f(j-1),dT0f(j),T0f(j),f(j),dx,D(j));
549 end
```

```
550
551 %---End Station 1 to 2---%
552
553 %---Station 2 to 3---%
554
555 %---Bartz equation---%
556
557 muam = zeros(NT,1);
558 rhoam = zeros(NT,1);
559 Tam = zeros(NT,1);
560
561 for j = Idx2:Idx3
562         Tam(j) = (Tf(j)+Ts)/2;
563         if mdotH2_extra > 0 && mdotO2_extra == 0
564         TempOut2 = CEA('problem','tp','equilibrium','p,bar',Pf_bar(j),...
565             't,K',Tam(j),'reactants','name','H2O(g)','H',2,'O',1,...
566             'wt%',mdotSteam,'reactants','name','H2(g)','H',2,...
567             'wt%',mdotH2_extra,'output','transport','short','end');
568         elseif mdotO2_extra > 0 && mdotH2_extra == 0
569             TempOut2 = CEA('problem','tp','equilibrium','p,bar',Pf_bar(j),...
570             't,K',Tam(j),'reactants','name','H2O(g)','H',2,'O',1,...
571             'wt%',mdotSteam,'reactants','name','O2(g)','O',2,...
572             'wt%',mdotO2_extra,'output','transport','short','end');
573         else
574             fprintf('\n\nInvalid values for mdotH2_extra or mdotO2_extra.\n\n')
575         end
576         muam(j) = TempOut2.output.viscosity/10000;
577         % Dynamic viscosity at the wall temperature, kg/(m*s)
578         rhoam(j) = TempOut2.output.density;
579         % Density at the wall temperature, kg/(m^3)
580         % Value of the property at the arithmetic mean temperature of the
581         % local freestream static temperature and the wall temperature
582 end
```

```
583
584 TempOut3 = CEA('problem','tp','equilibrium','p,bar',P0inf_bar,...
585             't,K',Tad,'reactants','name','H2O(g)','H',2,'O',1,...
586             'wt%',100.,'output','transport','short','end');
587 mu0 = TempOut3.output.viscosity/10000;
588 % Dynamic viscosity at stagnation conditions, kg/(m*s)
589
590 hB = h;
591
592 for m = Idx2+1:Idx3
593
594     hB(m) = (.026./((2.*Rv(m-1)).^.2)).*((Cp2.*...
595         (mu2.^.2))./(Pr2.^.6)).*((rhof(m-1).*...
596         U(m-1)).^.8).*(rhoam(m-1)./rhof(m-1)).*((muam(m-1)./...
597         mu0).^.2);
598     % Bartz equation; computes convective heat transfer coefficient of the
599     % gas, W/((m^2)*K)
600     % From (6, pg. 314.)
601
602     Qfdotconv(m-1) = hB(m).*(Ts-Tf(m-1));
603     % Rate of heat flux to fluid, W/(m^2), (2, pg. 777)
604     qf(m-1) = Qfdotconv(m-1)./mdotinf; % Heat flux per unit mass, J/(kg*m^2)
605     q(m-1) = qf(m-1).*A2(m-1); % Specific heat transfer, J/kg
606     % Note that the capital letter "B" at the end of a variable name
607     % indicates use in the Bartz equation calculations, unless stated
608     % otherwise.
609
610     T0f(m) = T0f(m-1) + (1./Cp2).*q(m-1);
611     % Stagnation temperature accounting for friction, K
612     dT0f(m) = T0f(m) - T0f(m-1); % Differential of stagnation temperature, K
613     dA(m) = A(m) - A(m-1); % Differential of cross-sectional area, m^2
614 end
615
```

```
616 h(Idx2+1:Idx3) = hB(Idx2+1:Idx3);
617
618 for j = Idx2+1:Idx3
619     Mf(j) = SWR_Steady1D_Mach(gamma2,Mf(j-1),dA(j),A(j),dT0f(j),T0f(j),f(j),dx,D(j));
620     P0f(j) = SWR_Steady1D_Pressure(gamma2,Mf(j),P0f(j-1),dT0f(j),T0f(j),f(j),dx,D(j));
621 end
622
623 %---End Bartz equation---%
624
625 %---End Station 2 to 3---%
626
627 %---Station 3 to Shock Station---%
628
629 % For loop to assign stagnation temperatures accounting for friction
630
631 if strcmp(ShockStation,'4') == 1
632     IdxShk = IdxShk4;
633 elseif strcmp(ShockStation,'3') == 1
634     IdxShk = IdxShk3;
635 end
636
637 for m = Idx3+1:NT
638     T0f(m) = T0f(m-1) + (1./Cp2).*q(m-1);
639     % Stagnation temperature accounting for friction, K
640     dT0f(m) = T0f(m) - T0f(m-1); % Differential of stagnation temperature, K
641     dA(m) = A(m) - A(m-1); % Differential of cross-sectional area, m^2
642 end
643
644 Mf(Idx3) = 1;
645 % Assume Mach number at the throat is exactly 1.
646 P0f(Idx3:Idx3+2) = P0f(Idx3);
647 % Assume stagnation pressure one and two increments downstream of the
648 % throat is equal to the value at the throat.
```

```
649 Mf(Idx3+2) = M(Idx3+2);
650 % Assume Mach number two increments downstream of the throat is equal to
651 % the adiabatic, isentropic Mach number at that point.
652
653 for j = Idx3+3:IdxShk
654     Mf(j) = SWR_Steady1D_Mach(gamma2,Mf(j-1),dA(j),A(j),dT0f(j),T0f(j),f(j),dx,D(j));
655     P0f(j) = SWR_Steady1D_Pressure(gamma2,Mf(j),P0f(j-1),dT0f(j),T0f(j),f(j),dx,D(j));
656 end
657
658 %---Shock Station to Test Section---%
659
660 %---Shock relations---%
661
662 % Account for a normal shock midway through the feedstock injector:
663 Mfps = ((1+C2.*Mf(IdxShk).^2)./((gamma2.*Mf(IdxShk).^2)-C2)).^.5;
664 % Post-shock Mach number, []
665 Mf(IdxShk+1) = Mfps;
666 % From Anderson, pg. 597
667
668 Pf(IdxShk) = P0f(IdxShk)./((1+C2.*(Mf(IdxShk).^2)).^(gamma2/(gamma2-1)));
669 % Static pressure immediately prior to the normal shock, Pa
670
671 Pfratio = (1+((2.*gamma2)./(gamma2+1))*((Mf(IdxShk).^2) - 1));
672 Pfps = Pfratio*Pf(IdxShk);
673 % Static pressure immediately after the normal shock, Pa
674 Pf(IdxShk+1) = Pfps;
675
676 P0f(IdxShk+1) = Pf(IdxShk+1).*((1+C2.*(Mf(IdxShk+1).^2)).^(gamma2/(gamma2-1)));
677 % Static pressure immediately prior to the normal shock, Pa
678
679 %---End shock relations---%
680
681 if strcmp(ShockStation,'3') == 1
```

```
682 for j = IdxShk+2:Idx5
683     Mf(j) = SWR_Steady1D_Mach(gamma2,Mf(j-1),dA(j),A(j),dT0f(j),T0f(j),f(j),dx,D(j));
684     P0f(j) = SWR_Steady1D_Pressure(gamma2,Mf(j),P0f(j-1),dT0f(j),T0f(j),f(j),dx,D(j));
685 end
686
687 % Calculate the Mach number post area expansion (pae = post area
688 % expansion).
689 Mfpaetest = Mf(Idx5+1);
690 Mfpae = 0;
691 while abs(Mfpae - Mfpaetest) > .00002
692     Mfpae = Mf(Idx5).*(A(Idx5)./A(Idx5+1)).*( ((1 + C2.*Mf(Idx5)).^(-G2))./((1 + C2.*Mfp
693     if Mfpaetest > Mfpae
694        Mfpaetest = Mfpaetest - .00001;
695     elseif Mfpaetest < Mfpae
696        Mfpaetest = Mfpaetest + .00001;
697     end
698 end
699
700 Mf(Idx5+1) = Mfpae;
701 P0f(Idx5+1) = P0f(Idx5);
702
703 for j = Idx5+2:NT
704     Mf(j) = SWR_Steady1D_Mach(gamma2,Mf(j-1),dA(j),A(j),dT0f(j),T0f(j),f(j),dx,D(j));
705     P0f(j) = SWR_Steady1D_Pressure(gamma2,Mf(j),P0f(j-1),dT0f(j),T0f(j),f(j),dx,D(j));
706 end
707 elseif strcmp(ShockStation,'4') == 1
708    for j = IdxShk+2:NT
709     Mf(j) = SWR_Steady1D_Mach(gamma2,Mf(j-1),dA(j),A(j),dT0f(j),T0f(j),f(j),dx,D(j));
710     P0f(j) = SWR_Steady1D_Pressure(gamma2,Mf(j),P0f(j-1),dT0f(j),T0f(j),f(j),dx,D(j));
711    end
712 end
713
714 %---End Shock Station to Test Section---%
```

```
715
716 %---Static values with friction ---%
717
718 Tf = T0f./(1+C2.*Mf.^2);
719 % Static temperature, K
720
721 Pf = P0f./((1+C2.*Mf.^2).^(gamma2./(gamma2-1)));
722 % Static pressure, Pa
723
724 rhof = Pf./(R2.*Tf);
725 % Static density assuming ideal gas, kg/(m^3)
726
727 %---End static values with friction---%
728
729 if mdot4 > 0;
730
731 %---N2 mixing---%
732
733     d4_in = .194; % Diameter of injection ports, in
734     r4_in = d4_in/2; % Radius of injector port, in
735     r4 = r4_in.*I2M; % Radius of injector port, m
736     N = 8; % Number of injector ports
737
738     thetaa_deg = 60; % Angle of four of the injector ports, degrees
739     thetab_deg = 30; % Angle of the other four injector ports, degrees
740
741     thetaa = thetaa_deg*pi/180; % Angle of four of the injector ports, radians
742     thetab = thetab_deg*pi/180; % Angle of the other four injector ports, radians
743
744     CosCor = .5*(cos(thetaa)+cos(thetab));
745     % Cosine correction term to account for angled injector ports.
746
747     A4a = N.*pi.*(r4.^2);
```

```
748     A4 = N.*pi.*(r4.^2).*CosCor;
749     A5 = A(Idx4);
750
751     alpha = mdot4./mdotinf; % Ratio of mass flow rates, mdot3/mdotinf, []
752     % Vary from .1 to 3
753
754     gamma4 = 1.4;
755     Cp4 = 1070;
756     % Specific heat at constant pressure of N2 at 300K and 1 atm, J/(kg*K)
757     MW4 = 28; % Molecular mass of injectant, g/mol
758     M4 = 1; % Mach number of injectant, []
759     % Assume injectant enters at sonic velocity
760     T4 = 298.15; % Temperature of injectant, K
761     R4 = Rbar./MW4; % Gas law constant for injectant
762     a4 = sqrt(gamma4*R4*T4); % Speed of sound of N2, m/s
763
764     gamma5 = gamma2;
765     M5 = Mf(Idx4); % Mach number of incoming freestream, []
766     % Assume adiabatic isentropic Mach number for now.
767
768     C4 = (gamma4-1)/2;
769     B4 = 2/(gamma4+1);
770     G4 = (gamma4+1)/(2*(gamma4-1));
771
772     % Remember, these are intermediate variables to make the code less
773     % jumbled.
774     C5 = (gamma5-1)/2;
775     B5 = 2/(gamma5+1);
776     G5 = (gamma5+1)/(2*(gamma5-1));
777
778     Astar4 = pi.*(r4.^2); % Area of just one of the injectors, m^2
779
780     T04 = T4*(1+C4*M4^2);
```

```
781     % Stagnation temperature of injectant, K
782 %     P4 = .5.*((mdot4./A4a).*sqrt(R4./gamma4).*sqrt(T04).*(1/M4).*...
783 %          ((1+C4.*M4.^2).^(-.5))).*(cos(thetaa) + cos(thetab));
784     P04 = (mdot4./A4a).*sqrt(R4.*T04./gamma4).*((1./B4).^(G4));
785     P4 = P04./((1+C4.*M4.^2).^(gamma4./(gamma4-1)));
786
787     % Pressure of injectant, Pa
788     P4_bar = P4/100000;
789     % Convert P3 from Pascals to bar
790
791     T05 = T0f(Idx4);
792     % Stagnation temperature of the incoming freestream, K
793     T5 = T05./(1+C5.*M5.^2);
794     P05 = P0f(Idx4);
795     % Stagnation pressure of the incoming freestream, Pa
796     P5 = Pf(Idx4);
797     % Static pressure of the incoming freestream, Pa
798     P5_bar = P5/100000;
799     % Convert P5 from Pascals to bar
800
801     P7_old = P4 + P5;
802     P7_bar = P4_bar + P5_bar;
803
804     Cp7a = (mdotinf*Cp2 + mdot4*Cp4)/(mdotinf + mdot4);
805     R7a = (mdotinf*R2 + mdot4*R4)/(mdotinf + mdot4);
806     gamma7a = Cp7a/(Cp7a-R7a);
807
808     CEAout7 = CEA('problem','hp','frozen','p,bar',P7_bar,...
809             'reactants','name','H2O(g)','H',2,'O',1,...
810             'wt%',mdotSteam,'t(K)',T5,'name','H2(g)','H',2,...
811             'wt%',mdotH2_extra,'t(K)',T5,'name','O2(g)','O',2,...
812             'wt%',mdotO2_extra,'t(K)',T5,'name','N2(g)','N',2,...
813             'wt%',mdot4,'t(K)',T4,'output','transport','short','end');
```

```
814         Cp7_kJ = CEAout7.output.cp_tran.froz; % Specific heat at constant pressure, [kJ/
815         Cp7 = Cp7_kJ.*1000; % Convert to J/(kg*K)
816         mu7 = CEAout7.output.viscosity./10000; % Dynamic Viscosity, kg/(m*s)
817         % Note that default output from CEAM is in millipoise.
818         % 10 P = 1 kg/(m*s), 1 P = 1000 mP
819         cond7 = CEAout7.output.conduct.froz*.1; % Conductive heat transfer coefficient,
820         % Note that the default output from CEAM is in mW/(cm*K)
821         Pr7 = CEAout7.output.prandtl.froz; % Specific heat at constant pressure, kJ/(kg*
822         gamma7 = CEAout7.output.gamma; % Ratio of specific heats from CEAM, []
823         MW7 = CEAout7.output.mw; % Molecular weight, check units
824         % Educated guess based on order of magnitude (10^1): kg/kmol
825         a7 = CEAout7.output.sonvel; % Sonic velocity, m/s
826         T7ad = CEAout7.output.temperature;
827         % Adiabatic flame temperature of mixture, K
828
829         R7 = Rbar/MW7;
830
831         C7 = (gamma7-1)/2;
832         B7 = 2/(gamma7+1);
833         G7 = (gamma7+1)/(2*(gamma7-1));
834
835         a5 = a2;
836         Cp5 = Cp2;
837         R5 = R2;
838
839         u4a = M4*a4*cos(thetaa);
840         u4b = M4*a4*cos(thetab);
841
842         u4 = (u4a + u4b)/2;
843         u5 = M5*a5;
844
845         ke4 = .5*(u4^2);
846         ke5 = .5*(u5^2);
```

```
847
848         fM4 = (M4.^2).*(1+C4.*M4.^2).*((1+gamma4.*M4.^2).^(-2));
849         fM5 = (M5.^2).*(1+C5.*M5.^2).*((1+gamma5.*M5.^2).^(-2));
850
851 %         M7test = .00001:.00001:5;
852
853             a7M72fun = @(M7,a7) .5.*(a7.*M7).^2;
854             alpha4 = alpha./(alpha+1);
855             alpha5 = 1./(alpha+1);
856             CpTke4 = alpha4.*(Cp4.*T4+ke4);
857             CpTke5 = alpha5.*(Cp5.*T5+ke5);
858
859             T7fun = @(M7,CpTke4,CpTke5,Cp7) (-a7M72fun(M7,a7) + CpTke4 + CpTke5)./Cp7;
860
861             T07fun = @(M7,C7) T7fun(M7,CpTke4,CpTke5,Cp7).*(1+C7.*M7.^2);
862             % Stagnation temperature of mixed fluid, K
863
864             fM7 = @(M7,alpha,R7,gamma7,T05,CosCor,R4,gamma4,fM4,R5,gamma5,fM5) ((1+alpha
865         (((alpha.*CosCor.*sqrt(R4.*T04./(gamma4.*T05.*fM4)))+...
866         sqrt(R5./(gamma5.*fM5))).^2);
867
868         M7fun = @(M7) M7 - sqrt(2.*fM7(M7,alpha,R7,gamma7,T05,CosCor,R4,gamma4,fM4,R5,ga
869         % Mach number of mixed fluid, []
870
871         % M7Real = real(M7);
872
873         options = optimset('TolX',.0002);
874         M7 = fzero(M7fun,M5,options);
875
876         T7 = T7fun(M7,CpTke4,CpTke5,Cp7);
877         T07 = T07fun(M7,C7);
878
879         BlkA = (1+alpha).*(M5./M7);
```

```
880          BlkB = sqrt(T07.*R7.*gamma5./(T05.*R5.*gamma7));
881          BlkC = (1 + C7.*M7.^2).^G7;
882          BlkD = (1 + C5.*M5.^2).^G5;
883
884          P07 = P05.*BlkA.*BlkB.*BlkC./BlkD;
885          P7 = P07/((1+C7*M7^2)^(gamma7/(gamma7-1)));
886
887  %---End N2 mixing---%
888
889  %---Shocks with N2---%
890  Amach7 = (Astar./Marea).*((B7.*(1+C7.*Marea.^2)).^G7);
891  if strcmp(ShockStation,'4') == 1
892  M2pm = M2; % Assign a post mixing Mach number, []
893  M2pm(Idx4+1:Idx5) = M7;
894
895  Mpaetest = M2pm(Idx5);
896  Mpae = 0;
897  while abs(Mpae - Mpaetest) > .00002
898
899              D = (M2pm(Idx5)./Mpaetest).*(A(Idx5)./A(Idx5+1));
900              E = 1;
901              DE = D.*E;
902              F = 1+C7.*(M2pm(Idx5).^2);
903              DEG = DE.^(-1./G7);
904              DEGF = DEG.*F;
905              CDEGF = (1./C7).*(DEGF-1);
906
907      Mpae = CDEGF.^.5;
908      if Mpaetest > Mpae
909         Mpaetest = Mpaetest - .00001;
910      elseif Mpaetest < Mpae
911         Mpaetest = Mpaetest + .00001;
912      end
```

```
913 end
914
915 M2pm(Idx5+1:IdxShk4) = Mpae;
916 % Mach number with mixing inside the 4" section but upstream of the shock.
917
918 % Account for a normal shock midway through the mixer section:
919 Mps2 = ((1+C7.*M2pm(IdxShk4).^2)./((gamma7.*M2pm(IdxShk4).^2)-C7)).^.5;
920 % Post-shock Mach number, []
921 M2pm(IdxShk4+1:NT) = Mps2*ones(NT-IdxShk4,1);
922 % From Anderson, pg. 597
923
924 P2pm = P2;
925 P2pm(Idx4+1:IdxShk4) = P07./((1+C7.*M2pm(Idx4+1:IdxShk4).^2).^(gamma7./(gamma7-1)));
926
927 Pratio2pm = (1+((2.*gamma7)./(gamma7+1))*((M2pm(IdxShk4).^2) - 1));
928 Pps2pm = Pratio2pm*P2pm(IdxShk4);
929 P2pm(IdxShk4+1:end) = Pps2pm.*ones(NT-IdxShk4,1);
930
931 T2pm = T2;
932 T2pm(Idx4+1:NT) = T07./(1+C7.*(M2pm(Idx4+1:NT).^2)); % Static temperature, K
933
934 elseif strcmp(ShockStation,'3') == 1
935 M3pm = M3; % Assign a post mixing Mach number, []
936 M3pm(Idx4+1:IdxShk3) = M7;
937
938 % Account for a normal shock midway through the feedstock injector:
939 Mps3pm = ((1+C7.*M3pm(IdxShk3).^2)./((gamma7.*M3pm(IdxShk3).^2)-C7)).^.5;
940 % Post-shock Mach number, []
941 M3pm(IdxShk3+1:NT) = Mps3pm*ones(NT-IdxShk3,1);
942 % From Anderson, pg. 597
943
944 P3pm = P3;
945 P3pm(Idx4+1:IdxShk3) = P07./((1+C7.*(M3pm(Idx4+1:IdxShk3).^2)).^...
```

```
946      (gamma7/(gamma7-1))); % Static pressure, Pa
947
948  Pratio3pm = (1+((2.*gamma7)./(gamma7+1))*((M3pm(IdxShk3).^2) - 1));
949  Pps3pm = Pratio3pm*P3pm(IdxShk3);
950  P3pm(IdxShk3+1:NT) = Pps3pm.*ones(NT-IdxShk3,1);
951
952  % Calculate the Mach number post area expansion (pae = post area
953  % expansion).
954  Mpaetest = M3(Idx5+1);
955  Mpae = 0;
956  while abs(Mpae - Mpaetest) > .00002
957      Mpae = M3pm(Idx5).*(A(Idx5)./A(Idx5+1)).*( ((1 + C7.*M3pm(Idx5)).^(-G7))./((1 + C7.*
958      if Mpaetest > Mpae
959         Mpaetest = Mpaetest - .00001;
960      elseif Mpaetest < Mpae
961         Mpaetest = Mpaetest + .00001;
962      end
963  end
964
965  M3pm(Idx5+1:NT) = Mpae*ones(NT-Idx5,1);
966
967  P03ps = P3pm(Idx5)*((1 + C7*M3pm(Idx5)^2)^(gamma7/(gamma7 - 1)));
968  % Stagnation pressure after the shock, Pa
969  Ppae = P03ps/((1 + C7*Mpae^2)^(gamma7/(gamma7 - 1)));
970  % Post area expansion static pressure, Pa
971  P3pm(Idx5+1:NT) = Ppae*ones(NT-Idx5,1);
972  % Static pressure, Pa
973
974  T3pm = T3;
975  T3pm(Idx4+1:NT) = T07./(1+C7.*(M3pm(Idx4+1:NT).^2)); % Static temperature, K
976
977  else
978      fprintf('\n\nNot a valid shock station.\nShockStation must equal either 3 or 4.\n\n'
```

```
979 end
980
981 %---End shocks with N2---%
982
983 %---Frictional considerations for mixed flow---%
984
985 %---Shocks with N2 and friction---%
986 Amach7 = (Astar./Marea).*((B7.*(1+C7.*Marea.^2)).^G7);
987 if strcmp(ShockStation,'4') == 1
988 M2pm_b = Mf; % Assign a post mixing Mach number, []
989
990 M2pm_b(Idx4+1:Idx5) = M7;
991
992 Mpaetest = Mf(Idx5+1);
993 Mpae = 0;
994 while abs(Mpae - Mpaetest) > .00002
995
996             D = (M2pm_b(Idx5)./Mpaetest).*(A(Idx5)./A(Idx5+1));
997             E = 1;
998             DE = D.*E;
999             F = 1+C7.*(M2pm_b(Idx5).^2);
1000            DEG = DE.^(-1./G7);
1001            DEGF = DEG.*F;
1002            CDEGF = (1./C7).*(DEGF-1);
1003
1004    Mpae = CDEGF.^.5;
1005    if Mpaetest > Mpae
1006       Mpaetest = Mpaetest - .00001;
1007    elseif Mpaetest < Mpae
1008       Mpaetest = Mpaetest + .00001;
1009    end
1010 end
1011
```

```
M2pm_b(Idx5+1:IdxShk4) = Mpae;
% Mach number with mixing inside the 4" section but upstream of the shock.

% Account for a normal shock midway through the mixer section:
Mps2_b = ((1+C7.*M2pm_b(IdxShk4).^2)./((gamma7.*M2pm_b(IdxShk4).^2)-C7)).^.5;
% Post-shock Mach number, []
M2pm_b(IdxShk4+1:NT) = Mps2_b*ones(NT-IdxShk4,1);
% From Anderson, pg. 597

P2pm_b = Pf;
P2pm_b(Idx4+1:IdxShk4) = P07./((1+C7.*M2pm_b(Idx4+1:IdxShk4).^2).^(gamma7./(gamma7-1)));

Pratio2pm_b = (1+((2.*gamma7)./(gamma7+1))*((M2pm_b(IdxShk4).^2) - 1));
Pps2pm_b = Pratio2pm_b*P2pm_b(IdxShk4);
P2pm_b(IdxShk4+1:end) = Pps2pm_b.*ones(NT-IdxShk4,1);

T2pm_b = Tf;
T2pm_b(Idx4+1:NT) = T07./(1+C7.*(M2pm_b(Idx4+1:NT).^2)); % Static temperature, K

elseif strcmp(ShockStation,'3') == 1
M3pm_b = Mf; % Assign a post mixing Mach number, []
M3pm_b(Idx4+1:IdxShk3) = M7;

% Account for a normal shock midway through the feedstock injector:
Mps3pm_b = ((1+C7.*M3pm_b(IdxShk3).^2)./((gamma7.*M3pm_b(IdxShk3).^2)-C7)).^.5;
% Post-shock Mach number, []
M3pm_b(IdxShk3+1:NT) = Mps3pm_b*ones(NT-IdxShk3,1);
% From Anderson, pg. 597

P3pm_b = Pf;
P3pm_b(Idx4+1:IdxShk3) = P07./((1+C7.*(M3pm_b(Idx4+1:IdxShk3).^2)).^...
    (gamma7/(gamma7-1))); % Static pressure, Pa

```

```
1045 Pratio3pm_b = (1+((2.*gamma7)./(gamma7+1))*((M3pm_b(IdxShk3).^2) - 1));
1046 Pps3pm_b = Pratio3pm_b*P3pm_b(IdxShk3);
1047 P3pm_b(IdxShk3+1:NT) = Pps3pm_b.*ones(NT-IdxShk3,1);
1048
1049 % Calculate the Mach number post area expansion (pae = post area
1050 % expansion).
1051 Mpaetest = Mf(Idx5+1);
1052 Mpae = 0;
1053 while abs(Mpae - Mpaetest) > .00002
1054     Mpae = M3pm(Idx5).*(A(Idx5)./A(Idx5+1)).*( ((1 + C7.*M3pm(Idx5)).^(-G7))./((1 + C7.*
1055     if Mpaetest > Mpae
1056        Mpaetest = Mpaetest - .00001;
1057     elseif Mpaetest < Mpae
1058        Mpaetest = Mpaetest + .00001;
1059     end
1060 end
1061
1062 M3pm_b(Idx5+1:NT) = Mpae*ones(NT-Idx5,1);
1063
1064 P03ps_b = P3pm_b(Idx5)*((1 + C7*M3pm_b(Idx5)^2)^(gamma7/(gamma7 - 1)));
1065 % Stagnation pressure after the shock, Pa
1066 Ppae_b = P03ps_b/((1 + C7*Mpae^2)^(gamma7/(gamma7 - 1)));
1067 % Post area expansion static pressure, Pa
1068 P3pm_b(Idx5+1:NT) = Ppae_b*ones(NT-Idx5,1);
1069 % Static pressure, Pa
1070
1071 T3pm_b = Tf;
1072 T3pm_b(Idx4+1:NT) = T07./(1+C7.*(M3pm_b(Idx4+1:NT).^2)); % Static temperature, K
1073
1074 end
1075
1076 elseif mdot4 < 0;
1077     fprintf('\n\nNot a valid value for mdot4.\n\n')
```

```
1078 end
1079
1080 %---End shocks with N2 and friction---%
1081
1082 if strcmp(ShockStation, '4') == 1
1083     Tfpm = T2pm_b;
1084     Pfpm = P2pm_b;
1085     Mfpm = M2pm_b;
1086 elseif strcmp(ShockStation, '3') == 1
1087     Tfpm = T3pm_b;
1088     Pfpm = P3pm_b;
1089     Mfpm = M3pm_b;
1090 end
1091
1092 mdot7 = mdotinf + mdot4;
1093
1094 rhofpm = rhof;
1095 Upm = U;
1096 P0fpm = P0f;
1097 P0fpm_bar = P0f_bar;
1098 Pfpm_bar = Pf_bar;
1099 Repm = Re;
1100 fpm = f;
1101 Nupm = Nu;
1102 hpm = h;
1103 qfpm = qf;
1104
1105 Upm(Idx4+1:NT) = a7.*Mfpm(Idx4+1:NT);
1106 P0fpm(Idx4+1:NT) = Pfpm(Idx4+1:NT).*((1+C7.*Mfpm(Idx4+1:NT).^2).^(gamma7./(gamma7-1)));
1107 P0fpm_bar(Idx4+1:NT) = P0fpm(Idx4+1:NT)/100000;
1108 Pfpm_bar(Idx4+1:NT) = Pfpm(Idx4+1:NT)/100000;
1109 rhofpm(Idx4+1:NT) = Pfpm(Idx4+1:NT)./(R7.*Tfpm(Idx4+1:NT));
1110
```

```
Repm(Idx4+1:NT) = (rhofpm(Idx4+1:NT).*Upm(Idx4+1:NT).*2.*Rv(Idx4+1:NT))./mu7;
    % Reynolds number
    fpm(Idx4+1:NT) = (.79*log(Repm(Idx4+1:NT))-1.64).^(-2); % First Petukhov equation,
    % Friction factor, valid for 3000 < Re < 5*10^6 in smooth tubes.
    Nupm(Idx4+1:NT) = (fpm(Idx4+1:NT)/8).*(Repm(Idx4+1:NT)-1000).*Pr7./(1+12.7.*((fpm(Id
    % Nusselt number, Gnielinski equation (2, pg. 806).
    % Valid for .5 <= Pr <= 2000 and 3000 < Re < 5*10^6
    hpm(Idx4+1:NT) = Nupm(Idx4+1:NT).*cond7./(2.*Rv(Idx4+1:NT)); % Convective heat trans
    Qfdotconvpm = hpm.*(Ts-Tfpm);
    % Rate of heat flux to fluid, W/(m^2), (2, pg. 777)
    qfpm(Idx4+1:NT) = Qfdotconvpm(Idx4+1:NT)./mdot7; % Heat flux per unit mass, J/(kg*m^
    qpm = qfpm.*A2; % Specific heat transfer, J/kg

    T0fpm = T0f;
    dT0fpm = dT0f;
    T0fpm(Idx4+1) = T07;
    dT0fpm(Idx4+1) = T0fpm(Idx4+1) - T0fpm(Idx4); % Differential of stagnation temperatu
    Mfpm(Idx4+1) = M7;
    P0fpm(Idx4+1) = P07;

for m = Idx4+2:NT
    T0fpm(m) = T0fpm(m-1) + (1./Cp7).*qpm(m-1);
    % Stagnation temperature accounting for friction, K
    dT0fpm(m) = T0fpm(m) - T0fpm(m-1); % Differential of stagnation temperature, K
    dA(m) = A(m) - A(m-1); % Differential of cross-sectional area, m^2
end

for j = Idx4+2:IdxShk
    Mfpm(j) = SWR_Steady1D_Mach(gamma7,Mfpm(j-1),dA(j),A(j),dT0fpm(j),T0fpm(j),fpm(j),dx
    P0fpm(j) = SWR_Steady1D_Pressure(gamma7,Mfpm(j),P0fpm(j-1),dT0fpm(j),T0fpm(j),fpm(j)
end

%---Shock Station to Test Section---%
```

```
1144
1145 %---Shock relations---%
1146
1147 % Account for a normal shock midway through the feedstock injector:
1148 Mfpspm = ((1+C7.*Mfpm(IdxShk).^2)./((gamma7.*Mfpm(IdxShk).^2)-C7)).^.5;
1149 % Post-shock Mach number, []
1150 Mfpm(IdxShk+1) = Mfpspm;
1151 % From Anderson, pg. 597
1152
1153 Pfpm(IdxShk) = P0fpm(IdxShk)./((1+C7.*(Mfpm(IdxShk).^2)).^(gamma7/(gamma7-1)));
1154 % Static pressure immediately prior to the normal shock, Pa
1155
1156 Pfpmratio = (1+((2.*gamma7)./(gamma7+1))*((Mfpm(IdxShk).^2) - 1));
1157 Pfpspm = Pfpmratio*Pfpm(IdxShk);
1158 % Static pressure immediately after the normal shock, Pa
1159 Pfpm(IdxShk+1) = Pfpspm;
1160
1161 P0fpm(IdxShk+1) = Pfpm(IdxShk+1).*((1+C7.*(Mfpm(IdxShk+1).^2)).^(gamma7/(gamma7-1)));
1162 % Static pressure immediately prior to the normal shock, Pa
1163
1164 %---End shock relations---%
1165
1166 if strcmp(ShockStation,'3') == 1
1167 for j = IdxShk+2:Idx5
1168     Mfpm(j) = SWR_Steady1D_Mach(gamma7,Mfpm(j-1),dA(j),A(j),dT0fpm(j),T0fpm(j),fpm(j),dx
1169     P0fpm(j) = SWR_Steady1D_Pressure(gamma7,Mfpm(j),P0fpm(j-1),dT0fpm(j),T0fpm(j),fpm(j)
1170 end
1171
1172 % Calculate the Mach number post area expansion (pae = post area
1173 % expansion).
1174 Mfpaepmtest = Mfpm(Idx5+1);
1175 Mfpaepm = 0;
1176 while abs(Mfpaepm - Mfpaepmtest) > .00002
```

```
1177      Mfpaepm = Mfpm(Idx5).*(A(Idx5)./A(Idx5+1)).*( ((1 + C7.*Mfpm(Idx5)).^(-G7))./((1 + C
1178      if Mfpaepmtest > Mfpaepm
1179         Mfpaepmtest = Mfpaepmtest - .00001;
1180      elseif Mfpaepmtest < Mfpaepm
1181         Mfpaepmtest = Mfpaepmtest + .00001;
1182      end
1183  end
1184
1185  Mfpm(Idx5+1) = Mfpaepm;
1186  P0fpm(Idx5+1) = P0fpm(Idx5);
1187
1188  for j = Idx5+2:NT
1189      Mfpm(j) = SWR_Steady1D_Mach(gamma7,Mfpm(j-1),dA(j),A(j),dT0fpm(j),T0fpm(j),fpm(j),dx
1190      P0fpm(j) = SWR_Steady1D_Pressure(gamma7,Mfpm(j),P0fpm(j-1),dT0fpm(j),T0fpm(j),fpm(j)
1191  end
1192  elseif strcmp(ShockStation,'4') == 1
1193     for j = IdxShk+2:NT
1194      Mfpm(j) = SWR_Steady1D_Mach(gamma7,Mfpm(j-1),dA(j),A(j),dT0fpm(j),T0fpm(j),fpm(j),dx
1195      P0fpm(j) = SWR_Steady1D_Pressure(gamma7,Mfpm(j),P0fpm(j-1),dT0fpm(j),T0fpm(j),fpm(j)
1196     end
1197  end
1198
1199  %---End shock station to test section---%
1200
1201  %---Static values with friction ---%
1202
1203  Tfpm = Tf;
1204  Tfpm(Idx4+1:NT) = T0fpm(Idx4+1:NT)./(1+C7.*Mfpm(Idx4+1:NT).^2);
1205  % Static temperature, K
1206
1207  Pfpm = Pf;
1208  Pfpm(Idx4+1:NT) = P0fpm(Idx4+1:NT)./((1+C7.*Mfpm(Idx4+1:NT).^2).^(gamma7./(gamma7-1)));
1209  % Static pressure, Pa
```

```
1210
1211 rhofpm = rhof;
1212 rhofpm(Idx4+1:NT) = Pfpm(Idx4+1:NT)./(R7.*Tfpm(Idx4+1:NT));
1213 % Static density assuming ideal gas, kg/(m^3)
1214
1215 %---End static values with friction---%
1216
1217 %---End frictional considerations for mixed flow---%
1218
1219 %---Data output---%
1220
1221 if mdot4 > 0
1222     fprintf('\n\nTest section M = %.4f',Mfpm(end))
1223     fprintf('\nTest section T = %.f K',Tfpm(end))
1224     fprintf('\nTest section P = %.f kPa',Pfpm(end)/1000)
1225     fprintf('\nTest section U = %.f m/s',Upm(end))
1226     fprintf('\nTest section mdotSteam = %.f g/s',mdotSteam*1000)
1227     fprintf('\nTest section mdotH2_extra = %.2f g/s',mdotH2_extra*1000)
1228     fprintf('\nTest section mdotN2 = %.f g/s',mdot4*1000)
1229     fprintf('\nTest section MW = %.2f g/mol',MW7)
1230     fprintf('\nTest section mu = %.4f millipoise',CEAout7.output.viscosity)
1231     fprintf('\nTest section k = %.3f mW/(cm*K)',CEAout7.output.conduct.froz)
1232     fprintf('\nTest section Nu = %.1f ',Nupm(end))
1233     fprintf('\nTest section h_c = %.1f W/(m^2*K)\n\n',hpm(end))
1234 elseif mdot4 == 0
1235     fprintf('\n\nTest section M = %.4f',Mf(end))
1236     fprintf('\nTest section T = %.f K',Tf(end))
1237     fprintf('\nTest section P = %.f kPa',Pf(end)/1000)
1238     fprintf('\nTest section U = %.f m/s',U(end))
1239     fprintf('\nTest section mdotSteam = %.f g/s',mdotSteam*1000)
1240     fprintf('\nTest section mdotH2_extra = %.2f g/s',mdotH2_extra*1000)
1241     fprintf('\nTest section mdotN2 = %.f g/s',mdot4*1000)
1242     fprintf('\nTest section MW = %.2f g/mol',MW2)
```

```
1243      fprintf('\nTest section mu = %.4f millipoise',CEAout2.output.viscosity)
1244      fprintf('\nTest section k = %.3f mW/(cm*K)',CEAout2.output.conduct.froz)
1245      fprintf('\nTest section Nu = %.1f ',Nu(end))
1246      fprintf('\nTest section h_c = %.1f W/(m^2*K)\n\n',h(end))
1247  end
1248
1249  %---Plots!---%
1250
1251  %---Plot as a function of axial position---%
1252  figure
1253  plot(X,Rv,'-','Color',[.9 .4 .09],'LineWidth',2)
1254  title('{\fontname{Times New Roman}Mach Number}')
1255  title('{\fontname{Times New Roman}Geometry}')
1256  xlabel('{\fontname{Times New Roman}Axial Position, [m]}')
1257  ylabel('{\fontname{Times New Roman}Radius, [m]}')
1258  ax = gca;
1259  ax.FontName = 'Times New Roman';
1260  figure
1261  % plot(X,M,'-','Color',[.45 .5 1],'LineWidth',2)
1262  % hold on
1263  if strcmp(ShockStation,'4') == 1
1264  plot(X,M2,'-','Color',[.2 .4 .8],'LineWidth',2)
1265  elseif strcmp(ShockStation,'3') == 1
1266      plot(X,M3,'-','Color',[.2 .4 .8],'LineWidth',2)
1267  end
1268  if mdot4 > 0;
1269  hold on
1270  if strcmp(ShockStation,'4') == 1
1271  plot(X,M2pm,'-','Color',[.45 .5 1],'LineWidth',2)
1272  elseif strcmp(ShockStation,'3') == 1
1273      plot(X,M3pm,'-','Color',[.45 .5 1],'LineWidth',2)
1274  end
1275  end
```

```
hold on
plot(X,Mf,'-','Color',[.7 .2 .65],'LineWidth',2)
if mdot4 > 0;
hold on
plot(X,Mfpm,'-','Color',[.58 .75 .68],'LineWidth',2)
end
title('{\fontname{Times New Roman}Mach Number}')
xlabel('{\fontname{Times New Roman}Axial Position, [m]}')
ylabel('{\fontname{Times New Roman}Mach number, []}')
legend('No Mixing','Mixing','With Friction','With Friction and Mixing')
l = legend;
l.FontName = 'Times New Roman';
ax = gca;
ax.FontName = 'Times New Roman';
    figure
%     plot(X,T,'-','Color',[.2 .9 .7],'LineWidth',2)
%     hold on
if strcmp(ShockStation,'4') == 1
    plot(X,T2,'-','Color',[.2 .4 .8],'LineWidth',2)
elseif strcmp(ShockStation,'3') == 1
    plot(X,T3,'-','Color',[.2 .4 .8],'LineWidth',2)
end
if mdot4 > 0;
hold on
if strcmp(ShockStation,'4') == 1
    plot(X,T2pm,'-','Color',[.45 .5 1],'LineWidth',2)
elseif strcmp(ShockStation,'3') == 1
    plot(X,T3pm,'-','Color',[.45 .5 1],'LineWidth',2)
end
end
    hold on
    plot(X,T0f,'-','Color',[.7 .2 .65],'LineWidth',2)
    hold on
```

```
1309      plot(X,Tf,':','Color',[.7 .2 .65],'LineWidth',2)
1310  if mdot4 > 0;
1311  hold on
1312  plot(X,T0fpm,'-','Color',[.58 .75 .68],'LineWidth',2)
1313  hold on
1314  plot(X,Tfpm,':','Color',[.58 .75 .68],'LineWidth',2)
1315  end
1316      title('{\fontname{Times New Roman}Temperature}')
1317      xlabel('{\fontname{Times New Roman}Axial Position, [m]}')
1318      ylabel('{\fontname{Times New Roman}Temperature, [K]}')
1319      legend('No Mixing','Mixing','T_0 with Friction',...
1320          'T with Friction','T_0 with Friction and Mixing',...
1321          'T with Friction and Mixing')
1322      l = legend;
1323      l.FontName = 'Times New Roman';
1324      ax = gca;
1325      ax.FontName = 'Times New Roman';
1326      figure
1327  %     plot(X,P,'-','Color',[.5 .1 .7],'LineWidth',2)
1328  %     hold on
1329  if strcmp(ShockStation,'4') == 1
1330      plot(X,P2,'-','Color',[.2 .4 .8],'LineWidth',2)
1331  elseif strcmp(ShockStation,'3') == 1
1332      plot(X,P3,'-','Color',[.2 .4 .8],'LineWidth',2)
1333  end
1334  if mdot4 > 0;
1335  hold on
1336  if strcmp(ShockStation,'4') == 1
1337      plot(X,P2pm,'-','Color',[.45 .5 1],'LineWidth',2)
1338  elseif strcmp(ShockStation,'3') == 1
1339      plot(X,P3pm,'-','Color',[.45 .5 1],'LineWidth',2)
1340  end
1341  end
```

```
1342      hold on
1343      plot(X,P0f,'-','Color',[.7 .2 .65],'LineWidth',2)
1344      hold on
1345      plot(X,Pf,':','Color',[.7 .2 .65],'LineWidth',2)
1346  if mdot4 > 0;
1347  hold on
1348  plot(X,P0fpm,'-','Color',[.58 .75 .68],'LineWidth',2)
1349  hold on
1350  plot(X,Pfpm,':','Color',[.58 .75 .68],'LineWidth',2)
1351  end
1352      title('{\fontname{Times New Roman}Pressure}')
1353      xlabel('{\fontname{Times New Roman}Axial Position, [m]}')
1354      ylabel('{\fontname{Times New Roman}Pressure, [Pa]}')
1355      legend('No Mixing','Mixing','P_0 with Friction','P with Friction',...
1356          'P_0 with Friction and Mixing','P with Friction and Mixing')
1357      l = legend;
1358      l.FontName = 'Times New Roman';
1359      ax = gca;
1360      ax.FontName = 'Times New Roman';
```

SWR_Steady1D_Mach.m:

```
1  %%%%%%%%%%%%%%%%%%%%%%%%%%%%%%%%%%%%%%%%
2  %----Dan Drabiak-------------------------%
3  %----University of Washington-----------%
4  %----Steady 1-D Mach Number Function--%
5  %%%%%%%%%%%%%%%%%%%%%%%%%%%%%%%%%%%%%%%%
6
7  % This function is intended for use with the latest version of the SWR
8  % Modeling Function.
9
10 function [M2] = SWR_Steady1D_Mach(gamma,M1,dA,A,dT0,T0,f,dx,D)
```

```
11
12 BlkA = ((1 + ((gamma-1)./2).*M1.^2)./(1-M1.^2));
13 BlkB = -2.*dA./A;
14 BlkC = (1 + gamma.*M1.^2).*dT0./T0;
15 BlkD = gamma.*(M1.^2).*f.*dx./D;
16
17 BlkE = BlkA.*(BlkB + BlkC + BlkD);
18
19 M2 = sqrt((M1.^2).*(1+BlkE));
20
21 end
```

SWR_Steady1D_Pressure.m:

```
1  %%%%%%%%%%%%%%%%%%%%%%%%%%%%%%%%%%%%%%%%
2  %---Dan Drabiak-------------------------%
3  %---University of Washington-----------%
4  %---Steady 1-D Pressure Function-------%
5  %%%%%%%%%%%%%%%%%%%%%%%%%%%%%%%%%%%%%%%%
6
7  % This function is intended for use with the latest version of the SWR
8  % Modeling Function.
9
10 function [P02] = SWR_Steady1D_Pressure(gamma,M,P01,dT0,T0,f,dx,D)
11
12 BlkA = (-gamma.*M.^2)./2;
13 BlkB = dT0./T0;
14 BlkC = f.*dx./D;
15
16 BlkD = BlkA.*(BlkB + BlkC);
17
18 P02 = P01.*(1+BlkD);
```

```
19
20  end
```